Biological Nitrogen Removal in an Aerobic Granular Sludge Reactor Using Sensor-Mediated Control

by

Zerihun Bekele

A dissertation submitted in partial fulfillment
of the requirements for the degree of
Doctor of Philosophy
(Environmental Engineering)
in The University of Michigan
2020

Doctoral Committee:

Dr. Charles B. Bott, Co-Chair
Professor Nancy G. Love, Co-Chair
Professor Glen Daigger
Assistant Professor Branco Kerkez
Dr. Imre Takacs
Professor Henry Wang

2020

zerualem@umich.edu

ORCID iD: 0000-0002-0570-0941

Acknowledgments

This PhD dissertation work was supported through NSF GOALI grant number CBET1438560. I have also received a significant support from Hampton Roads Sanitation District to conduct this research. In addition I have also recieved support from the Department of Civil and Environmental Engineering and Rackham Graduate School. I am grateful to have received these funding supports to conduct my research without any financial restrictions.

I would like to thank my co-advisors Dr. Nancy Love and Dr. Charles Bott for their ever present support and mentrorship. I am greatful to have found such wonderful mentors that believed in me and guided me throughout my research work. They were also equally interested to the growth of personal well being and my research work through thier valuable advise and support. They have listened and understood my potential and needs, and allowed me pursue my research in the direction I wanted to go. I would like to thank my disseration committee Dr. Glen Daigger, Dr. Branko Kerkez, Dr. Henry Wang and Dr Imre Tacaks for offering your guidance, mentorship and support along the way.

I would like to thank the wonderul group of researchers that have helped this research work to come to success. I am greatful to have had work with Dr. Jeseth Delgado who have contributed significanlty to the work done in Chapter 3 both in lab and writing the chapter. I would like to thank Robert Smith (Xylem Inc.) for providing the ammonium/nitrate sensors that were used in this work. I would to thank the 'Downstream' research group Andrea McFarland, Brett Wagner and undergraduate researchers Adriana Arcelay, and Yan Du for their assistance in the laboratory. I also am greatful to have been part of the larger amazing Environmental

Biotechnology group who have offered thier hand whenever I needed.help. I want to extend my gratitude also the entire Civil and Environmental Engineering staffs particulalry to Tom Yavaraski for his assistance with analytical equipments in training and assitance. I would like also to thank the admistrative staff including Matt Blank, Stephanie Ford and Tabitha Rohn,

Finally, I would like to thank my familty who have been my backbone and cheer leaders to go after my passion and do this work. Thank you for encouraging me and sharing the burden with me. You have been there with me and believed in me even in times I doubt myself.

Table of Contents

List of Tables

List of Figures

List of Appendices

Abstract

Water resource recovery facilities (WRRFs) are infrastructure systems that are built to protect the water environment and recover valuable resources, such as water, nutrient and energy. However, full realization of this goals has been limited due to stringent effluent standard requirements and the lack of commercialization of WRRF technologies to date. consequently, research, technology development, and innovations have intensified to close these gaps. One area where such efforts have been focused is in biological nitrogen removal (BNiR), which is commonly achieved using conventional activated sludge systems. These systems have drawback, such as high aeration expense, larger footprints, and poor resource efficiency. To address these issues, novel technologies have been conceived over the last two decades and are moving toward wider full-scale adoption. One such technology is aerobic granular sludge reactor (GSR). In a GSR, a dense and self-immobilized biofilm called granules are formed that are round fast settling particles containing a consortium of microbial groups that allow for the simultaneous removal of substrates. These unique characteristics allow aerobic GSR to be small footprint and resource efficient. Consequently, the aerobic GSR technology shows great promise as novel state-of-the-art nitrogen removal technology for wastewater management. Coupled with aerobic GSR, a novel BNR process that has both low aeration and resource demand is partial nitritation and anammox (PN/A). Aerobic GSR with PN/A has been applied previously for high strength wastewater; however, little has been done to advance its application with low strength wastewater. This is due to several challenges associated with dilute wastewater, such as developing aerobic granules and sustaining them for long periods of operation; suppressing competing microbial organisms such as nitrite oxidizing bacteria (NOB), and maintaining the activity of desired organisms such as anammox. While addressing these challenges to improve N removal process, it is also desirable

to do it with as little aeration expense as possible. Hence, this dissertation presents advancements that can be used to address these standing challenges and accelerate wider adaption of AGS with PN/A.

This research developed an aerobic GSR operating scheme modeled as a B-stage system downstream of an A-stage carbon capture technology (i.e., moving away from single-sludge treatment systems). For this, we designed and developed lab scale reactor sequencing batch reactor (SBR) with a novel sensor-mediated control (SMC) aeration control strategy. Synthetic wastewater that mimics a dilute mainstream wastewater that is pre-treated via an anaerobic membrane reactor A-stage was used for the laboratory experimental portion of this study. Three different aeration strategies (1) low dissolved oxygen (DO) setpoint, (2) high DO setpoint, and (3) low DO setpoint with residual ammonium control (RAC) were tested, and the aerobic GSR performance was characterized. The result show that it is possible to develop stable granules with aerobic GSR using a low strength wastewater. Of the three tested aeration controls, we found that using a low DO setpoint with RAC gives better partial nitritation and effective suppression of undesired microbial activity by NOB. However, overall N removal was limited to 60%, indicating a need to further optimize the process.

To assess long term process stability and improve overall N removal, an investigation into an improved SMC scheme was conduct over 650 days. For this, we used intermittent aeration with variable aerobic and anaerobic durations on top of the existing DO setpoint and RAC to allow each reaction cycle to further adapt to the dynamics of the reactor. In addition, the long-term experiment was done under varying organic loading rates (OLRs) to investigate its impact on granulation. Our results show that OLR has a strong effect on granule development and that stable granules can be formed at a minimum OLR of 0.2 kg-COD/m^3/day, consistent with the previous experiment. In terms of N removal, the improved SMC scheme resulted in a higher efficiency up to 90%, which was also stable over a long period of operation (100 days).

To understand the performance of the system under varying organic carbon and ammonium loading conditions, representative of a range of A-stage technology options, a simulation-based investigation was done. We developed a 1-D biofilm model representing the lab-scale reactor with the same operation practices and SMC. Several influent compositions and operational settings were evaluated. The results from the model reveal that the developed SMC increased the robustness of the system by allowing the handling of different substrate loads and effectively removed N up to 94% percent. This is a promising finding suggests that a B-stage aerobic GSR can handle different loading conditions effectively without compromising N removal capacity. Overall, the results in this dissertation highlight the importance of using a robust real-time control scheme to advance the potential application of aerobic GSR with PN/A as a mainstream N removal system. In addition, this study improves our understanding of the aerobic GSR reactor technology.

Chapter 1

Introduction

1.1 Background

Wastewater treatment plants are crucial for the protection of the environment and a healthy water cycle. Moreover, recovering water, energy, and resources from wastewater is gaining momentum as a result of our increased focus on sustainable practices and revolutionary innovative designs in the wastewater treatment industry. Managing wastewater in a sustainable manner have a broader impact, including enhanced public health; improved water security; improved environmental quality; societal benefits; and economic benefits. Although, conventional wastewater treatment technologies, such as conventional activated sludge (CAS), has supported the majority of high income country (HIC) urban populations over the last 50 years, there is ample room for improvement if cost-effective and energy-efficient nutrient management is to be realized. For example, in the USA it is estimated that 3-4% of a city's electricity demand is for wastewater collection and treatment (Gude, 2015), and up to 50-60% of the energy demand associated with CAS treatment plants is due to aeration (Bellucci et al., 2011; Mccarty et al., 2011). Furthermore, managing the excess sludge generated incurs extra expense, and energy recovery efficiency from CAS sludge is limited to 50-60% of the total energy expense (Shi, 2011). In addition, some wastewater treatment technologies cannot meet new and increasingly stringent effluent standards that exist in parts of the U.S. and the world (Freed, 2007; Hendriks & Langeveld, 2017). Hence, further research and innovations are needed to achieve the desired sustainability goals.

To improve upon the sustainability of wastewater treatment technologies, several advances are under development that reduce both energy and resource requirements while meeting more stringent effluent standards and resource recovery requirements. One approach includes moving from a single-sludge system to multistage treatment systems that, once coupled, offer an opportunity to optimize distinct treatment goals per stage and enhance resource recovery and energy reduction. Use of novel biological processes and advanced sensor-based technologies offer an innovative approach to achieve these sustainable, multistage water systems. This dissertation focuses on expanding our understanding of a particular component of a sustainable, multistage water system for municipal applications.

One multistage water system strategy that has been advocated for because of its potential to recover energy and resources is the A-B (adsorption-biooxidation) treatment system (Jetten et al., 1997; Rodriguez-Sanchez et al., 2016; Versprille et al., 1985). The A-B process call for separate units and processes to achieve carbon capture for energy recovery in the A-stage, and minimize carbon and energy requirements for nitrogen and phosphorus removal and recovery in the B-stage. The most common A-stage technologies include: high rate activated sludge (HRAS), chemically enhanced primary treatment (CEPT), and anaerobic mainstream treatment such as anaerobic membrane biofilm reactors (AnMBRs). The B-stage takes the effluent from the A-stage process and treats it further for nitrogen and phosphorus removal or recovery. Some of the main technologies that are proposed for use in B-stage processes are moving bed biofilm reactors (MBBRs) (Odegaard, 2006), membrane aerated biofilm reactors (MABRs) (Martin & Nerenberg, 2012) and granular sludge reactors (GSRs) (Zhang et al., 2016).

More recently, two-step biological nitrogen removal processes such as short-cut nitrogen removal and deammonification processes are seen as game-changers for B-stage processes. These two-step nitrogen removal processes are biologically efficient and cost effective compared to the traditional nitrification/denitrification processes. For instance, deammonification, also known as the partial nitritation-anammox (PN/A) process where approximately half the ammonia is

oxidized to nitrite and then removed by anaerobic nitrogen removal via anammox (Wett, 2007), has proven to be efficient in sidestream configurations by reducing aeration energy, external carbon, alkalinity demands, and excess sludge (Lackner et al., 2014). The development of these technologies is deemed worthwhile; for instance, according to McCarty (2018), mainstream anammox systems can be sustainable solutions that save energy by reducing aeration energy demand and produce fewer biosolids compared to traditional nitrification/denitrification systems.

Two-step nitrogen removal, such as PN/A, can happen simultaneously in a single biofilm reactor such as a membrane aerated biofilm reactor (MABR) and aerobic granular sludge reactor (GSR) (Lackner et al., 2014). For systems that require external carbon as electron donor, theoretically, these processes can reduce organic carbon requirements by 40%, aeration energy by 25% and sludge production by 40% (Cao et al., 2017; Gilbert et al., 2015; Ma et al., 2015; Regmi et al., 2015). Despite these advantages, PN/A , has not yet been successfully implemented in mainstream setups other than in lab and pilot scale installations (Agrawal et al., 2018; Lotti et al., 2015; McCarty, 2018). This is due to that fact that the dilute characteristics of mainstream wastewater are not as readily suitable for direct application of PN/A as they are for sidestream systems.

In addition to adopting novel biological processes, more economical reactor configurations are desirable to the overall sustainability of water resource recovery facilities. As an example, the development of the aerobic GSR is a major advancement in wastewater treatment technology. Aerobic GSR offer a unique set of advantages compared to conventional activated sludge reactors, including: smaller footprint, lower operational costs, and avoidance of settleability issues (Nancharaiah & Sarvajith, 2019). Furthermore, aerobic granules host a consortium of microbial communities in different redox biofilm layers. As a result, simultaneous substrate removal can occur on an individual granule. Hence, these unique attributes of the aerobic GSR

technology make it an ideal B-stage technology for nitrogen removal using simultaneous PN/A and denitrification (SNAD).

To successfully use aerobic GSR for SNAD as mainstream B-stage nitrogen removal technologies, several bottlenecks must be overcome: (i) developing aerobic granules, (ii) sustaining granules over long periods of time in systems receiving dynamic inputs (Tay et al., 2004), and; (iii) properly channeling aeration and substates to the desired microbial processes while avoiding competition by others (Cao et al., 2017). Progress on approaches that develop and sustain granules for B-stage SNAD systems has been slow; hence detailed theoretical and experimental investigations must be carried out to understand and implement reactor operational strategies that support both. The second challenge is related to the PN/A process where co-existing microbial communities compete for the same resources. For example, nitrite oxidizing bacteria (NOB) and anammox (AMX) both compete for nitrite, and ordinary heterotrophic organisms (OHO) and ammonium oxidizing bacteria (AOB) compete for oxygen. Therefore, on/off aeration strategies based on real-time sensor-mediated control (SMC) are needed if granular SNAD technologies are to be scalable. SMC allows for robust control over aeration to supply only the minimum aeration needed to derive the bio-oxidation of nitrogen via desired metabolic pathways. For example, applying ammonia-based aeration control dictates that a minimum residual ammonia concentration be maintained to promote partial nitritation of ammonium to nitrite followed by anammox-based nitrogen removal while suppressing NOB.

Overall, integrating engineering advancements with novel microbial processes is key for the successful implementation of AGS with SNAD with mainstream wastewater treatment. Additional research is needed to understand the underlying processes and develop actionable insights. To make progress, experimental and modelling research are needed to identify gaps and overcome bottlenecks that will lead to scalable solutions that include SNAD in granular systems.

1.2. Overview of Dissertation

The objective of the research described in this dissertation was to investigate developmental elements for aerobic GSR with SNAD with a specific emphasis on how to optimize SMC-based aeration to meet multiple treatment goals. Both experimental and modeling approaches are used to elucidate the governing processes and mechanisms that lead to successful SNAD in aerobic GSR for dilute mainstream wastewater. The work is completed in the context of a B-stage system that receives effluent from an A-stage process (e.g., HRAS, CEPT or AnMBR). Chapter 2 provides background information based on: (i) the development of aerobic GSR and mainstream PN/A processes; (ii) the application of real-time sensor mediated control to maximize N removal; and (iii) strategies for aerobic GSR modeling and simulation. Chapter 3 reports on a laboratory SNAD system that receives simulated AnMBR A-stage effluent as its feed. The study evaluated the impact of the first-generation SMC on granulation, NOB suppression, total inorganic nitrogen removal, anammox retention, and extent of aeration. The study showed that it was possible to achieve granulation and sufficient partial nitritation while suppressing NOB using a very low strength wastewater with an organic loading rate of 0.2 kg-COD/m^3/d (Bekele et al., 2020). Even though, it was possible to maintain anammox activity and biomass throughout the experiment, total inorganic nitrogen removal was not very high (57 ± 3%). We concluded that further research is needed to optimize aeration and achieve a higher degree of N removal, presumably by increasing anammox retention capacity. Thus, in Chapter 4 we evaluated a lab scale reactor coupled with a second-generation SMC that was used to calibrate a simulation model. Our overall goal was to create a revised granulation process and SMC approach that can further improve N removal capacity. The findings from this study indicate that it is possible to improve N removal in SNAD systems by using adaptive intermittent aeration control and longer anaerobic duration that allows granules to retain a higher anammox population. In addition, the revised operational strategy resulted in smaller granules (diameter = 0.4 mm) compared to the previous experiment where granules had an average granule diameter of 1 mm. Furthermore, the data from the second study was used to calibrate a simulation model that can predict performance of the laboratory GSR. Finally, to further investigate the feasibility of the results

obtained in Chapters 3 and 4, we used simulation to investigate how different influent (A-stage effluent) conditions may influence SNAD performance.

The final chapter highlights the key findings of the dissertation and its significance for future adoption of mainstream SNAD using aerobic GSR. It also highlights additional research questions that need to be addressed through future studies. Overall, this dissertation contributes new, mechanistic understanding to the ongoing body of work that is striving to move wastewater treatment facilities towards energy reduction and resource efficiency.

1.3. References

Agrawal, S., Seuntjens, D., Cocker, P. De, Lackner, S., & Vlaeminck, S. E. (2018). Success of mainstream partial nitritation/anammox demands integration of engineering, microbiome and modeling insights. In *Current Opinion in Biotechnology* (Vol. 50, pp. 214–221). Elsevier Current Trends. https://doi.org/10.1016/j.copbio.2018.01.013

Bekele, Z. A., Delgado Vela, J., Bott, C. B., & Love, N. G. (2020). Sensor-mediated granular sludge reactor for nitrogen removal and reduced aeration demand using a dilute wastewater. *Water Environment Research*, 1–11. https://doi.org/10.1002/wer.1296

Bellucci, M., Ofiteru, I. D., Graham, D. W., Head, I. M., & Curtis, T. P. (2011). Low-dissolved-oxygen nitrifying systems exploit ammonia-oxidizing bacteria with unusually high yields. *Applied and Environmental Microbiology*, *77*(21), 7787–7796. https://doi.org/10.1128/AEM.00330-11

Cao, Y., van Loosdrecht, M. C. M., & Daigger, G. T. (2017). Mainstream partial nitritation–anammox in municipal wastewater treatment: status, bottlenecks, and further studies. *Applied Microbiology and Biotechnology*, *101*(4), 1365–1383. https://doi.org/10.1007/s00253-016-8058-7

Freed, T. (2007). Wastewater Industry Moving Toward Enhanced Nutrient Removal Standards - WaterWorld. *WaterWorld*, *23*(3). http://www.waterworld.com/articles/print/volume-23/issue-3/editorial-feature/wastewater-industry-moving-toward-enhanced-nutrient-removal-standards.html

Gilbert, E. M., Agrawal, S., Schwartz, T., Horn, H., & Lackner, S. (2015). Comparing different reactor configurations for Partial Nitritation/Anammox at low temperatures. *Water Research*, *81*, 92–100. https://doi.org/10.1016/j.watres.2015.05.022

Gude, V. G. (2015). Energy and water autarky of wastewater treatment and power generation systems. In *Renewable and Sustainable Energy Reviews* (Vol. 45, pp. 52–68). Elsevier Ltd. https://doi.org/10.1016/j.rser.2015.01.055

Hendriks, A. T. W. M., & Langeveld, J. G. (2017). Rethinking Wastewater Treatment Plant Effluent Standards: Nutrient Reduction or Nutrient Control? *Environmental Science & Technology*, *51*, 4735–4737. https://doi.org/10.1021/acs.est.7b01186

Jetten, M. S. M., Horn, S. J., & van Loosdrecht, M. C. M. (1997). Towards a more sustainable municipal wastewater treatment system. *Water Science and Technology*, *35*(9). http://wst.iwaponline.com/content/35/9/171

Lackner, S., Gilbert, E. M., Vlaeminck, S. E., Joss, A., Horn, H., & van Loosdrecht, M. C. M. (2014). Full-scale partial nitritation/anammox experiences – An application survey. *Water Research*, *55*, 292–303. https://doi.org/10.1016/J.WATRES.2014.02.032

Lotti, T., Kleerebezem, R., Hu, Z., Kartal, B., De Kreuk, M. K., Van Erp Taalman Kip, C., Kruit, J., Hendrickx, T. L. G., & Van Loosdrecht, M. C. M. (2015). Pilot-scale evaluation of anammox-based mainstream nitrogen removal from municipal wastewater. *Environmental Technology (United Kingdom)*, *36*(9), 1167–1177. https://doi.org/10.1080/09593330.2014.982722

Ma, B., Bao, P., Wei, Y., Zhu, G., Yuan, Z., & Peng, Y. (2015). Suppressing Nitrite-oxidizing Bacteria Growth to Achieve Nitrogen Removal from Domestic Wastewater via Anammox Using Intermittent Aeration with Low Dissolved Oxygen. *Scientific Reports*, *5*(April), 13048. https://doi.org/10.1038/srep13048

Martin, K. J., & Nerenberg, R. (2012). The membrane biofilm reactor (MBfR) for water and wastewater treatment: Principles, applications, and recent developments. *Bioresource Technology*, *122*, 83–94. https://doi.org/10.1016/J.BIORTECH.2012.02.110

McCarty, P. L. (2018). What is the Best Biological Process for Nitrogen Removal: When and Why? *Environmental Science and Technology*, *52*(7), 3835–3841. https://doi.org/10.1021/acs.est.7b05832

Mccarty, P. L., Bae, J., & Kim, J. (2011). Domestic Wastewater Treatment as a Net Energy Producer: Can This be Achieved? *Environ. Sci. Technol*, *45*, 7100–7106. https://doi.org/10.1021/es2014264

Nancharaiah, Y. V., & Sarvajith, M. (2019). Aerobic granular sludge process: a fast growing biological treatment for sustainable wastewater treatment. In *Current Opinion in Environmental Science and Health* (Vol. 12, pp. 57–65). Elsevier B.V. https://doi.org/10.1016/j.coesh.2019.09.011

Odegaard, H. (2006). Innovations in wastewater treatment: -the moving bed biofilm process. *Water Science and Technology*, *53*(9), 17–33. https://doi.org/10.2166/wst.2006.284

Regmi, P., Holgate, B., Miller, M. W., Park, H., Chandran, K., Wett, B., Murthy, S., & Bott, C. B. (2015). Nitrogen polishing in a fully anoxic anammox MBBR treating mainstream nitritation-denitritation effluent. *Biotechnology and Bioengineering*, n/a-n/a. https://doi.org/10.1002/bit.25826

Rodriguez-Sanchez, A., Purswani, J., Lotti, T., Maza-Marquez, P., van Loosdrecht, M. C. M., Vahala, R., & Gonzalez-Martinez, A. (2016). Distribution and microbial community

structure analysis of a single-stage partial nitritation/anammox granular sludge bioreactor operating at low temperature. *Environmental Technology*, *3330*(June), 1–36. https://doi.org/10.1080/09593330.2016.1147613

Shi, C. Y. (2011). Mass Flow and Energy Efficiency of Municipal Wastewater Treatment Plants. *Water Intelligence Online*, *10*, 9781780400907. https://doi.org/10.2166/9781780400907

Tay, J. H., Pan, S., He, Y., & Tay, S. T. L. (2004). Effect of organic loading rate on aerobic granulation. I: Reactor performance. *Journal of Environmental Engineering*, *130*(10), 1094–1101. https://doi.org/10.1061/(ASCE)0733-9372(2004)130:10(1094)

Versprille, A. I., Zuurveen, B., & Stein, T. (1985). THE A-B PROCESS: A NOVEL TWO STAGE WASTEWATER TREATMENT SYSTEM. *Wat. Sci. Tech*, *17*, 235–246. http://wst.iwaponline.com/content/ppiwawst/17/2-3/235.full.pdf

Wett, B. (2007). Development and implementation of a robust deammonification process. *Water Science & Technology*, *56*(7), 81–88. https://doi.org/10.2166/wst.2007.611

Zhang, Q., Hu, J., & Lee, D.-J. (2016). Aerobic granular processes: Current research trends. *Bioresource Technology*, *210*, 74–80. https://doi.org/10.1016/j.biortech.2016.01.098

Chapter 2

Background

2.1. Introduction

Current water scarcity around the globe and the need to further protect receiving water bodies motivates stricter effluent quality requirements that demand higher levels of treatment at wastewater treatment facilities. Many innovative approaches have been proposed to address these needs, but those that can achieve economic and environmental sustainability (e.g., reduced greenhouse gas emissions, reasonable life cycle costs) are most likely to be viewed both as being responsive to the needs and scalable. This dissertation attempts to address an innovative technology focused on biological nitrogen removal (BNiR) that is both responsive and scalable.

The water industry has substantial experience in designing and operating conventional, single-sludge BNiR processes, where carbon, nitrogen and phosphorus are all degraded or sequestered biological with a single mixed liquor that sequences between aerobic, anaerobic and anoxic zones. BNiR, specifically, involves multiple microbially-mediate metabolic processes (Figure 2.1). The first metabolic process to achieve BNiR is complete nitrification, which is the aerobic oxidation of total ammonium-nitrogen (NH_4^+ and NH_3) to nitrate in a two-step microbial process. The first step in complete nitrification is performed by ammonium-oxidizing bacteria (AOB) that convert ammonia (NH_3 plus the NH_4^+ converted to NH_3) to nitrite. The second step involves further oxidation of the nitrite to nitrate by nitrite oxidizing bacteria (NOB).

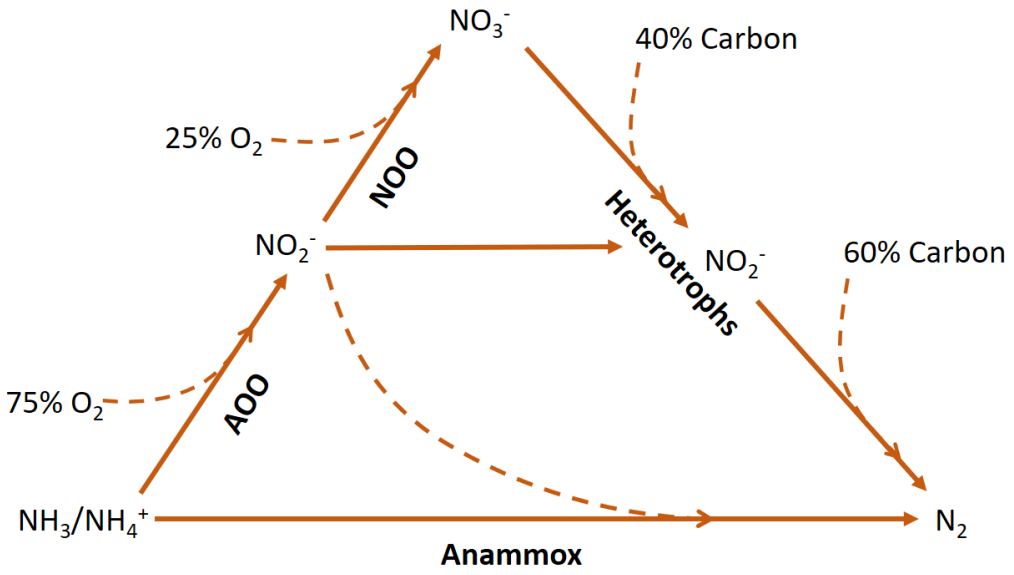

Figure 2.1. Steps involved in biological nitrogen removal, which is in the form of ammonia/ammonium getting converted to nitrogen gas.

Nitrification requires a substantial amount of oxygen, with 4.6 g O_2 demand per g of ammonia-N fully nitrified. This oxygen demand is distributed between AOB- and NOB-mediated steps, with 75% going for conversion of ammonia to nitrite and 25% used for conversion of nitrite to nitrate. Both nitrification steps produce oxidized inorganic nitrogen forms (NO_2^-, NO_3^-) that can serve as electron acceptors for denitrification by ordinary heterotrophic organisms (OHOs), many strains of which can convert these nitrogen compounds to dinitrogen gas (Leslie et al., 2011). However, there are different functional groups that categorize denitrification, including: complete denitrification to N_2 starting with nitrate, or partial denitrification from nitrate to nitrite, or nitrite to N_2. (cite). Furthermore, most single-sludge BNiR treatment configurations require recirculation of nitrate-rich mixed liquor to anoxic zones that support OHO denitrification via nitrate. Doing so eliminates the need to provide aeration for a portion of the carbon treatment. While this reduces the aeration demand relative to that demanded for conventional activated sludge systems that only perform aerobic carbon and ammonia conversion, recirculation incurs increased energy demands due to pumping that can eliminate the gains realized due to reduced

aeration for carbon oxidation.. Some BNiR systems that need to achieve very low concentrations of total nitrogen also require an additional electron donor for denitrification, typically provided as an organic carbon source. In addition, all conventional BNiR systems produce a significant amount of sludge that needs to be managed. Thus, while conventional single-sludge BNiR systems have been successful at accomplishing nitrogen removal goals across a range of technologies, many improvements are required to achieve greater energy efficiency and overcome the mentioned shortcomings while accomplishing nitrogen removal from wastewater streams.

Biological nutrient removal (BNuR) technologies have been broadly applied in nutrient sensitive areas of the world; however, these technologies need to be more sustainable and energy efficient (McCarty, 2018). Many BNuR technologies that have been deployed full-scale use a "single sludge" approach where carbon, nitrogen and phosphorus are all degraded or sequestered biological with a single mixed liquor that sequences between aerobic, anaerobic, and anoxic zones. Although these systems met the need for the initial generation of BNuR technologies, the systems are energetically costly (Svardal & Kroiss, 2011). Over the last decade, there has been a research emphasis on separating carbon management (A-stage) from nitrogen (B-stage) and phosphorus management in multi-stage systems (Liu et al., 2020; Wan et al., 2016; Wett et al., 2007). Innovation around each stage has been occurring separately. This dissertation is focused on innovative developments around a B-stage technology that uses operational and automation adjustments to achieve energy efficiency and scalability. The rest of this Background Chapter covers the state of knowledge for BNiR processes and, specifically, the application of B-stage BNiR systems coupled with three types of A-stage carbon removal and capture processes: specifically, anaerobic membrane bioreactors (AnMBR); chemically-enhanced primary treatment (CEPT); and high rate activated sludge (HRAS). Of the three A-stage processes evaluated, anaerobic processes (such as AnMBR) produce the most complex effluent characteristics to achieve BNR with. Hence, as a proof of concept, the experimental work of the dissertation

focuses on nitrogen removal from a simulated AnMBR effluent (Chapters 3 and 4). Since the effluent from the different A-stage processes share similar characteristics with AnMBR effluents, such as low soluble COD and similar ammonium content, much of the applications discussed for anaerobic A-stage effluent are applicable for the other A-stage processes. A comparison of all three types of A-stage systems are further investigated in Chapter 5 through modeling and simulation. Consequently, this chapter provides a review of: what is known about BNiR from effluents treated through the three kinds of A-stage systems noted; microbial processes relevant to low carbon BNiR systems; the granular sludge bioreactor technology; modeling and simulation approaches; and sensor-mediated control strategies to enhance the performance of BNiR.

2.2. Nitrogen removal from anaerobic effluents

Conventional single-sludge BNR has been used to treat effluents from A-stage municipal wastewater systems, but it is not well suited in all cases. For example, anaerobic mainstream A-stage processes that are focused on carbon removal creates an effluent that contains methane and sulfide, slightly higher concentrations of ammonia and organic nitrogen relative to untreated domestic wastewater, and low amounts of readily biodegradable, soluble COD (Delgado Vela et al., 2015). Using conventional BNR to treat such kind of wastewater would require multistep processes or units as they lack a significant potential to support simultaneous processes. Hence, they are less resource efficient and require larger footprint. Consequently, alternative nitrogen removal technologies that employ novel metabolisms, such as completely autotrophic processes, and advanced process engineering are worthy of consideration.

Autotrophic BNiR processes can substantially reduce aeration, the demand for exogenous electron donor, and the mass of sludge that needs to be managed (Jetten et al., 2005; Kartal et al., 2010; Lotti et al., 2015; Morales et al., 2015; M.-K.H. Winkler et al., 2012). One such group of microorganisms are the **an**aerobic **amm**onia **ox**idizers (**anammox**) that are classified under the

phylum Planctomacetes (Jetten et al., 2005). They are capable of converting ammonia to dinitrogen gas under anoxic conditions using nitrite as electron acceptor (see equation 1, van de Graaf et al., 1996). This metabolic pathway, shown in Figure 1, requires 25% less oxygen, no organic carbon to support denitrification and produces about 80% less sludge compared to the heterotrophic denitrification processes. Given the broad range of benefits associated with autotrophic denitrification processes such as anammox, attention has shifted towards finding ways to apply it for mainstream BNiR.

$$1NH_4^+ + 1.31NO_2^- + 0.0425CO_2 \rightarrow 1.045N_2 + 0.22NO_3^- + 1.87H_2O + 0.09OH^- + 0.0425CH_2O \quad \text{(eq. 2.1)}$$

Although not fully addressed in this dissertation, denitrifying anaerobic methane oxidizers (DAMO) are another recently discovered group of microorganisms that are capable of autotrophic denitrification. DAMO can use dissolved methane from anaerobic effluents as a carbon and electron source coupled with nitrite or nitrate as electron acceptors to produce dinitrogen gas (see eq. 2.1) (Raghoebarsing et al., 2006). The DAMO groups include bacteria classified as NC10 and archaea related to **AN**aerobic **ME**thanotrophs (ANME-2d) (Ettwig et al., 2010; He et al., 2013). Ettwig et al. (2010) identified the bacteria that are responsible for nitrite-based anaerobic oxidation of methane (AOM) as *Candidatus* Methylomirabilis oxyfera. They showed that this group of bacteria were capable of reducing nitrite to dinitrogen (N_2) and diatomic oxygen (O_2), and using the O_2 to oxidize methane via an intra-aerobic pathway. Later, novel Archaea that are capable of ammonium oxidation by using nitrate as their electron acceptor via reverse methanogenesis were discovered by Haroon et al. (2013). They named this ANME-2d lineage *Candidatus* Methanoperedens nitroreducens. Researchers (Haroon et al., 2013; Raghoebarsing et al., 2006) have also shown that both types of AOM can co-exist in a single system, depending upon the type of substrate available. Since the first step in nitrogen removal involves aeration to convert some of the ammonium to nitrite, the dissolved methane can be

stripped out, resulting in greenhouse gas emission. To avoid this, reactors must be designed and operated in a way that allows oxidation to occur while eliminating or minimizing methane emissions and facilitating the use of methane by DAMO. The discovery of DAMO provides a possible solution that avoids the need for an external carbon source and reduces greenhouse gas emissions while contributing to the overall goal of BNiR.

Nitrite reduction to N_2 by DAMO bacteria (*M. oxyfera*) (Ettwig et al., 2010):

$$3NO_2^- + 8CH_4 + 8H^+ = 4N_2 + 3CO_2 + 10H_2O \ (\Delta G^0 = -928\ kJ^{-1}CH_4) \qquad \text{(eq. 2.2)}$$

Nitrate reduction to nitrite by DAMO archaea (*M. nitroreducens*) (Haroon et al., 2013):

$$4NO_3^- + CH_4 = 4NO_2^- + CO_2 + 2H_2O \ (\Delta G^0 = -503\ kJ^{-1}CH_4) \qquad \text{(eq. 2.3)}$$

Sulfide is another constituent commonly found in anaerobic effluents that is a potential electron donor that can drive autotrophic denitrification. Sulfide concentrations in anaerobic A-stage effluents vary depending on the source and treatment method used for drinking water (i.e., sulfate-based coagulant salts can increase sulfur concentrations in sewage), or the composition of industrial facilities that discharge into the sewer. Sulfide is toxic, corrosive and malodorous; therefore, appropriate treatment is needed to protect the environment (Anette Æsøy et al., 1998). Sulfide-based autotrophic denitrification can occur by using nitrite or nitrate as electron acceptor in wastewater bioreactors (Baldensperger and Garcia, 1975; Cardoso et al., 2006; Claus and Kutzner, 1985; Foresti et al., 2006; Gommers et al., 1988; Souza and Foresti, 2013). The best studied bacteria responsible for chemoautotrophic denitrification using reduced sulfide or thiosulfate are *Thiobacillus denitrificans* and *Sulfurimonas denitrificans* (Shao et al., 2010a). The presence of elevated sulfide is also known to have an inhibitory effect on nitrifiers (Anette Æsøy et al., 1998; Delgado Vela et al., 2018; Joye & Hollibaugh, 1995), anammox (Dapena-Mora et al.,

2007; Jin et al., 2012, 2013) and heterotrophic denitrifiers (Roger, 1982; S0rensen et al., 1980). Therefore, both the benefits and impact of sulfide on nitrogen removal will be very important to pursue for future studies.

The ultimate challenge in treating a wastewater for nitrogen removal that contains conventional (organic carbon) and multiple alternative (ammonium, methane, sulfide) electron donors is finding bioreactor operating conditions that can support multiple metabolisms while ensuring the available electron donors and acceptors are properly utilized. When we have multiple microbial groups capable of competing metabolisms and multiple substrates in a single reactor, the most competitive and synergetic groups are expected to prevail depending of the reactor type and how it is operated. Therefore, to have better control of the competition among organisms and to manage substrate fluxes, a major hypothesis of this dissertation states that SMC will offer a means to overcome these challenges.

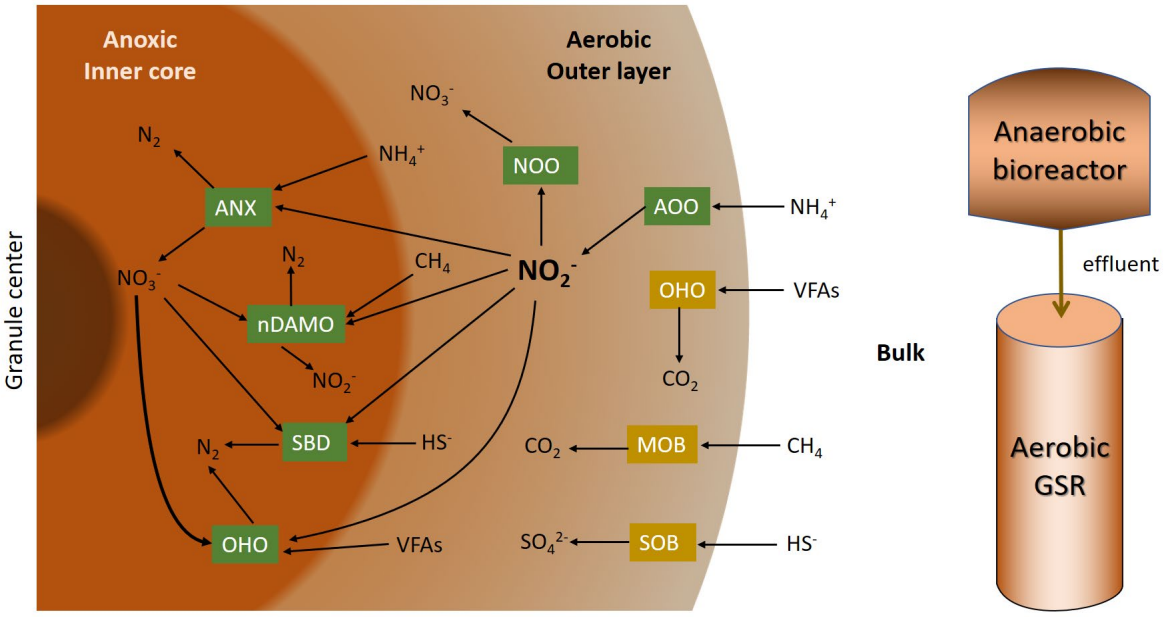

Figure 2.2. Potential metabolic pathways for removal of ammonia, VFA, methane, and sulfide present in mainstream anaerobically treated A-stage effluent fed to an aerobic granular sludge process, an example B-stage technology.

Figure 2.2 shows schematically what may happen in a B-stage system designed for NBiR that receives anaerobically-treated A-stage effluent. It shows all the possible microbial agents and how they might be spatially positioned in a granule from a granular sludge reactor, for example. It is unlikely that all would co-exist as shown in the schematic, which is intended to just show what is possible. More work is needed to delineate exactly how these microbial groups might assemble, depending upon operating conditions, reactor configuration, start-up protocol, and control strategies used.

2.3. Nitrogen removal from A-stage HRAS process effluent

One type of A-stage process in the A-B process paradigm is the high-rate activated sludge (HRAS) process for carbon adsorption and capture. The HRAS was developed with the aim of redirecting organic carbon for later energy conversion to biogas in an anaerobic digester. To maximize carbon capture, HRAS is operated with a high food-to-microorganism ratio and low solids retention time (SRT) with short hydraulic residence time (HRT). With this approach, HRAS can remove 50-70 % of total COD with relatively little aeration input. Since the SRT is short (less than 3 days), nitrification in this system is minimal or prevented. Thus, the effluent from HRAS systems contain low concentrations of soluble COD and most of the influent ammonia remains unconverted.

In order to meet effluent standards in regions with nitrogen removal limits, the A-stage HRAS process must be followed with a B-stage BNiR step. If nitrite-based autotrophic N removal is desired in the B-stage, it is necessary to target an appropriate COD:N ratio entering the B-stage. This ratio defines the competition between heterotrophic bacteria and autotrophs like nitrifiers and anammox and will vary depending upon the B-stage technology used. Given the aerobic nature of the effluent from an A-stage HRAS, the primary metabolic options for N removal include partial nitritation plus anammox (PN/A) and heterotrophic denitrification via either nitrite or nitrate. Focusing on heterotrophic denitrification using internal organic carbon as the

primary means to achieve N removal regulations requires a COD:N ratio around 5 so that the COD is available in excess. This is often hard to do after a COD reducing A-stage, and it would require use of an exogenous electron donor. Alternatively, targeting PN/A in the B-stage allows for autotrophic nitrogen removal and reduces the need for an exogenous electron donor. Furthermore, because the A-stage HRAS does not remove all organic carbon, some aerobic and anoxic organic carbon oxidation will occur. All these factors must be taken into consideration when selecting a B-stage technology.

2.4. Nitrogen removal from A-stage CEPT process effluent

Chemically enhanced primary treatment (CEPT) is an older advanced primary treatment method that is seeing renewed interest today. It is used to improve the performance of primary clarifiers for wastewater treatment, and to capture more organic matter as part of a resource recovery strategy than would be accomplished with a conventional primary clarifier. This technology uses coagulants to improve the settleability of particulate and colloidal matter. Therefore, CEPT removes mainly particulate and colloidal COD, leaving the soluble COD for secondary treatment. In addition, some nitrogen removal occurs due to nitrogen contained in suspended solids and colloids, but it is not highly efficient. If one considers CEPT an A-stage process, its effluent will contain mainly soluble COD and ammonia that could be well suited for a granular sludge B-stage system reliant upon a high enough COD:N ratio to support multi-redox granule formation. Depending upon the COD:N ratio of the CEPT effluent, nitritation and heterotrophic denitritation with or without anammox can be applied to remove nitrogen. If the COD:N ratio is less than 2 or if we are interested in minimizing aeration demand in general, integrating partial-nitritation plus anammox will be an ideal strategy.

2.5. Mainstream Partial Nitritation/Anammox (PN/A) Process.

Partial nitritation/anammox (PN/A) process has become the most important BNiR process in the last two decades since its discovery because it accomplishes multiple goals within the wastewater

sustainability paradigm (Agrawal et al., 2018). It is a completely autotrophic nitrogen removal process, which means no organic carbon is needed. In addition, it has a lower aeration requirement than other BNiR processes. For these reasons, PN/A is well suited to couple with effluents generated from A-stage systems that practice carbon capture. To date, the success of PN/A full-scale processes is mainly associated with environments where AOB and anammox organisms readily outcompete NOB and OHOs, such as in sidestream configurations (Nsenga Kumwimba et al., 2020).

Successful partial nitritation (oxidation of about half the ammonium to nitrite) is a key first step in PN/A systems. The nitrite produced can then be used by multiple microbial groups, including OHOs, DAMO bacteria, NOB, SBDs and anammox (see Figure 2.2 as an example). Of these microbial groups, uptake of nitrite by NOB is undesirable because it eliminates the opportunity to support nitrite-driven denitritation metabolic processes. For example, a high level of NOB activity means more oxygen consumption and lower N removal via the other metabolic pathways, including PN/A. Nitrate buildup because of high NOB activity will mainly support OHO-based denitrification, which works if sufficient organic carbon is available; however, often this is not the case, especially in dilute mainstream wastewater. Furthermore, excess nitrate will not be completely reduced by DAMO using methane, which reduces nitrate to nitrite, not to N_2 (Haroon et al., 2013). It will also limit any opportunity present for sulfide-driven N-removal, which favors nitrite as an electron acceptor over nitrate. Thus, creating an operating condition that promotes partial nitritation while suppressing NOB activity is critical if autotrophic BNiR removal is to be achieved in dilute mainstream conditions.

To achieve partial nitritation while suppressing NOB, different approaches have been shown to work effectively in sidestream systems that contain high concentrations of ammonium (>10x relative to mainstream systems). The approaches include inhibition of NOB by free ammonia (FA) (Philips et al., 2002), free nitrous acid (FNA), low SRT (Regmi et al., 2014) and high temperature (Kornaros et al., 2010; Poot et al., 2016; Cao et al., 2017). However, mainstream

effluents treated first in an A-stage system are dilute and have relatively low temperatures during the coldest months. Due to these conditions, suppressing NOB is challenging in a mainstream system.

Thus, to successfully implement PN/A under mainstream conditions, some operational strategies must be implemented to suppress NOB activity while maintaining a relatively higher AOB and anammox activity. To be successful, it is necessary to maintain some residual ammonium throughout the operating cycle since ammonium supports both AOB and anammox. That is, since ammonium is the electron donor for anammox, maintaining an ammonium residual allows anammox to compete. This technique has been shown to be successful for achieving mainstream NOB suppression (Kornaros et al., 2010; Regmi et al., 2014). Other techniques that have been used to suppress NOB activity relative to AOB in both sidestream and mainstream include manipulating DO setpoint and the use of intermittent aeration. The latter strategy is referred to as transient anoxia (Pollice et al., 2002).

The success of using a DO setpoint depends upon the genera and species of NOB and AOB present in the system. As such, their response to DO level will vary depending on their DO affinity difference. For example, the ammonia-oxidizer *Nitrosomonas* has a higher DO affinity than nitrite-oxidizing *Nitrospira* (Poot et al., 2016), which means operating at a lower DO will favor nitritation and suppress NOB. Furthermore, the affinity coefficients will depend on temperature; as a result, it will also have an impact on which species of AOB and NOB will be most active. For example, *Nitrosomonas* have a higher maximum growth rate (μ_{max}) than *Nitrospira* at low temperature, which is common during many months of the year in mainstream systems (Cao et. al., 2017). Together, this means *Nitrosomonas* will grow faster under low temperature and ammonia-sufficient conditions. Thus, the choice of the DO setpoint must consider the type of nitrifier species present in the sludge.

Transient anoxia is created using intermittent aeration (on/off aeration) and it has been used to support faster AOB growth relative to NOB. The differential growth achieved with transient anoxia is believed to occur because it has been shown that NOB growth lags behind AOB growth when transitioning from anoxic to aerobic environments (Kornaros et al., 2010; Ma et al., 2015b). Furthermore, intermittent aeration creates an opportunity for anoxic growth and reduced aeration costs. Therefore, incorporating transient anoxia requires a dynamic or real-time aeration control strategy. The use of intermittent aeration is one of the key techniques for successful implementation of PN/A in mainstream BNiR.

2.6. Aerobic Granular Sludge Technology

2.6.1. **Technology Background**

Aerobic granular sludge reactor (GSR) technology is an advanced wastewater treatment process that is economically competitive when compared to conventional completely mixed activated sludge systems (Merle K. de Kreuk & van Loosdrecht, 2006; Liu & Tay, 2004). Granules are self-immobilized and dense microbial aggregates enmeshed and crosslinked in extracellular polymeric substances (EPS) structure (Adav et al., 2008; Saurabh Jyoti Sarma et al., 2017). They are normally developed in sequencing batch reactors (SBRs) under aerobic conditions by applying shear stress and other selection pressures, such as short settling times and feast-famine phases (Beun et al., 2002; de Kreuk and van Loosdrecht, 2004; Derlon et. al., 2016; Liu et. al., 2015a; Morgenroth et. al., 1997; Winkler et. al., 2011). The granules are microbial aggregates that have an aerobic outer layer, anaerobic middle layer and a core dominated by dead cells (Aqeel et al., 2016). Consequently, the outer layer mainly consists of aerobic microorganisms, and the middle layer mainly consists of facultative and obligate anaerobic microorganisms.

A number of studies have shown that the main factors affecting granule formation are substrate composition, loading rate and operating conditions (de Kreuk and van Loosdrecht, 2004; Li et al.,

2008; Linlin et al., 2005; Liu and Tay, 2002; McSwain et al., 2004; Mosquera-Corral et al., 2005; Qin et al., 2004; Van Der Star et al., 2007; Wang et al., 2007; Yang et al., 2005). The operating conditions that are reported to influence the granulation process are shear stress, settling time, aeration intensity, seed sludge, cycle time, reactor height to diameter ratio, aerobic starvation and volume exchange ratio. Thus, optimizing all or a subset of these operating conditions is key to developing stable granules.

Granules have gained special interest recently due to their competitive advantage over the conventional activated sludge process. One advantage is that granules have layers of redox zones that are capable of supporting simultaneous aerobic and anaerobic biodegradation in a single granule. This is comparable to what is currently accomplished with single sludge aerobic/anoxic systems but avoids the need for multiple reactors (Saurabh Jyoti Sarma et al., 2017). Granules are also dense microbial aggregates that can retain large amounts of biomass, resulting in reduced reactor volumes. They have excellent settling characteristics that eliminate the need for large clarifiers. In addition, due to their compact nature, granules have been shown to be resistant to moderate shock loads up to 15 kg COD/m^3-d and 0.72 kg N/m^3-d (Tay et al., 2004; Thanh et al., 2009; Zhao et al., 2013), toxic chemicals such as phenol up to 2.5 kg/m^3-d, and salinity up to 10 g-NaCl/L (Adav et al., 2010; Jiang et al., 2004; Moussavi et al., 2010; Taheri et al., 2012). Finally, they produce less excess sludge due to low biomass loss (Khan et al., 2013).

Despite its multifaceted advantages, the AGS technology also has major bottlenecks that prevents its wide-spread adoption. The main challenge are slow startup times for granule formation (Pijuan et al., 2011; S J Sarma & Tay, 2018) and long-term stability of granules (Franca et al., 2018; Kang & Yuan, 2017; Lee et al., 2010). The former is especially relevant for low loaded wastewater. For instance, the reported organic loading rate needed in order to form stable granules and retain them for long periods of time is >1 kg COD/m^3-day (Derlon et al., 2016; Tay et al., 2004; Wagner & da Costa, 2013). This organic loading is higher than many domestic wastewaters; therefore, wide-spread implementation of full-scale granular sludge reactors is

limited to treatment plants that receive medium and high organic loads. Overall, the challenges that come about due to slow granule development may be partly attributed to the lack of knowledge about biomolecular mechanisms that drive the granulation process. Hence, understanding the biomolecular mechanism for stable granules remains a potential area of research, especially for low strength wastewaters (Nancharaiah & Kiran Kumar Reddy, 2018).

2.6.2. **Application of GSR as a B-Stage Technology**

Granular sludge reactor (GSR) systems have been applied to treat a variety of wastewaters, such as organic carbon- or nutrient-rich wastewaters from domestic as well as industrial sources (Campo et al., 2017; de Kreuk et al., 2005; Derlon et al., 2016; Liu and Tay, 2007; Liu et al., 2015b; Wang et al., 2007). GSRs have also been used for the removal of toxic substances and emerging contaminants (Balest et al., 2008; Caluwé et al., 2017; He-Long Jiang et al., 2006; Sarma et al., 2016). Furthermore, they have been used to bioaugment conventional activated sludge systems to improve performance and capacity (Figdore et al., 2018). However, there is limited research to expand the application of AGS to low strength wastewater. Overall, these examples illustrate that GSR systems have the potential for a wide range of applications compared to conventional activated sludge systems. In this thesis, we focus on their use as a B-stage technology that receives wastewater with characteristics consistent with three-different A-stage technology options: anaerobic membrane bioreactor, CBET, and HRAS.

First, we consider coupling AnMBR as an A-stage treatment step with aerobic GSR for the B-stage treatment step to accomplish BNiR. The granules of aerobic GSRs have an aerobic outer layer and anoxic/anaerobic inner layer within which multiple microbial groups can be retained and compete simultaneously (see Figure 2-2). In the outer layer of a granule receiving AnMBR effluent, OHOs, MOB, AOB and NOB can compete for oxygen and their respective donors. At the same time, OHOs, DAMO, anammox and SBD can compete in the inner layer for alternative electron acceptors. Our goal is to use nitrite for this role as much as possible to support

autotrophic BNiR as much as possible. However, the exact location and abundance of desired microorganisms depends on how the system is operated from startup up through steady state operation. We assume that the organic carbon present in an AnMBR A-stage effluent will be mostly organic acids and is likely to be used by OHOs both in the aerobic and anaerobic layers. There is also some evidence that certain anammox species can outcompete OHOs to autotrophically oxidize VFAs with nitrate as an electron acceptor, which produces CO_2, ammonium and nitrite as a byproduct (Güven et al., 2005; M.-K.H. Winkler et al., 2012; M. K. H. Winkler et al., 2012). In granular systems, ammonium is mainly used by AOB to convert it to nitrite in the aerobic layer, and anammox can autotrophically oxidize the remaining ammonium with nitrite as an electron acceptor in the anoxic layer. In addition, the nitrite produced can also be oxidized by NOB and converted to nitrate in the aerobic layer. If not stripped completely, methane can be oxidized aerobically by MOB in the aerobic layer and anaerobically by DAMO bacteria and archaea using nitrite and nitrate as electron acceptors, respectively. Sulfide can also be used for autotrophic denitrification using nitrate or nitrite as electron acceptors by T. *denitrificans* or S. *denitrificans* (Shao et al., 2010b). As all these metabolisms can possibly occur in a single granule, a common chemical that all these microbial groups, except AOB, will compete for is nitrite. If any of these alternative nitrite-utilizing metabolisms is to be retained in a granular system, then the first step in achieving full or partial nitritation is crucial for a system's success. Because of the complexity associated with multiple possible nitrite-based anoxic metabolisms, numerical models are a helpful tool that can guide experimental research. Experiments can further inform the models, provide evidence that explains microbial interactions, and identify the best operating strategy that will lead to improved BNiR.

The GSR technology is a viable B-stage option when coupled with HRAS because it can achieve the integration of PN/A and heterotrophic denitrification. A large enough COD:N ratio is needed to grow granules large enough to create the range of redox zones needed for the three primary metabolisms to thrive, and so that the microorganisms that mediate these metabolisms

can be retained over time. Furthermore, the competition between NOB, anammox and heterotrophs for nitrite needs to be managed. This need provides an opportunity for a real-time sensor-mediated control system that controls aeration so that autotrophic processes are favored over heterotrophic processes. One example of deploying this approach occurred at the Strass treatment plant (Wett, 2007; Wett et al., 2013), which integrates mainstream deammonification in an A-B process as part of an energy positive treatment plant. They use an intermittent aeration strategy to suppress NOB activity in the mainstream. However, it should be noted that the plant includes a sidestream anammox process and with the help of cyclones they are able to augment AOB and anammox biomass into the mainstream B-stage to allow for stable mainstream anammox.

Similar to the case with an HRAS A-stage, aerobic GSR could be an economical and reliable B-stage option for BNiR from a CEPT effluent, even though this A-B combination has not been reported in the literature. This could be particularly useful if the CEPT A-stage converts much of the residual COD into biodegradable forms such as organic acids. Because little is known about this A-B combination, modeling can be used to investigate both the energy efficiency and stability of an A-B coupled CEPT and GSR process.

2.6.3. **Modeling of Aerobic Granular Sludge Reactors**

Granules are structurally the same as biofilms with dense microbial aggregates that form substrate concentration gradients (Gao et al., 2011; Jang, 2003; Reino et al., 2016; Rodriguez-Sanchez et al., 2016). The substrate's concentration profile depends on the size and density of the granule, reaction rates, diffusion coefficients and other environmental factors. Generally, aerobic granules are oxygen diffusion limited, which creates aerobic, anoxic, and anaerobic zones that allow for multiple microbial metabolic groups to grow. They require enough substrate in the bulk liquid to drive the concentration gradient into the granular core, where it become substrate-limited (**Error! Reference source not found.**). Altogether, individual granules support

simultaneous aerobic and anoxic/anaerobic bioconversions within the granules in a single reactor (M K De Kreuk et al., 2007), and given sufficient granules can achieve low bulk-liquid substrate concentrations of target pollutants to meet effluent regulations.

Granules are mathematically modelled as co-diffusional biofilms, as shown in Figure 2.3 (Kreuk et al., 2007; Ni and Yu, 2010). They have three zones including the bulk liquid, the liquid diffusion layer (LDL), and the biofilm matrix. Although a three-dimensional representation and biofilm model might provide more detailed information, they are complex and difficult to simulate. Hence, most of the aerobic granule modeling has been done using a one-dimensional biofilm model, which is sufficient to address our needs in this research study (Bing-Jie Ni, 2008; Castro-Barros et al., 2017; Kagawa et al., 2015; M K De Kreuk et al., 2007; Ni et al., 2008; M-K.H Winkler et al., 2015). Furthermore, the size of the granule is commonly assumed to be constant and at steady-state, which can be one limitation on the currently used models (Baeten et al., 2019). In one-dimensional biofilm models, each redox zone is assumed to be homogenous. That is, granules are assumed to be perfectly spherical, uniform in density and porosity, and have a constant diffusion coefficient between layers. Despite this simplification, a one-dimensional biofilm model usually offers satisfactory results to understand the performance and impact of operational conditions for a granular sludge reactor, and it has been widely used to date to generate and test different hypotheses.

The physicochemical and microbial processes in granules are modeled like other biofilm systems which is based on the Activated Sludge Model (ASMs) framework (using Gujer or Petersen matrix). Modifications can be easily incorporated, such as using two-step nitrification and simultaneous growth and storage (Kreuk et al., 2007; Ni et al., 2008a, 2008b; Zhou et al., 2013). Physicochemical processes such as aeration, gas stripping, and precipitation can also be easily integrated in the matrix with the biological processes. The reactor model is configured as a sequencing batch reactor (SBR) which is typically used to develop aerobic granules (Ni et al., 2010). Important operational parameters or selection pressures that need to be included in the

model to capture the granulation process includes settling time and efficiency, effluent discharge time, and exchange ratio or discharge depth. These parameters are easily translated between the model and the physical SBR reactor.

A common modeling platform that has been used by many researchers to model aerobic GSR is AQUASIM (Wanner and Morgenroth, 2004). In AQUASIM, Kreuk et al. (2007) modeled the granular sludge reactor using an SBR by artificially linking a constant volume biofilm compartment to represent the granular biomass, and a variable mixed compartment to represent the SBR. The bioconversions included in this model include COD, nitrogen, and phosphorus removal, and it was derived from the Delft metabolic bio-P activated sludge model (Meijer 2004).

For this research we use SUMO which is a modern whole plant modeling software developed Dynamita Inc., France. As compared to AQUASIM, SUMO gives much more flexibility to add both kinetic models and to model reactor control strategies. SUMO comes with predefined set of kinetic models and commonly known reactor configurations. In addition, SUMO allows to develop new reactor configuration and integrate it to existing kinetic models. The user can easily develop the kinetic model, reactor configuration and control strategies using an Excel spreadsheet and using SUMO's high-level language called SUMO slang and integrate it to the SUMO's core software.

2.6.4. **Real-time Control strategy for aerobic granular sludge.**

Due to the inherent dynamic nature of wastewater characteristics and processes, several studies have been reported since the early 1970's promoting the adoption of real-time control, ranging from a single wastewater treatment unit to an entire catchment level wastewater management system. For example, at a larger scale for integrated wastewater management, Brandstetter et al. (1973) developed a mathematical model for real-time control of a metropolitan wastewater management system where they used real-time rainfall data to determine the required flow diversions that minimize the discharge of pollutants. At a unit scale, Olsson and Andrews (1978)

developed a model demonstrating the use of oxygen level profiles to control reaction rates in an activated sludge process. Since then, real-time control strategies from simple on-off to more complex model predictive control have been used (Åmand et al., 2013) for different wastewater treatment systems (Andrews, 1974; Holenda et al., 2008; O'Brien et al., 2011; Patry & Takács, 1990; Schilling et al., 1996; Tong et al., 1980; Williams et al., 1990).With the evolution of wastewater treatment plants to resource recovery facilities (Mccarty et al., 2011; Wan et al., 2016), real-time control strategies are playing an increasingly important and critical role, both to minimize energy requirements and to improve nutrient removal or recovery, leading to cost effective and sustainable treatment systems. This is especially relevant as effluent standards are becoming more stringent.

Real-time control systems are also relevant to specific cases; for instance, when we want to use a mix of microbial metabolic processes to treat a complex wastewater such as reject (dewatering) waters from an anaerobically stabilized municipal primary and secondary sludge. In such complex systems, several operating parameters can be better optimized by using real-time control systems to yield improved process performance. For example, Daigger and Littleton (2014) indicated that having a control strategy is as an important factor to achieve effective simultaneous BNuR in a single reactor.

The critical operating parameters needed for simultaneous nitrification and denitrification (SNAD) to minimize energy demand and improve N-removal include oxygen load, aerobic vs anaerobic duration, and residual ammonia. That is, it is important to supply the right amount of aeration for the right amount of time to partially convert ammonium to nitrite while, at the same time, suppressing NOB activity. Excessive amounts of DO will significantly impact N-removal by favoring NOB to convert nitrite to nitrate, leaving less ammonium and no nitrite for anammox, reducing the size of the anoxic zone in the granules, and inhibiting obligate anaerobes. In addition to its impact on N-removal, it means also higher aeration energy consumption for the system.

To implement real-time control strategies, different sensors can be used by installing them in the reactor and making decisions based on the observed changes, termed as sensor-mediated (real-time) control (SMC). Real-time control has been widely applied for conventional nitrogen removal for municipal wastewater (Zanetti et al., 2012) to optimize process performance. However, only a few lab-scale studies have reported on the application of real-time controls specific to aerobic granular sludge reactors (Kishida et al., 2008; Yuan et al., 2010; Gao et al., 2011). The sensors that have been used for real-time control strategy in these studies include DO, ORP and pH. The studies used one or more of these sensors to indirectly determine the endpoints of different biological conversions, such as to control the length of aerobic and anaerobic durations. Although ammonium sensors have been used successfully in flocculent activated sludge systems (Letizia eta l., 2012; Regmi et al., 2014), to date, it has not been reported for use in an aerobic GSR that is being used with real-time control. Hence, one hypothesis is that such advanced, multi-sensor (pH, DO setpoint, ammonium-based aeration) system will provide robust control to achieve excellent and stable N-removal and energy efficiency.

Sensors can be used either directly or indirectly to determine the endpoints of nitrification and denitrification. The indirect detection of the endpoints are done using pH, DO, and ORP sensors while direct detection (measuring the concentration of target species that define water quality in the effluent), is done using NH_4^+, NO_2^-, and NO_3^- sensors. Using the combination of direct and indirect methods, we can automatically control the DO level, and the duration of aerobic and anaerobic cycles. This becomes particularly important for real wastewaters where influent conditions can be very dynamic. Furthermore, avoiding under- or over-aeration will enhance energy efficiency and process performance.

Real-time control systems go hand in hand with mathematical simulation programs that allow prediction of operational conditions before they are implemented. For relatively simple systems, PID and simple concentration based on-off control techniques can be included in mathematical models relatively easily. Generally, PID-based control is useful when we need to maintain a

desired concentration for a certain input parameter such as oxygen supply. On the other hand, a simple concentration-based on-off control can be used to change operational conditions, such as the duration of aerobic/anaerobic cycles. For example, Kagawa et al. (2015) included in their granular sludge model a simple DO setpoint control based on ammonium and nitrate concentrations in the reactor to adjust the DO setpoint by a fixed proportion. Their simulation results showed that adopting such a simple control technique would yield improved and stable reactor performance.

More recently, ammonium-based aeration has been applied to advance shortcut nitrogen removal via nitrite-based denitrification processes. Ammonium-based aeration are applied in two different ways: to maintain a minimum residual ammonium concentration (RAC) throughout the reaction time, and to maintain a desired ammonium to NOx ratio (the so called AvN control) in the effluent (Regmi et al., 2014). Both techniques aim at suppressing NOB activity so that enough ammonium and nitrite are present to support denitrification (preferably, anammmox). For example, Balslev et al. (1996) used simple threshold-based control using on-line ammonium and nitrate sensors to control aeration and sludge recirculation to improve process performance and power consumption in an activated sludge system. Others (Thornberg et al., 1993; Guo et al., 2009; Lemaire et al., 2008) also used similar rule-based real-time control strategies with on-line sensors to control aerobic/anaerobic phase lengths and aeration intensity in a flocculent activated sludge systems. Regmi et al. (2014) used a novel AvN control in a pilot-scale system to maintain an equal proportion of ammonium to NOx (i.e. nitrite + nitrate) concentrations to favor partial nitritation and out-selection of NOB in a first stage reactor and support anammox activity in a downstream. Therefore, it is natural to follows on these important initial studies with the hypothesis that similar ammonium-based aeration control strategies can be used to improve the energy efficiency and nitrogen removal performance of aerobic granular sludge reactors.

2.7. References

Adav, S. S., Lee, D.-J., & Tay, J.-H. (2008). Extracellular polymeric substances and structural stability of aerobic granule. *Water Research*, *42*(6–7), 1644–1650. https://doi.org/10.1016/j.watres.2007.10.013

Agrawal, S., Seuntjens, D., Cocker, P. De, Lackner, S., & Vlaeminck, S. E. (2018). Success of mainstream partial nitritation/anammox demands integration of engineering, microbiome and modeling insights. In *Current Opinion in Biotechnology* (Vol. 50, pp. 214–221). Elsevier Current Trends. https://doi.org/10.1016/j.copbio.2018.01.013

Åmand, L., Olsson, G., & Carlsson, B. (2013). Aeration control - A review. *Water Science and Technology*, *67*(11), 2374–2398. https://doi.org/10.2166/wst.2013.139

Andrews, J. F. (1974). Dynamic models and control strategies for wastewater treatment processes. *Water Research*, *8*(5), 261–289. https://doi.org/10.1016/0043-1354(74)90090-6

Anette Æsøy, Ødegaard, H., & Bentzen, G. (1998). The effect of sulphide and organic matter on the nitrification activity in a biofilm process. *Water Science and Technology*, *37*(1), 115–122. https://doi.org/10.1016/S0273-1223(97)00760-9

Aqeel, H., Basuvaraj, M., Hall, M., Neufeld, J. D., & Liss, S. N. (2016). Microbial dynamics and properties of aerobic granules developed in a laboratory-scale sequencing batch reactor with an intermediate filamentous bulking stage. *Applied Microbiology and Biotechnology*, *100*(1), 447–460. https://doi.org/10.1007/s00253-015-6981-7

Baeten, J. E., Batstone, D. J., Schraa, O. J., van Loosdrecht, M. C. M., & Volcke, E. I. P. (2019). Modelling anaerobic, aerobic and partial nitritation-anammox granular sludge reactors - A review. In *Water Research*. https://doi.org/10.1016/j.watres.2018.11.026

Balslev, P., Lynggaard-Jenson, A., & Nickelsen. C. (1996). Nutrient sensor based real-time on-line process control of a wastewater treatment plant using recirculation. *Water Science & Yechnology*, *33*(1), 183–192. http://wst.iwaponline.com/content/ppiwawst/33/1/183.full.pdf

Bing-Jie Ni, H.-Q. Y. (2008). Storage and Growth of Denitrifiers in Aerobic Granules: Part I. Model Development. *Biotechnology and Bioengineering*, *189 (Pt 3*(Ii), 503–505. https://doi.org/10.1002/bit

Brandstetter, A., Engel, R. L., & Cearlock, D. B. (1973). A Mathematical Model For Optimum Design And Control Of Metropolitan Wastewater Management Systems. *Water Resources Bulletin*, *9*(6), 1188–1200.

Castro-Barros, C. M., Jia, M., Van Loosdrecht, M. C. M., Volcke, E. I. P., & Winkler, M. K. H. (2017). Evaluating the potential for dissimilatory nitrate reduction by anammox bacteria for municipal wastewater treatment. *Bioresource Technology*, *233*, 363–372. https://doi.org/10.1016/j.biortech.2017.02.063

Daigger, G. T., & Littleton, H. X. (2013). Simultaneous biological nutrient removal: A state-of-the art review. *86th Annual Water Environment Federation Technical Exhibition and Conference, WEFTEC 2013*, *6*(3), 3389–3416.

https://doi.org/10.2175/106143013X13736496908555
Dapena-Mora, A., Fernandez, I., Campos, J. L., Mosquera-Corral, A., Mendez, R., & Jetten, M. S. M. (2007). Evaluation of activity and inhibition effects on Anammox process by batch tests based on the nitrogen gas production. *Enzyme and Microbial Technology*, *40*, 859–865. https://ac-els-cdn-com.proxy.lib.umich.edu/S0141022906003450/1-s2.0-S0141022906003450-main.pdf?_tid=f014a20c-d3e9-11e7-b4bd-00000aab0f26&acdnat=1511838917_face9cbfe7c669915f6ef3f4bab14781
de Kreuk, Merle K., & van Loosdrecht, M. C. (2006). Formation of Aerobic Granules with Domestic Sewage. *Journal of Environmental Engineering*, *132*(6), 694–697. https://doi.org/10.1061/(ASCE)0733-9372(2006)132:6(694)
Delgado Vela, J., Dick, G. J., & Love, N. G. (2018). Sulfide inhibition of nitrite oxidation in activated sludge depends on microbial community composition. *Water Research*, *138*, 241–249. https://doi.org/10.1016/j.watres.2018.03.047
Delgado Vela, J., Stadler, L. B., Martin, K. J., Raskin, L., Bott, C. B., & Love, N. G. (2015). Prospects for Biological Nitrogen Removal from Anaerobic Effluents during Mainstream Wastewater Treatment. *Environmental Science & Technology Letters*, *2*(9), 234–244. https://doi.org/10.1021/acs.estlett.5b00191
Derlon, N., Wagner, J., da Costa, R. H. R., & Morgenroth, E. (2016). Formation of aerobic granules for the treatment of real and low-strength municipal wastewater using a sequencing batch reactor operated at constant volume. *Water Research*, *105*, 341–350. https://doi.org/10.1016/j.watres.2016.09.007
Ettwig, K. F., Butler, M. K., Le Paslier, D., Pelletier, E., Mangenot, S., Kuypers, M. M. M., Schreiber, F., Dutilh, B. E., Zedelius, J., de Beer, D., Gloerich, J., Wessels, H. J. C. T., van Alen, T., Luesken, F., Wu, M. L., van de Pas-Schoonen, K. T., Op den Camp, H. J. M., Janssen-Megens, E. M., Francoijs, K.-J., … Strous, M. (2010). Nitrite-driven anaerobic methane oxidation by oxygenic bacteria. *Nature*, *464*(7288), 543–548. https://doi.org/10.1038/nature08883
Figdore, B. A., Stensel, H. D., Karoliina, M.-, & Winkler, H. (2018). *Comparison of different aerobic granular sludge types for activated sludge nitrification bioaugmentation potential*. https://doi.org/10.1016/j.biortech.2017.11.004
Franca, R. D. G., Pinheiro, H. M., van Loosdrecht, M. C. M., & Lourenço, N. D. (2018). Stability of aerobic granules during long-term bioreactor operation. *Biotechnology Advances*, *36*(1), 228–246. https://doi.org/10.1016/J.BIOTECHADV.2017.11.005
Gao, D., Liu, L., Liang, H., & Wu, W.-M. (2011). Aerobic granular sludge: characterization, mechanism of granulation and application to wastewater treatment. *Critical Reviews in Biotechnology*, *31*(2), 137–152. https://doi.org/10.3109/07388551.2010.497961
Guo, J. H., Peng, Y. Z., Wang, S. Y., Zheng, Y. N., Huang, H. J., & Ge, S. J. (2009). Effective and robust partial nitrification to nitrite by real-time aeration duration control in an SBR treating domestic wastewater. *Process Biochemistry*, *44*(9), 979–985.

https://doi.org/10.1016/J.PROCBIO.2009.04.022
Güven, D., Dapena, A., Kartal, B., Schmid, M. C., Maas, B., van de Pas-Schoonen, K., Sozen, S., Mendez, R., Op den Camp, H. J. M., Jetten, M. S. M., Strous, M., & Schmidt, I. (2005). Propionate oxidation by and methanol inhibition of anaerobic ammonium-oxidizing bacteria. *Applied and Environmental Microbiology*, *71*(2), 1066–1071. https://doi.org/10.1128/AEM.71.2.1066-1071.2005
Haroon, M. F., Hu, S., Shi, Y., Imelfort, M., Keller, J., Hugenholtz, P., Yuan, Z., & Tyson, G. W. (2013). Anaerobic oxidation of methane coupled to nitrate reduction in a novel archaeal lineage. *Nature*, *500*(7464), 567–570. https://doi.org/10.1038/nature12375
He, Z., Cai, C., Geng, S., Lou, L., Xu, X., Zheng, P., & Hu, B. (2013). Mdodeling a nitrite-dependent anaerobic methane oxidation process: Parameters identification and model evaluation. *Bioresource Technology*, *147*, 315–320. https://doi.org/10.1016/j.biortech.2013.08.001
Holenda, B., Domokos, E., Rédey, Á., & Fazakas, J. (2008). Dissolved oxygen control of the activated sludge wastewater treatment process using model predictive control. *Computers & Chemical Engineering*, *32*(6), 1270–1278. https://doi.org/10.1016/J.COMPCHEMENG.2007.06.008
Jang, A. (2003). Characterization and evaluation of aerobic granules in sequencing batch reactor. *Journal of Biotechnology*, *105*(1–2), 71–82. https://doi.org/10.1016/S0168-1656(03)00142-1
Jetten, M., Schmid, M., van de Pas-Schoonen, K., Sinninghe Damsté, J., & Strous, M. (2005). Anammox Organisms: Enrichment, Cultivation, and Environmental Analysis. *Methods in Enzymology*, *397*, 34–57. https://doi.org/10.1016/S0076-6879(05)97003-1
Jin, R.-C., Yang, G.-F., Yu, J.-J., & Zheng, P. (2012). The inhibition of the Anammox process: A review. *Chemical Engineering Journal*, *197*, 67–79. https://doi.org/10.1016/j.cej.2012.05.014
Jin, R.-C., Yang, G.-F., Zhang, Q.-Q., Yu, J.-Ji., & Xing, B.-S. (2013). The effect of sulfide inhibition on the ANAMMOX process. *Water Research*, *47*(3), 1459–1469. https://doi.org/10.1016/J.WATRES.2012.12.018
Joye, S. B., & Hollibaugh, J. T. (1995). Influence of Sulfide Inhibition of Nitrification on Nitrogen Regeneration in Sediments. *Source: Science, New Series*, *270*(5236), 623–625. http://www.jstor.org/stable/2888331
Kagawa, Y., Tahata, J., Kishida, N., Matsumoto, S., Picioreanu, C., van Loosdrecht, M. C. M., & Tsuneda, S. (2015). Modeling the nutrient removal process in aerobic granular sludge system by coupling the reactor- and granule-scale models. *Biotechnology and Bioengineering*, *112*(1), 53–64. https://doi.org/10.1002/bit.25331
Kang, A. J., & Yuan, Q. (2017). *Long-term stability and nutrient removal efficiency of aerobic granules at low organic loads*. https://doi.org/10.1016/j.biortech.2017.03.057
Kartal, B., Kuenen, J. G., & van Loosdrecht, M. C. M. (2010). Sewage Treatment with Anammox. *Science*, *328*(5979), 702–703. https://doi.org/10.1126/science.1185941
Kreuk, M K De, Picioreanu, C., Hosseini, M., Xavier, J. B., & Loosdrecht, M. C. M. Van. (2007).

Kinetic Model of a Granular Sludge SBR: Influences on Nutrient Removal. *Biotechnology and Bioengineering*, *97*(4), 801–815.

Lee, D.-J., Chen, Y.-Y., Show, K.-Y., Whiteley, C. G., & Tay, J.-H. (2010). Advances in aerobic granule formation and granule stability in the course of storage and reactor operation. *Biotechnology Advances*, *28*(6), 919–934. https://doi.org/10.1016/j.biotechadv.2010.08.007

Lemaire, R., Marcelino, M., & Yuan, Z. (2008). Achieving the nitrite pathway using aeration phase length control and step-feed in an SBR removing nutrients from abattoir wastewater. *Biotechnology and Bioengineering*, *100*(6), 1228–1236. https://doi.org/10.1002/bit.21844

Leslie, G., Daigger, G., Love, N., & Filipe, C. (2011). *Biological Wastewater Treatment* (Third Edit). CRC Press.

Liu, Y., Gu, J., & Zhang, M. (2020). Approaches to energy and resource recovery from municipal wastewater. In *A-B Processes: Towards Energy Self-sufficient Municipal Wastewater Treatment* (pp. 29–67). IWA Publishing. https://doi.org/10.2166/9781789060089_0029

Liu, Y., & Tay, J.-H. (2004). State of the art of biogranulation technology for wastewater treatment. *Biotechnology Advances*, *22*(7), 533–563. https://doi.org/10.1016/j.biotechadv.2004.05.001

Lotti, T., Kleerebezem, R., Hu, Z., Kartal, B., De Kreuk, M. K., Van Erp Taalman Kip, C., Kruit, J., Hendrickx, T. L. G., & Van Loosdrecht, M. C. M. (2015). Pilot-scale evaluation of anammox-based mainstream nitrogen removal from municipal wastewater. *Environmental Technology (United Kingdom)*, *36*(9), 1167–1177. https://doi.org/10.1080/09593330.2014.982722

McCarty, P. L. (2018). What is the Best Biological Process for Nitrogen Removal: When and Why? *Environmental Science and Technology*, *52*(7), 3835–3841. https://doi.org/10.1021/acs.est.7b05832

Mccarty, P. L., Bae, J., & Kim, J. (2011). Domestic Wastewater Treatment as a Net Energy Producer: Can This be Achieved? *Environ. Sci. Technol*, *45*, 7100–7106. https://doi.org/10.1021/es2014264

Morales, N., Val del Río, Á., Vázquez-Padín, J. R., Méndez, R., Mosquera-Corral, A., & Campos, J. L. (2015). Integration of the Anammox process to the rejection water and main stream lines of WWTPs. *Chemosphere*, *140*, 99–105. https://doi.org/10.1016/j.chemosphere.2015.03.058

Nancharaiah, Y. V., & Kiran Kumar Reddy, G. (2018). Aerobic granular sludge technology: Mechanisms of granulation and biotechnological applications. *Bioresource Technology*, *247*, 1128–1143. https://doi.org/10.1016/J.BIORTECH.2017.09.131

Ni, B.-J., Yu, H.-Q., & Sun, Y.-J. (2008). Modeling simultaneous autotrophic and heterotrophic growth in aerobic granules. *Water Research*, *42*(6), 1583–1594. https://doi.org/10.1016/j.watres.2007.11.010

Nsenga Kumwimba, M., Lotti, T., Şenel, E., Li, X., & Suanon, F. (2020). Anammox-based processes: How far have we come and what work remains? A review by bibliometric

analysis. In *Chemosphere* (Vol. 238, p. 124627). Elsevier Ltd. https://doi.org/10.1016/j.chemosphere.2019.124627

O'Brien, M., Mack, J., Lennox, B., Lovett, D., & Wall, A. (2011). Model predictive control of an activated sludge process: A case study. *Control Engineering Practice*, *19*(1), 54–61. https://doi.org/10.1016/J.CONENGPRAC.2010.09.001

Olsson, G., & Andrews, J. F. (1978). The dissolved oxygen profile—A valuable tool for control of the activated sludge process. *Water Research*, *12*(11), 985–1004. https://doi.org/10.1016/0043-1354(78)90082-9

Patry, G. G., & Takács, I. (1990). MODULAR/MULTI-PURPOSE MODELLING SYSTEM FOR THE SIMULATION AND CONTROL OF WASTEWATER TREATMENT PLANTS: AN INNOVATIVE APPROACH. In *Instrumentation, Control and Automation of Water and Wastewater Treatment and Transport Systems* (pp. 385–392). Elsevier. https://doi.org/10.1016/B978-0-08-040776-0.50052-4

Philips, S., Laanbroek, H. J., & Verstraete, W. (2002). Origin, causes and effects of increased nitrite concentrations in aquatic environments. In *Reviews in Environmental Science and Biotechnology*. https://doi.org/10.1023/A:1020892826575

Pijuan, M., Werner, U., & Yuan, Z. (2011). Reducing the startup time of aerobic granular sludge reactors through seeding floccular sludge with crushed aerobic granules. *Water Research*, *45*(16), 5075–5083. https://doi.org/10.1016/j.watres.2011.07.009

Pollice, A., Tandoi, V., & Lestingi, C. (2002). Influence of aeration and sludge retention time on ammonium oxidation to nitrite and nitrate. *Water Research*, *36*(10), 2541–2546. https://doi.org/10.1016/S0043-1354(01)00468-7

Raghoebarsing, A. A., Pol, A., Van De Pas-Schoonen, K. T., Smolders, A. J. P., Ettwig, K. F., Rijpstra, W. I. C., Schouten, S., Sinninghe Damsté, J. S., Op Den Camp, H. J. M., Jetten, M. S. M., & Strous, M. (2006). A microbial consortium couples anaerobic methane oxidation to denitrification. *Nature*, *440*(7086), 918–921. https://doi.org/10.1038/nature04617

Regmi, P., Miller, M. W., Holgate, B., Bunce, R., Park, H., Chandran, K., Wett, B., Murthy, S., & Bott, C. B. (2014). Control of aeration, aerobic SRT and COD input for mainstream nitritation/denitritation. *Water Research*, *57*, 162–171. https://doi.org/10.1016/j.watres.2014.03.035

Reino, C., Suárez-Ojeda, M. E., Pérez, J., & Carrera, J. (2016). Kinetic and microbiological characterization of aerobic granules performing partial nitritation of a low-strength wastewater at 10 °C. *Water Research*, *101*, 147–156. https://doi.org/10.1016/j.watres.2016.05.059

Rodriguez-Sanchez, A., Purswani, J., Lotti, T., Maza-Marquez, P., van Loosdrecht, M. C. M., Vahala, R., & Gonzalez-Martinez, A. (2016). Distribution and microbial community structure analysis of a single-stage partial nitritation/anammox granular sludge bioreactor operating at low temperature. *Environmental Technology*, *3330*(June), 1–36. https://doi.org/10.1080/09593330.2016.1147613

Roger, K. (1982). Denitrification. *Microbiological Reviews*, *46*(1), 43–70. https://www.ncbi.nlm.nih.gov/pmc/articles/PMC373209/pdf/microrev00066-0053.pdf

S0rensen, J., Tiedje, J. M., & Firestone2, R. B. (1980). Inhibition by Sulfide of Nitric and Nitrous Oxide Reduction by Denitrifying Pseudomonas fluorescenst. *APPLIED AND ENVIRONMENTAL MICROBIOLOGY*, *39*(1), 105–108. https://www.ncbi.nlm.nih.gov/pmc/articles/PMC291291/pdf/aem00231-0125.pdf

Sarma, S J, & Tay, J. H. (2018). Aerobic granulation for future wastewater treatment technology: challenges ahead. *Environ. Sci.: Water Res. Technol*, *4*(9). https://doi.org/10.1039/c7ew00148g

Sarma, Saurabh Jyoti, Tay, J. H., & Chu, A. (2017). Finding Knowledge Gaps in Aerobic Granulation Technology. In *Trends in Biotechnology* (Vol. 35, Issue 1, pp. 66–78). https://doi.org/10.1016/j.tibtech.2016.07.003

Schilling, W., Andersson, B., Nyberg, U., Aspegren, H., Rauch, W., & Harremoës, P. (1996). Real time control of wastewater systems. *Journal of Hydraulic Research*, *34*(6), 785–797. https://doi.org/10.1080/00221689609498450

Svardal, K., & Kroiss, H. (2011). Energy requirements for waste water treatment. *Water Science and Technology*, *64*(6), 1355–1361. https://doi.org/10.2166/wst.2011.221

Tay, J.-H., Pan, S., He, Y., & Tay, S. T. L. (2004). Effect of Organic Loading Rate on Aerobic Granulation. II: Characteristics of Aerobic Granules. *Journal of Environmental Engineering*, *130*(10), 1102–1109. https://doi.org/10.1061/(ASCE)0733-9372(2004)130:10(1102)

Tong, R. M., Beck, M. B., & Latten, A. (1980). Fuzzy control of the activated sludge wastewater treatment process. *Automatica*, *16*(6), 695–701. https://doi.org/10.1016/0005-1098(80)90011-4

van de Graaf, A. A., de Bruijn, P., Robertson, L. A., Jetten, M., & Gijs Kuenen, J. (1996). Autotrophic growth of anaerobic ammonium-oxidizing micro-organisms in a fluidized bed reactor. *Microbiology*, *142*(2), 187–2. http://www.microbiologyresearch.org/docserver/fulltext/micro/142/8/mic-142-8-2187.pdf?expires=1511799911&id=id&accname=sgid023964&checksum=BB2E0070FBF23AF46281FBB65E735421

Wagner, J., & da Costa, R. H. R. (2013). Aerobic Granulation in a Sequencing Batch Reactor Using Real Domestic Wastewater. *Journal of Environmental Engineering*, *139*(11), 1391–1396. https://doi.org/10.1061/(ASCE)EE.1943-7870.0000760

Wan, J., Gu, J., Zhao, Q., & Liu, Y. (2016). *COD capture: a feasible option towards energy self-sufficient domestic wastewater treatment*. https://doi.org/10.1038/srep25054

Wett, B. (2007). Development and implementation of a robust deammonification process. *Water Science & Technology*, *56*(7), 81–88. https://doi.org/10.2166/wst.2007.611

Wett, B., Buchauer, K., & Fimml, C. (2007). Energy self - sufficiency as a feasible concept for wastewater treatment systems. *IWA Leading Edge Technology Conference*. https://www.researchgate.net/profile/Bernhard_Wett/publication/228684984_Energy_self-

sufficiency_as_a_feasible_concept_for_wastewater_treatment_systems/links/0f31752fde1a2d3d13000000/Energy-self-sufficiency-as-a-feasible-concept-for-wastewater-treatment-s

Wett, B., Omari, A., Podmirseg, S. M., Han, M., Akintayo, O., Gómez Brandón, M., Murthy, S., Bott, C., Hell, M., Takács, I., Nyhuis, G., & O'Shaughnessy, M. (2013). Going for mainstream deammonification from bench to full scale for maximized resource efficiency. *Water Science and Technology*, *68*(2), 283–289. https://doi.org/10.2166/wst.2013.150

Williams, G. L., Rhinehart, R. R., & Riggs, B. (1990). In-Line Process-Model-Based Control of Wastewater pH Using Dual Base Injection. *Ind. Eng. Chem. Res. Ind. Eng. Chem. Res*, *29*(7), 1254–1259. https://pubs.acs.org/doi/pdf/10.1021/ie00103a026

Winkler, M-K.H, Ettwig, K. F., Vannecke, T. P. W., Stultiens, K., Bogdan, A., Kartal, B., & Volcke, E. I. P. (2015). Modelling simultaneous anaerobic methane and ammonium removal in a granular sludge reactor. *Water Research*, *73*, 323–331. https://doi.org/10.1016/j.watres.2015.01.039

Winkler, M.-K.H., Kleerebezem, R., & van Loosdrecht, M. C. M. (2012). Integration of anammox into the aerobic granular sludge process for main stream wastewater treatment at ambient temperatures. *Water Research*, *46*(1), 136–144. https://doi.org/10.1016/j.watres.2011.10.034

Winkler, M. K. H., Yang, J., Kleerebezem, R., Plaza, E., Trela, J., Hultman, B., & van Loosdrecht, M. C. M. (2012). Nitrate reduction by organotrophic Anammox bacteria in a nitritation/anammox granular sludge and a moving bed biofilm reactor. *Bioresource Technology*, *114*, 217–223. https://doi.org/10.1016/j.biortech.2012.03.070

Zanetti, L., Frison, N., Nota, E., Tomizioli, M., Bolzonella, D., & Fatone, F. (2012). Progress in real-time control applied to biological nitrogen removal from wastewater. A short-review. *DES*, *286*, 1–7. https://doi.org/10.1016/j.desal.2011.11.056

Chapter 3

Sensor-mediated granular sludge reactor for nitrogen removal and reduced aeration demand using a dilute wastewater

Zerihun A. Bekele[1], Jeseth Delgado Vela[2], Charles B. Bott[3], and Nancy G. Love[1,*]

[1]Department of Civil Engineering and Environmental Engineering, University of Michigan, 1351 Beal Ave, Ann Arbor, MI 48109, USA (Email: *zerualem@umich.edu, nglove@umich.edu*)

[2] Current address: Department of Civil and Environmental Engineering, Howard University, 2300 Sixth St NW, Washington, DC 20059, USA (Email: jeseth.delgadovela@howard.edu)

[3]Hampton Roads Sanitation District, 1434 Air Rail Ave, Virginia Beach, Virginia 23455, USA (Email: *cbott@hrsd.com*)

Abstract

A sensor-mediated strategy was applied to a lab-scale granular sludge reactor (GSR) to demonstrate that energy efficient inorganic nitrogen removal is possible with a dilute mainstream wastewater. The GSR was fed a dilute wastewater designed to simulate an A-stage mainstream anaerobic treatment process. DO, pH, and ammonia/nitrate sensors measured water quality as part of a real-time control strategy that resulted in low-energy nitrogen removal. At a low COD (0.2 kg/m^3/day) and ammonia (0.1 kg-N/m^3/day) load, the average degree of ammonia oxidation was 86.2±3.2% and total inorganic nitrogen removal was 56.7±2.9% over the entire reactor operation. Aeration was controlled using a DO setpoint, with and without residual ammonia control. Under both strategies, maintaining a low bulk oxygen level (0.5 mg/L) and

alternating aerobic/anoxic cycles resulted in a higher level of nitrite accumulation and supported shortcut inorganic nitrogen removal by suppressing nitrite oxidizing bacteria. Furthermore, coupling a DO setpoint aeration strategy with residual ammonia control resulted in more stable nitritation and improved aeration efficiency. The results show that sensor-mediated controls, especially coupled with a DO setpoint and residual ammonia controls, are beneficial for maintaining stable aerobic granular sludge.

Key words: NOB suppression, aeration control, partial nitritation/anammox, mainstream N removal

3.1. Introduction

There is great interest in systems that are energy neutral or positive to also achieve resource recovery using means that meet stringent effluent standards. The A-B (adsorption-biooxidation) process targets this end point. The A-stage is dedicated to maximizing carbon capture for later energy production and is commonly deployed using high rate activated sludge (HRAS) (Jimenez et al., 2015) or chemically enhanced primary treatment (CEPT) (Diamantis et al., 2013). Recently, the anaerobic membrane biofilm reactor (AnMBR) has been proposed as a viable A-stage technology that could become an energy efficient option (Smith et al., 2014). The B-stage is focused on energy efficient nutrient (commonly nitrogen) management (Jetten et al., 1997; Wan et al., 2016). Most of the energy expense in an A-B process occurs due to aeration in the B-stage, where the remaining carbon and nitrogen (N) are removed. In some cases, it is possible for the energy expense in the B-stage to negate the energy gained in the A-stage, making A-B process inefficient for energy recovery (Zhou et al., 2013).

Processes that require less oxygen and do not require external substrate are desirable to minimize aeration demand in the B-stage. Traditionally, N removal is done via complete nitrification (first by ammonium oxidizing bacteria (AOB), then by nitrite oxidizing bacteria (NOB)) followed by

heterotrophic denitrification via ordinary heterotrophic organisms (OHOs). This process has a high aeration demand and requires a higher theoretical oxygen demand (ThOD) to nitrogen (ThOD/N) ratio (> 5) compared to other novel processes (Daigger, 2014). In particular, A-stage processes such as HRAS and CEPT are less efficient at removing nitrogen (de Graaff et al., 2016; Miller et al., 2016), resulting in an effluent ThOD/N ratio < 5. This ratio is insufficient for N removal , because additional carbon will be lost during aeration for nitrification. In this case, exogenous electron donor may be needed to achieve high levels of N removal.

Compared to HRAS and CEPT, the AnMBR A-stage process may be better suited to achieve an overall A-B process energy efficiency. The effluent from mainstream anaerobic treatment typically contains organic carbon (45-145 mg COD/L), ammonium (19-53 mg N/L), dissolved methane (40-140 mg ThOD/L) and sulfide (0-145 mg ThOD/L) (Delgado Vela et al., 2015). Hence, if we consider dissolved methane, sulfide and ammonium as potential electron donors in addition to organic carbon for N removal in a downstream B-stage system, it will be enough for complete N-removal. Methane and sulfide in the AnMBR effluent are possible electron donors for N removal with nitrite/nitrate as electron acceptors via denitrifying anaerobic methane oxidation (DAMO) (Raghoebarsing et al., 2006) and sulfide oxidation (Souza & Foresti, 2013). Among these options, pursuing N removal via nitrite is preferred as it uses less electron donor and less aeration for nitritation. Ammonia can be used as electron donor for anaerobic ammonia oxidation (anammox), which requires nitrite as an e^- acceptor (Strous et al., 1998). However, any of these approaches requires an operational strategy that reliably allows nitritation and minimizes loss of electron donors. Assuming this can be done, then partial nitritation and anammox (PN/A) becomes the most attractive B-stage N removal option, as its low aeration demand and no organic carbon demand (Winkler et al., 2012).

Besides targeting for efficient N removal processes, the use of advanced biofilm systems such as aerobic granular sludge reactor (GSR) as a prospective B-stage technology has significant advantages over conventional activated sludge systems (Sarma et al., 2017). Noted advantages of

aerobic GSR include: the presence of different redox zones within the granules that support a diverse microbial ecology; high rates of settleability; and a high biomass retention which is ideal for slow growing N-removing bacteria (de Kreuk et al., 2005; Liu et al., 2003; Szabó et al., 2017). Figure 3.1 shows the potential key microbial groups and their interactions during complete nitrogen removal via nitrite in a single stage GSR downstream of an AnMBR A-stage. The schematic emphasizes that competition for nitrite will occur among different anaerobic organisms, and suggests that successful N removal requires sustained partial nitritation while supressing nitrite oxidation by NOB. Therefore, the success of an energy efficient aerobic GSR as a B-stage N removal system requires a robust operating strategy that favors simultaneous partial nitritation and denitritation by suppressing NOB.

One of the main challenges for N-removal in mainstream wastewater via nitrite is suppression of NOB. In particular, the suppression of NOB in PN/A process has been demonstrated at full-scale for concentrated sidestream applications, which have favorable conditions such as: low C/N ratio (<2 g COD/g N); high temperature (20 to 30 ^{o}C); high free ammonia concentrations (> 0.1 mg N/L) (Philips et al., 2002); and high (> 0.2 mg N/L) free nitrous acid (Kornaros et al., 2010). Unfortunately, most of these conditions are atypical for dilute mainstream systems (Cao et al., 2017). However, if a sequencing batch reactor (SBR) is used and a minimum residual ammonium concentration (RAC) is maintained throughout the reaction time, NOB suppression can still be achieved via free ammonia that is present in sufficient concentration during most of the reaction cycle.

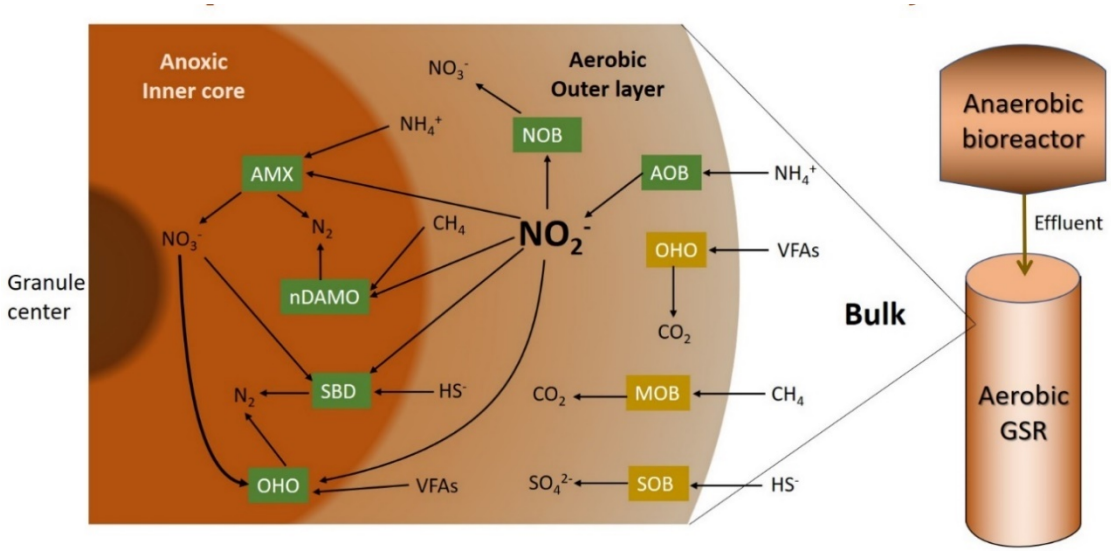

Figure 3.1. Potential metabolic pathways in a B-stage GSR for removal of ammonia, VFA, methane and sulfide present in an anaerobically-treated A-stage. SBD: sulfur based denitrification, MOB: methane oxidizing bacteria, and SOB: sulfur oxidizing bacteria.

Nonetheless, since this alone may not be enough to effectively suppress NOB, new strategies are needed for NOB suppression. For this reason, we propose the use of real-time sensor-mediated control (SMC) for robust aeration control to suppress NOB. Online sensors have been used to suppress NOB in sidestream applications by manipulating the DO setpoint, or by using intermittent aeration and ammonium-based aeration control (ABAC). For example, Regmi et al. (2014) used real-time ABAC with intermittent aeration to suppress NOB in a suspended culture for mainstream nitritation. Lemaire et al. (2008) used DO and pH sensors to control aerobic duration for shortcut N removal by suppressing NOB. Both studies demonstrate that SMC for mainstream NOB suppression is a viable option.

A-stage effluent has a low organic load in concert with a much lower N load than side-stream granular systems, which can tolerate low organic loads given the high N loading (Wett et al., 2015). The combination of low organic and N loading with a low C/N ratio in dilute mainstream A-B applications makes it challenging to develop and sustain granules. Tay et al. (2004) reported that they were not able to produce granules when the organic loading was below 2 kg COD m^{-3} d^{-1}. The lowest organic loading rate that we found reported to date for successful granule formation

came from Ni et al. (2008) and Zhang et al. (2015) who used 0.6-1 and 0.37-0.56 kg COD m^{-3} d^{-1}, respectively. Hence, developing stable granules in low loaded circumstances is another challenge that must be addressed to advance the GSR technology.

In this study, we focused on developing and operating an aerobic GSR as an exemplary B-stage N removal system for an A-stage AnMBR effluent. We use this reactor configuration to develop and demonstrate an SMC strategy that supports NOB suppression and reduces aeration energy. We evaluated the degree to which the strategy supports PN/A for N removal, and highlight the conditions needed to support stable granule formation.

3.2. Methods

3.2.1. Reactor setup.

A glass bubble column reactor with 76.2 mm (3 inches) diameter and 711.2 mm (28 inches) height with a working volume of 4.5 L was operated for 474 days. The reactor was initially inoculated by mixing a nitrifying activated sludge from the Ann Arbor Wastewater Treatment Plant (Michigan, USA) and biomass from a full-scale deammonification (DEMON) unit (Hampton Roads Sanitation District, Virginia, USA). The reactor was fed with a simulated mainstream anaerobic digester effluent containing ammonium (48 ± 6 mg/L-N), VFAs (acetate and propionate, 100 mg/L-COD), dissolved methane at saturation (~22 mg/L-CH_4) and other trace elements. Details of the media preparation procedure can be found in the Appendix Section 12. The COD:N ratio, considering VFA and ammonium, was from 1.85 to 2.5. The reactor was monitored and controlled using online optical DO (WTW, FDO 925, Xylem Inc.), pH (accumet® Electrode, Fisher Scientific), and NH_4^+/NO_3^- (IQ SensorNet VARiON® Plus Sensors, Xylem Inc.) probes to suppress NOB and favor the growth of AOB and anammox species. A bulk DO concentration was held at specific DO levels between 0.2 and 1.5 (± 0.1 mg/L O_2). The pH was

monitored using an online probe and was maintained between 7.3 $\pm$ 0.2 and 8.0 $\pm$ 0.2 by dosing $NaHCO_3$. The entire experiment was conducted at an ambient temperature between 20 and 23^{o}C.

3.2.2. Cycle operation

The reactor was operated in a sequencing batch mode with a 40 min anoxic slow feed from the bottom of the reactor, followed by intermittent aeration with anoxic and aerobic cycles for 220-300 min, a settling time of 4 to 10 min, and 4 min of decanting with a volumetric exchange ratio of 50%. Air was supplied using a glass diffuser with a superficial upflow velocity of 1.6 cm/sec. During the anoxic phase, gas from the head space of the reactor was pressurized by diaphragm pump, blended with dinitrogen gas and recirculated through the reactor. This supported the development of anoxic conditions and resupplied stripped methane gas to enhance the chance for its dissolution and metabolism. During the aerobic phase a mixture of dry air, dinitrogen gas and head space gas were pumped into the reactor. The dry air flow rate was controlled with a mass flow controller (MFC) device to maintain the desired setpoint using in-house developed partial differential and integral (PID) controller (developed in LabView® software).

3.2.3. Sensor-mediated control development

Across the aerobic phases of a single SBR cycle, DO was controlled in the first two phases based on a specific setpoint, and ammonia-based aeration control was used for the last phase of operation. Both aeration schemes were implemented by developing a PID controller in LabView (Appendix A, Figure A-5). The developed LabView SMC program was designed to allow time-based aeration for DO setpoint only and ABAC with a DO setpoint. The program also controls all the pumps and sensor-based devices, thus automating the entire operation. Information reported as sensor-derived concentration was adjusted based on correction factors determined by using simple linear regression between sensor output and analytically-determined concentrations

(i.e., for ammonium and nitrate). Effluent nitrite corrections reported in **Figure 3.5** only were derived from its correlations with effluent ammonium and nitrate.

3.2.4. Long-term reactor operation

The reactor was operated for 474 days, which can be broken down into four phases (Appendix A, Table A-2). During the first phase (days 1-60), granule development occurred and the reactor was operated at a DO setpoint of 1.5 mg/L. A lower DO setpoint (0.5 mg/L) without ABAC was used during the second phase (days 61-200). The third phase (days 201 - 410) was operated at a DO setpoint of 0.75 mg/L without ABAC. The final and fourth phase (days 411-474) was operated with low DO setpoint (0.5 mg/L) and ABAC. Ammonium-based aeration was implemented to maintain residual ammonium at or above 5 mg/L as N, both to promote anammox activity and to suppress NOB as indicated by Cao et al. (2017). During all phases, samples were usually collected three times a week from the reactor after settling using a sampling port, and analyzed for ammonium (Standard Method (SM) Sec. 4500-NH_3 F), nitrite (SM Sec. 4500-NO_2^- B), nitrate (SM Sec. 4110 B) and methane (SM 2720, 6211, and 6010). Biweekly cross-cycle sampling was done over a single operating cycle to obtain profiles of soluble N species, also volatile fatty acids (VFAs) using ion chromatography as described in Smith et al. (Smith et al., 2013). Additionally, in-situ batch activity tests were conducted for Phases 2, 3 and 4 to determine nitrification and anammox activities. The detailed procedure for this can be found in SI section 13. Physical characteristics of granules, such as size, sludge volume index (SVI), and solids retention time (SRT), were also monitored as described in the SI. All sensors data (i.e., NH_4^+, NO_3^-, DO and pH) and other operation information were logged every minute. All values errors are given at a 95% confidence interval from a t-test distribution.

3.2.5. Microbial community analysis

Biomass samples were taken during the first two months of the reactor granulation phase and at later stages of operation to monitor the microbial composition using 16S rRNA gene amplicon sequencing. The inoculum used to obtain an anammox organism was from a full-scale deammonification unit at Hampton Roads Sanitation District (HRSD), Virginia. DNA was extracted using three bead-beading steps followed by extraction with a Maxwell 16 LEV automated nucleic acid extractor (Promega, Madison WI) using DNA blood kits. Amplicon sequencing of the V4 region of the 16S rRNA gene was performed on the Illumina MiSeq (MiSeq Reagent Kit V2 500 cycles, Illumina Inc., San Diego, CA) platform using the previously developed dual-indexing sequencing strategy (Kozich et al., 2013). Additional details of the procedure can be found in Delgado Vela et al. (2018). Post-processing of the Illumina MiSeq data was done using the Mothur MiSeq SOP (Schloss et al., 2009) without rarefication and including archaea in the analysis. Data from the MiSeq analysis have been uploaded to NCBI and is openly available under accession number PRJNA549919.

3.3. Results

3.3.1. Phase 1: Granule formation

The initial phase of granule development took about 60 days (Figure 3.2), which is relatively rapid compared to other granular systems (Ni et al., 2009). For granule development and selection, the reactor was operated in SBR mode with a short (5 min) settling time and a superficial upflow velocity of 1.6 cm/sec. The granules went through different morphological transformations as they were formed (Figure 3.2a). First, micro-granules began to form after two weeks of operation. Then, large and fluffy granules formed after a month. Finally, the granules developed into mature granules after two months of operation. The mature granules had an average diameter of 0.97±0.06 mm (Appendix A, Figure A-2) and an average settling velocity of

12 m/hr. The steady state mean VSS concentration was 1,520 ± 176 mg/L with a mean 5 min SVI of 70 mg/L. We calculated an average SRT of 4.8±0.6 days, 12.2 ± 2.9 days, 11.9 ± 2.1 days, and 17.5 ± 3.5 days for Phase 1, Phase 2, Phase 3, and Phase 4, respectively (Appendix A, Figure A-1).

During granulation, the biomass color changed from dark red (inoculum, not shown) to pale yellow (Figure 3.2), indicating a shift in microbial composition. Whole community analysis based on the 16S rRNA gene was used to characterize how the microbial community shifted over the course of reactor operation, including during the granulation period (Figure 3.3). Community analysis showed that only anammox taxa (AMX) was detected in the inoculum of the order "Candidatus Brocadiales," and comprised approximately 13% of the community. Subsequently, the relative abundance of AMX decreased to 2.2% by the end of granulation. During this same period, nitrite and ammonium accumulated while nitrate was mostly absent. Although substrates required for anammox metabolism were present, the loss of AMX suggests that this metabolism was not occurring to a significant degree. Concurrently, the inoculum contained relatively equal fractions of AOB (genus *Nitrosomonas,* 3.7%) and NOB (genus *Nitrospira,* 3.4%); however, by the end of the granulation period AOB had a higher relative abundance (5.4%) than NOB (0.6%), consistent with NOB out-selection. The nitrite accumulation rate (NAR = 0.67±0.24) was consistent with this result (see Figure 3.4). Furthermore, OHOs increased from 20% to 50% over this same period; however, we presume that insufficient organic carbon was available as an electron donor to fully consume the accumulated nitrite as it was observed in Phase 2 and 3 (Appendix A, Figure A-6). These results suggest that a rapid, or aggressive, granulation period makes it difficult to establish stable redox niches that are needed to support slow growing microorganisms, such as AMX and NOB. Furthermore, the high DO of 1.5 mg/L used during the aerobic period might have reduced the size of the anoxic zone in the granules, which may have limited AMX activity. Collectively, these factors all likely contributed to the reduction in N removal during the granulation phase.

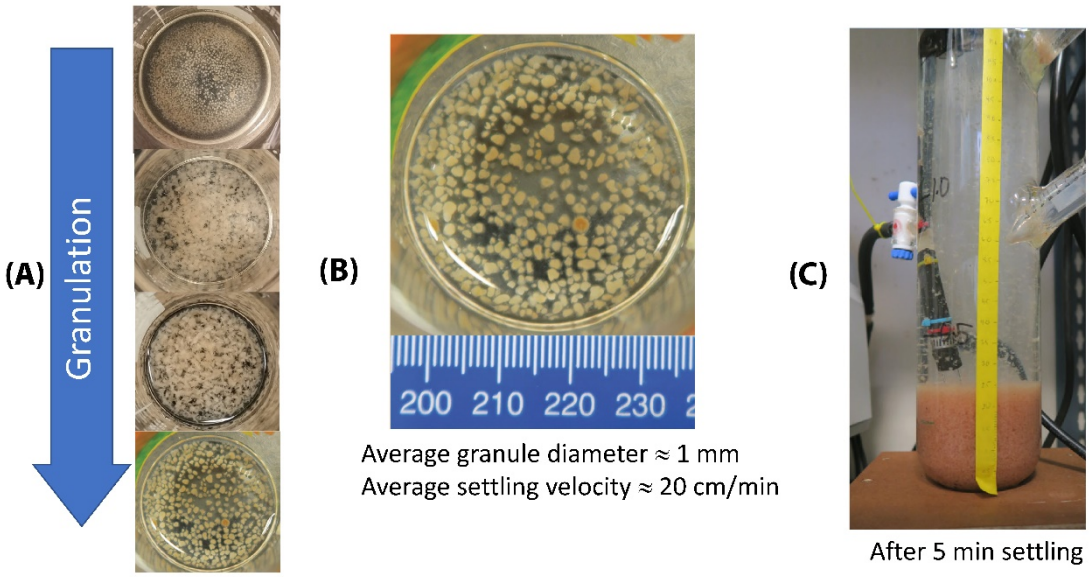

Figure 3.2. (a) Granules change over time during start-up Phase 1. They began as micro-granules, then became large and fluffy, and finally developed into mature granules. (b) Mature granules with an average size of 1 mm. (c) Granules in the reactor after 5 minutes of settling.

3.3.2. Phase 2: Low (0.5 mg/L) dissolved oxygen operational phase

In Phase 2 operation when the bulk DO setpoint was 0.5 mg-O_2/L, nitrite was routinely present in the effluent at an average concentration of 13.9 ± 3.4 mg N/L while nitrate averaged 0.4 ± 0.2 mg N/L with high NAR of 0.93±0.06 (Figure 3.4). The effluent ammonium concentration was 8.4 ± 3.5 mg N/L and quite variable (Appendix A, Figure A-4), ranging between 25 and below detection (seven of 25 measurements during this phase were at or below 0.1 mg/L as N). The overall TIN removal during this phase was 49.6±5.6% and the overall ammonia conversion was 80.7±8.1% (Figure 3.4). This broad range of performance during Phase 2 may have made it difficult to sustain significant anammox growth in the system.

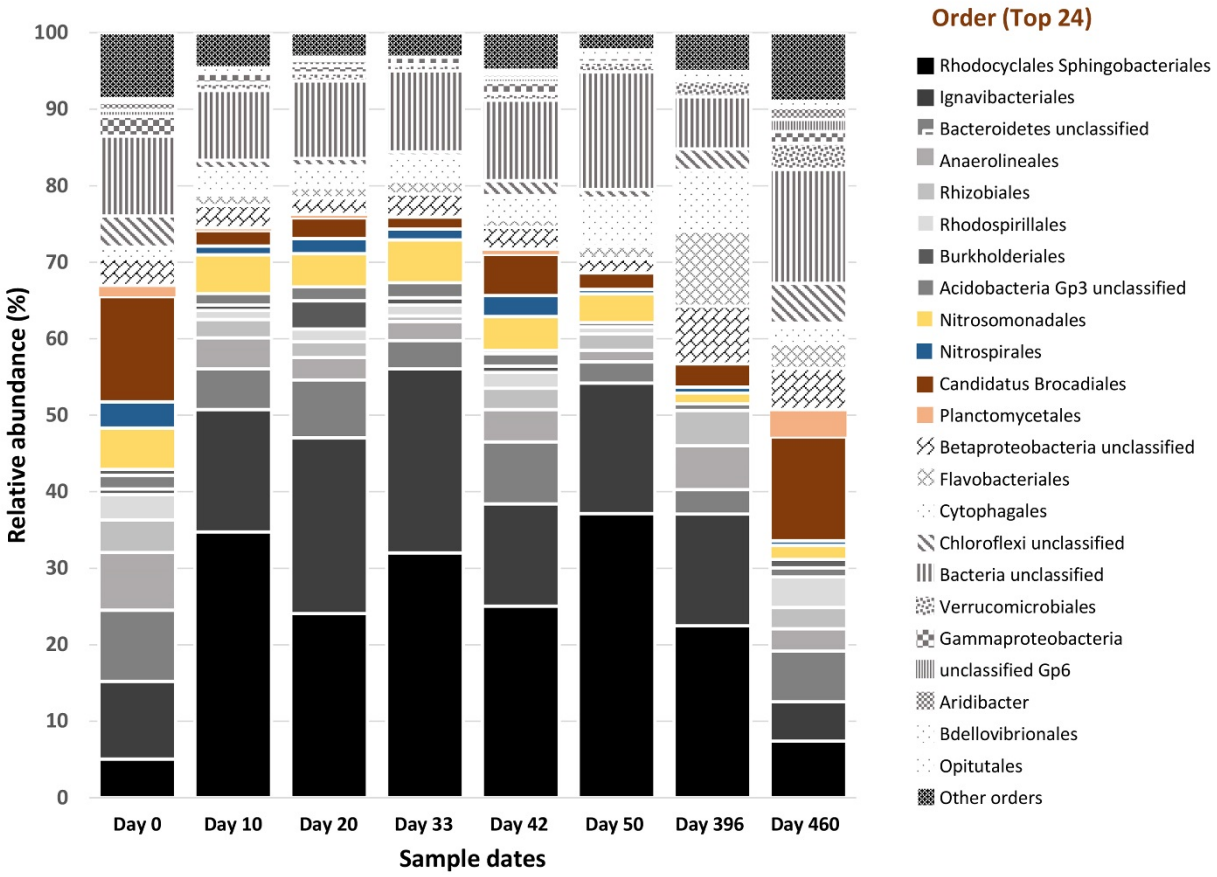

Figure 3.3. Microbial composition dynamics at order level OTUs for the period of granule development (through day 50), day 396 which is in phase 3, and day 460 which is in phase 4. Solid greytone colors are OHOs, hatched greytones are other bacteria with either known or unknown functions such as EPS production, hydrolysis, and filament formation, and solid non-greytone colors are AOB, NOB, anammox and the order plactomycetales.

To estimate of the relative contributions of AMX and OHOs to TIN removal, we used cross-cycle data (i.e., one batch cycle N and VFA profile data) with theoretical stoichiometric equation (See Appendix A Section 10, from Tables A-9 to A-16). The VFA data show that at least one-third was utilized by the end of the first anoxic period and was consumed at the same time as residual nitrite held over from the prior cycle was consumed, implying that nitrite served as the electron acceptor during that period. The remaining VFA was rapidly oxidized during the first aerobic period. After accounting for nitrogen consumption for cell growth, our calculations suggest that TIN removal via OHOs occurred up to the end of the first anoxic period, and for the rest of the cycle via anammox. Our stoichiometric predictive analysis shows that VFA removed up to 72%

of the oxidized inorganic nitrogen on average during Phase 2. We did not detect residual methane at the end of the anoxic feed period (Appendix A, Figure A-7) nor did we detect DAMO through our microbial community analysis; therefore, it is reasonable to assume that methane was stripped out as soon as mixing started in the first anoxic zone. Considering all these factors leaves an unaccounted source of TIN removal of at least 28%, which we assume is attributed to anammox during this Phase. Consequently, despite its low relative abundance, AMX may have contributed to TIN removal.

In-situ nitrification and anammox activity results from tests conducted during Phase 2 suggest that NOB were suppressed and AMX were active, corroborating the stoichiometric predictive analysis. AOB (0.32 g N-NO_2^- formed/g VSS/day) were 4 times more active than NOB (0.08 g N-NO_3^- formed/g VSS/day), even though DO exceeded 1.0 mg/L (Table A-6). The Phase 2 in-situ anammox activity test yielded a specific total inorganic nitrogen (ammonium + nitrite) utilization rate of 0.104 mg-N/mg-VSS/day, supporting our prior conclusion that anammox was likely actively involved in TIN removal (See Appendix A, Table A-3).

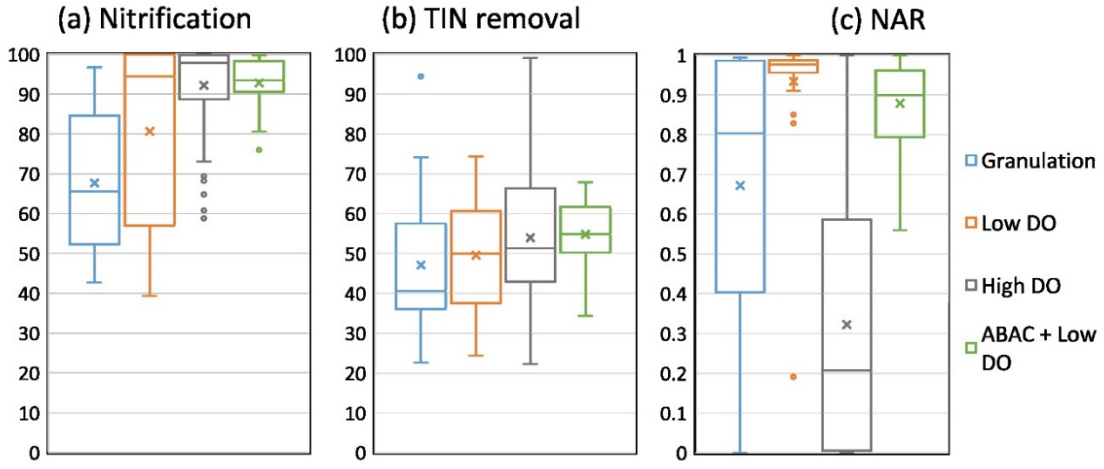

Figure 3.4. Boxplots showing comparisons across the four operation stages for (a) percent nitrification, (b) percent total inorganic nitrogen removal, and (c) nitrite accumulation ratio (NAR = effluent nitrite-N:effluent [nitrite-N + nitrate-N]). Note: 'x' indicates the mean, the inside horizontal line indicates the median.

3.3.3. Phase 3: high (0.75 mg/L) dissolved oxygen operational phase

Phase 3 was operated at a higher bulk DO setpoint of 0.75-1 mg-O_2/L, and resulted in both a sustained loss of nitrite and increase in nitrate. During this phase, effluent nitrite was present at an average concentration of 4.4 ± 1.1 mg N/L while the effluent nitrate increased to an average concentration of 14.7 ± 2.6 mg N/L, which resulted in low NAR of 0.33±0.08 (Figure 3.4). The effluent ammonium concentration was 4.0±1.5 mg N/L with an overall conversion rate of 92 ± 3%, which is higher than in Phase 2 ($p < 0.001$). The overall TIN removal for this phase was 53.2 ± 4.1%, which is similar to the performance of Phase 2 ($p > 0.05$).

Cross-cycle analysis showed that AMX and OHO both continued to contribute to TIN removal. VFA was predominantly consumed during the anoxic feed period via heterotrophic denitrification that used the residual nitrate from the prior cycle (see Appendix A, Figure A-6). The remaining VFA was oxidized rapidly during the first aerobic period. Consequently, any TIN removal observed after the first aerobic period was assumed to be due to AMX. Based on cross-cycle data (Appendix A, Tables A-17 through A-24) and after accounting for N loss for growth, we estimate that VFA could, at best, remove 66% of the oxidized inorganic nitrogen present in the influent. Since AMX are present in the system and exposed to intermittent anaerobic periods, and a persistent anaerobic inner core exists in the granules despite a measureable bulk DO, we conclude that AMX removed up to 34% of TIN.

In-situ nitrification and anammox activity tests indicated that NOB were more active than AOB, and anammox activity was detected but lower than what was measured during Phase 2 (See Appendix A, Table A-3 & A-6). The in-situ nitrification test conducted on day 376 showed that the NOB activity rate (0.32 g N-NO_3^- formed/g VSS/day) was at least 3 times more active than AOB (0.099 g N-NO_2^- formed/g VSS/day), indicating that the NOB suppression observed during Phase 2 was reversed. In addition, the in-situ anammox activity test conducted on day 362 showed that AMX had a specific total inorganic nitrogen utilization rate of 0.08 mg-N/mg-VSS/

day, indicating that AMX were active but at a lower rate than what was measured during Phase 2. As a confirmation, we estimated the average rate of the net TIN oxidized by AMX only during Phase 3 to be 0.06 mg-N/mg-VSS/day from the cross-cycles data. Since the in-situ activity tests show the highest rate achievable under ideal conditions, this comparison shows that the anammox activity measured can explain the loss of oxidized TIN residual during a single cycle.

Microbial community analysis produced results consistent with the in-situ activity experiments. Illumina Miseq results from samples collected on day 396 (toward the end of Phase 3) indicate that the granules continued to contain AMX, AOB and NOB but with a lower relative abundance compared to the granulation phase. In addition, granule size did not significantly change during Phase 2 (0.97±0.05 mm) and Phase 3 (0.92±0.02 mm) (two-tail t-Test p=0.1). This suggests that the shift in performance and establishment of nitrite oxidation was motivated primarily by the small change in bulk liquid DO, which could have supported higher NOB activity and caused loss of NOB suppression.

3.3.4. Phase 4: Ammonium-based aeration control (ABAC)

Phase 2 performance showed that a low bulk DO concentration could maintain a higher nitrite concentration and support anammox metabolism; however, nitrite was highly variable and made anammox-based total N removal vulnerable to instability. The variability observed likely occurred because the available ammonium was periodically used up before the end of a cycle, which would have reduced AMX growth and supported NOB growth. Hence, ABAC was implemented during Phase 4 to maintain a minimum residual ammonium concentration throughout each reaction cycle to create a condition that suppressed NOB and supported AOB and AMX activity (Lotti et al., 2014; Pérez et al., 2014). For an SBR, the suppression of NOB by residual ammonium is much more pronounced at the beginning of the reaction phase than the end given the concentration gradient in the reactor. This also allows for sufficient free ammonia to be present that can inhibit NOB, despite the eventual decrease in total ammonia-N by the end

of each reaction cycle. The ABAC strategy used an NH_4^+/NO_3^- sensor to maintain a residual ammonium concentration around 5 mg/L as N, and a DO sensor to maintain a low bulk DO setpoint (0.5 mg O_2/L). This strategy reduced variability in bulk liquid nutrient concentrations and increase aeration efficiency.

With ABAC, we saw a significant shift in both performance and microbial community population composition. Detectable effluent nitrite (16.0 ± 1.6 mg-N/L) and nitrate (2.26±0.72 mg-N/L) resulted in a high NAR of 0.88±0.04. Also, a lower residual ammonium concentration of 3.5 ± 1.3 mg/L was maintained. The average overall inorganic nitrogen removal efficiency improved slightly to 54.8 ± 3.3 % compared to the other phases (Figure 3.5); however, the improvement was not statistically significant compared to both Phase 2 ($p=0.12$) and Phase 3 ($p=0.75$). Nevertheless, we saw evidence of improved anammox activity. From the in-situ nitrification test on day 459 (Table SI A-8), AOB (0.31 g N-NO_2^- formed/g VSS/day) were 3.5 times more active than NOB (0.09 g N-NO_3^- formed/g VSS/day), while the in-situ anammox activity test performed on day 463 resulted in an anammox specific activity of 0.153 mg-N/mg-VSS day, which is about 1.5 times faster than Phase 2 and almost 2 times faster than Phase 3 (See Appendix A, Table A-4). From the cross-cycle data (Tables A-25-A-26) analysis, we estimated AMX contributed at least 40% of TIN removed. Illumina Miseq analysis (Day 460, Figure 3) provided additional evidence that the anammox population had recovered significantly during Phase 4 to a relative abundance of 13% while OHOs declined. Together, the performance and microbial community data demonstrate that coupling three aspects of SMC (low DO setpoint, intermittent aeration, and ABAC) created a favorable condition for partial nitritation/anammox in a granular system that received a simulated dilute mainstream anaerobic effluent and reduced the variability in TIN removal (Figure 3.4).

Our data also suggests that implementing ABAC improved aeration efficiency, as shown in Figure 3.5. To take a closer look at the improvement made by ABAC in our system, we show

sensor-based performance measurements from the reactor for 50 consecutive cycles as we transitioned from Phase 3 to Phase 4. ABAC determined the aerobic duration by limiting aeration up until the residual ammonium dropped below the setpoint of. This caused the overall aerobic duration to be shorter as compared to using a DO-based setpoint only. In this case, the overall aerobic duration was reduced by up to 25% and on average by 15% with the use of ABAC versus DO setpoint operation with fixed aerobic duration (Figure 3.5b).

3.4. Discussion

3.4.1. Stable granulation is possible in a B-stage nitrogen removing GSR system

Our results show that it is possible to produce stable granules in an aerobic granular sludge system receiving a dilute wastewater containing residual organic carbon and ammonium. Mature granules with a mean diameter of 1 mm were developed within two months of operation on a synthetic feed with a COD loading of 0.2 kg m^{-3} d^{-1} and nitrogen loading of 0.1 kg N m^{-3} d^{-1}. The larger granules are likely to have a larger intra-granular anaerobic zone that can support anaerobic metabolisms. Generally, granules are much easier to develop when the organic loading rate is higher than 1 kg m^{-3} d^{-1} (Jafari Kang & Yuan, 2017; Tay et al., 2004). A few studies have reported successful granulation at low organic loading rates (between 0.4 and 1 kg m^{-3} d^{-1}) but with a longer time for stable granulation (65 to 120 days) than what was observed in this study (60 days) (Ni et al., 2009; C. Zhang et al., 2015). Therefore, with this study we demonstrated that it is possible to produce granules at low organic loading conditions pertinent to mainstream applications.

The organic carbon load to the GSR played two major roles. First, it was a major contributor for N removal in all phases. Using stoichiometry, we estimate that it functioned as an electron donor and contributed around 60%, 64% and 60% of the oxidized TIN removal observed during Phases 2, 3 and 4, respectively. The loss of organic carbon due to its reaction with oxidized TIN was

limited to the first anoxic period and the availability of residual NO_X. Any residual organic carbon present in the first aerobic zone was oxidized by O_2. Second, the organic carbon load to the GSR provided the minimum loading needed to develop and sustain granules in our dilute system. Peyong (2012) observed that reducing the organic loading rate below 0.54 kg COD $m^{-3}day^{-1}$ resulted in disintegration of granules and the subsequent loss of biomass. Hence, our study showed that it is indeed possible to maintain a stable granular system with organic loading as low as 0.2 kg COD $m^{-3}day^{-1}$.

3.4.2. Low bulk DO with intermittent aeration supported NOB suppression

Operating the reactor at a bulk DO setpoint of 0.5 mg/L combined with intermittent aeration effectively suppressed NOB activity. The NAR observed during Phases 2 and 4 was significantly higher than Phase 3 ($p < 0.001$) and indicates that operating at low bulk DO was key to effective NOB suppression (Figure 4). Suppression of NOB by low DO is also known to occur in both activated sludge (Peng & Zhu, 2006) and biofilm systems (Brockmann & Morgenroth, 2010; Ma et al., 2015). Rapid intermittent aeration also suppressed NOB because they are known to adapt slowly under transient conditions when shifting from an anaerobic to an aerobic environment, and leads to an accumulated growth disadvantage (Gilbert et al., 2014; Kornaros et al., 2010; Regmi et al., 2014). Concurrently, specific to our system, the quick loss of both VFA and methane means the residual ammonia creates a condition that supports the growth of AOB and ANX more so than NOB for most of the reaction cycle. On top of this, the presence of residual ammonium between 2 and 5 mg NH_4^- N/L has been reported to differentially limit the activity of NOB relative to that of AOB (Pérez et al., 2014; Poot et al., 2016). Therefore, our SMC operation strategy with low and intermittent DO mainly favored AOB while suppressing NOB.

The success of using low bulk DO to achieve NOB suppression can be attributed in part to the known differences in growth rate between the AOB and NOB genera present in our system. A 16S rRNA gene-based community analysis showed that the only NOB types detected in our

reactor are from the genus *Nitrospira*, which are typically found to have a lower maximum specific growth rate and lower oxygen affinity (Blackburne et al., 2007) than the AOB detected in our system, the genus *Nitrosomonas*, which are typically found to have a higher maximum specific growth rate and oxygen affinity (Blackburne et al., 2008). These two genera of bacteria have been found to coexist in many partial nitritation systems, as summarized by Cao et al. (2017) and reported by other authors (Sinha et al., 2006; Wett et al., 2013). Hence, the AOB in our system are likely to have a higher oxygen affinity under low DO conditions than the NOB, resulting in suppression of the latter.

3.4.3. Coupling ABAC with low DO setpoint enhanced energy efficient, anammox-supported N removal

The performance of the GSR was stable and aeration energy demand was reduced with the addition of ABAC. When the reactor was operated without residual ammonium control during Phase 3, it was not possible to consistently maintain residual ammonium through the end of the reaction cycle; hence, the residual ammonium concentration tended to vary substantially (Figure 3.5a). This is undesirable since a minimum residual ammonium concentration is needed throughout the reaction zones for successful partial nitritation. Thus, this underscores the benefit brought by ABAC to ensure that an ammonium residue is maintained throughout the reaction time. When we added ABAC, aeration duration was reduced by up to 25% relative to what occurred when we used a DO setpoint only (Figure 3.5b). This reduction in aerobic duration translates into a reduction in aeration energy cost. Consequently, the use of ABAC resulted in tighter aeration control, which yielded more stable residual ammonium and overall TIN removal performance for the system. Translated to full-scale treatment systems that often have a dynamic influent composition, these results imply that the use of ABAC will be critical to the cost-effective deployment of mainstream B-stage GSR applications that must achieve stable nitrogen reduction.

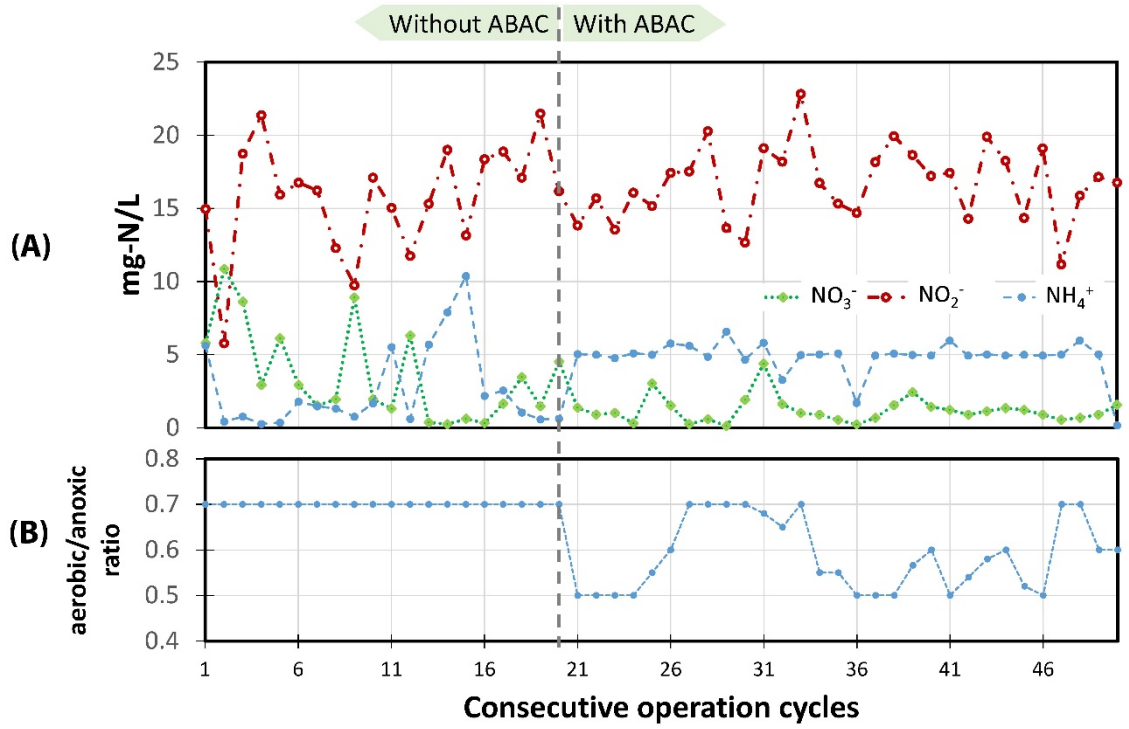

Figure 3.5. Reactor operation with and without ABAC (Days from 396 to 417). (a) Effluent nitrogen species concentration profile under both scenarios (measurements determined using sensors and corrected with analytically determined values). (b) The corresponding total aerobic/anoxic duration fraction.

The use of ABAC with low DO setpoint and intermittent aeration also improved the retention of AMX in our system. Whole community (16S rRNA gene) sequencing data showed that coupling ABAC with low intermittent DO setpoint control corresponded with the recovery of AMX to around 13% relative abundance, four times higher than was seen without ABAC (Figure 3.3). The increase in AMX relative abundance corresponded with a 1.5-fold increase in the in-situ rate of anammox specific activity relative to what was observed during Phase 2 (low-DO without ABAC). Furthermore, the specific anammox rate measured during Phase 4 (low DO with ABAC, 0.153 mg-N/mg-VSS-day) is similar the rate reported by Lotti et al. (2015b) for a partial nitritation/anammox SBR controlled with low DO and ABAC at 20°C (0.11 mg-N/mg-VSS day) and at 25°C (0.14 mg-N/mg-VSS day). To achieve N-removal via nitrite by suppressing NOB, other studies have used DO, pH and ORP in aerobic granular sludge reactors (Lochmatter et al., 2013; Tao et al., 2012) while DO and ABAC have been used in conventional activated sludge

systems (Regmi et al., 2014, 2015) to control DO setpoint and aerobic duration. All of these studies had higher organic and/or nitrogen volumetric loading than this study. Here, we developed and demonstrated a SMC strategy that integrated a DO setpoint, intermittent aeration and residual ammonia control to promote partial nitritation/anammox in a mainstream GSR fed with dilute wastewater to achieve N-removal with reduced aeration expense.

3.4.4. Less aggressive start-up is required for better nitrogen removal

The manner with which the GSR was operated during granulation influenced the system's ability to retain anammox activity. As the 16S rRNA sequencing results show, AMX was substantially reduced in abundance during the granulation period, consistent with the corresponding higher nitrite accumulation and lower levels of nitrate. We believe the observed reduction in AMX relative abundance has to do with two unfavorable start-up conditions. First, during the start-up period granules were developed with a short settling time to select against flocculent sludge. This created a short residence time of 4.8±0.6 days (Appendix A, Figure A-1), which was less than the minimum reported doubling time of 11 days for AMX (Strous et al., 1998) in an SBR, and this possibly caused washout within the first few days before granules started developing. While others have predicted that SRTs as short as three days are possible (Lotti et al., 2015a; Zhang et al., 2017), we did not observe that with our data. Second, since the influent contained only ammonium and not nitrite, AMX growth had to rely on AOB activity and achieving nitrite accumulation, neither of which was stable during the start-up period.

Collectively, these results suggest that a less aggressive start up condition is required to retain a higher percentage AMX population. A less aggressive start-up condition could be implemented to include: (i) gradually decreasing the settling time to maintain an adequate SRT until granules start to appear; (ii) supplementing the feed with nitrite during start-up until the initial development of granules is observed; and (iii) incorporating an anaerobic phase at the beginning of the run. The last two actions where demonstrated by Winkler et al. (2012) for integration of

anammox to out-compete acetate in a granular system that received a higher organic (0.6 kg-COD/m^3/d) and N (1.14 kg-N/m^3/d) loading than this study. In addition to these actions, start-up can be further improved by incorporating intermittent aeration to match the rate of nitritation with the rate of anammox activity in the system. This can be achieved by using a SMC to dynamically adjust the aerobic and anaerobic durations to promote partial nitritation/anammox while suppressing NOB. Further studies are needed to demonstrate the viability of these ideas.

3.5. Conclusions

We demonstrated that successful N-removal from a dilute mainstream wastewater requires a robust real-time control strategy for effective utilization of resources and reduced energy expense. We showed that it is possible to develop a granular sludge in a low carbon-loaded system that can effectively suppress NOB activity so that N-removal can be achieved via partial nitritation/anammox. Key operational strategies were identified and include using low DO intermittent aeration with ABAC (i.e. to maintain minimum residual ammonium). The findings of this research indicate that it is possible to remove nitrogen in a single compact system and with less aeration energy expended if simultaneous nitritation, anammox and heterotrophic denitrification are enabled with the assistance of SMC.

3.6. References

Barr, J. J., Cook, A. E., & Bond, P. L. (2010). Granule formation mechanisms within an aerobic wastewater system for phosphorus removal. *Applied and Environmental Microbiology*, *76*(22), 7588–7597. https://doi.org/10.1128/AEM.00864-10

Blackburne, R., Vadivelu, V. M., Yuan, Z., & Keller, J. (2007). Kinetic characterisation of an enriched Nitrospira culture with comparison to Nitrobacter. *Water Research*, *41*(14), 3033–3042. https://doi.org/10.1016/J.WATRES.2007.01.043

Blackburne, R., Yuan, Z., & Keller, J. (2008). Demonstration of nitrogen removal via nitrite in a sequencing batch reactor treating domestic wastewater. *Water Research*, *42*(8–9), 2166–2176. https://doi.org/10.1016/J.WATRES.2007.11.029

Brockmann, D., & Morgenroth, E. (2010). Evaluating operating conditions for outcompeting nitrite oxidizers and maintaining partial nitrification in biofilm systems using biofilm modeling and Monte Carlo filtering. *Water Research*, *44*, 1995–2009. https://doi.org/10.1016/j.watres.2009.12.010

Cao, Y., van Loosdrecht, M. C. M., & Daigger, G. T. (2017). Mainstream partial nitritation–anammox in municipal wastewater treatment: status, bottlenecks, and further studies. *Applied Microbiology and Biotechnology*, *101*(4), 1365–1383. https://doi.org/10.1007/s00253-016-8058-7

Daigger, G. T. (2014). Oxygen and Carbon Requirements for Biological Nitrogen Removal Processes Accomplishing Nitrification, Nitritation, and Anammox. *Water Environment Research*, *86*(3), 204–209. https://doi.org/10.2175/106143013X13807328849459

de Graaff, M. S., van den Brand, T. P. H., Roest, K., Zandvoort, M. H., Duin, O., & van Loosdrecht, M. C. M. (2016). Full-Scale Highly-Loaded Wastewater Treatment Processes (A-Stage) to Increase Energy Production from Wastewater: Performance and Design Guidelines. *Environmental Engineering Science*, *33*(8), 571–577. https://doi.org/10.1089/ees.2016.0022

de Kreuk, M. K., Heijnen, J. J., & van Loosdrecht, M. C. M. (2005). Simultaneous COD, nitrogen, and phosphate removal by aerobic granular sludge. *Biotechnology and Bioengineering*, *90*(6), 761–769. https://doi.org/10.1002/bit.20470

Delgado Vela, J., Dick, G. J., & Love, N. G. (2018). Sulfide inhibition of nitrite oxidation in activated sludge depends on microbial community composition. *Water Research*, *138*, 241–249. https://doi.org/10.1016/j.watres.2018.03.047

Delgado Vela, J., Stadler, L. B., Martin, K. J., Raskin, L., Bott, C. B., & Love, N. G. (2015). Prospects for Biological Nitrogen Removal from Anaerobic Effluents during Mainstream Wastewater Treatment. *Environmental Science & Technology Letters*, *2*(9), 234–244. https://doi.org/10.1021/acs.estlett.5b00191

Diamantis, V., Verstraete, W., Eftaxias, A., Bundervoet, B., Vlaeminck, S. E., Melidis, P., & Aivasidis, A. (2013). Sewage pre-concentration for maximum recovery and reuse at decentralized level. *Water Science and Technology*, *67*(6), 1188–1193. https://doi.org/10.2166/wst.2013.639

Gilbert, E. M., Agrawal, S., Brunner, F., Schwartz, T., Horn, H., & Lackner, S. (2014). Response of different Nitrospira Species to anoxic periods depends on operational DO. *Environmental Science and Technology*, *48*(5). https://doi.org/10.1021/es404992g

Jafari Kang, A., & Yuan, Q. (2017). Long-term stability and nutrient removal efficiency of aerobic granules at low organic loads. *Bioresource Technology*, *234*, 336–342. https://doi.org/10.1016/J.BIORTECH.2017.03.057

Jetten, M. S. M., Horn, S. J., & van Loosdrecht, M. C. M. (1997). Towards a more sustainable municipal wastewater treatment system. *Water Science and Technology*, *35*(9). http://wst.iwaponline.com/content/35/9/171

Jimenez, J., Miller, M., Bott, C., Murthy, S., De Clippeleir, H., & Wett, B. (2015). High-rate activated sludge system for carbon management – Evaluation of crucial process mechanisms and design parameters. *Water Research*, *87*, 476–482. https://doi.org/10.1016/J.WATRES.2015.07.032

Kornaros, M., Dokianakis, S. N., & Lyberatos, G. (2010). Partial nitrification/denitrification can be attributed to the slow response of nitrite oxidizing bacteria to periodic anoxic disturbances. *Environmental Science & Technology*, *44*(19), 7245–7253. https://doi.org/10.1021/es100564j

Kozich, J. J., Westcott, S. L., Baxter, N. T., Highlander, S. K., & Schloss, P. D. (2013). Development of a Dual-Index Sequencing Strategy and Curation Pipeline for Analyzing Amplicon Sequence Data on the MiSeq Illumina Sequencing Platform. *Applied and Environmental Microbiology*, *79*(17), 5112–5120. https://doi.org/10.1128/AEM.01043-13

Lemaire, R., Marcelino, M., & Yuan, Z. (2008). Achieving the nitrite pathway using aeration phase length control and step-feed in an SBR removing nutrients from abattoir wastewater. *Biotechnology and Bioengineering*, *100*(6), 1228–1236. https://doi.org/10.1002/bit.21844

Liu, Y., Yang, S.-F., & Tay, J.-H. (2003). Elemental compositions and characteristics of aerobic granules cultivated at different substrate N/C ratios. *Applied Microbiology and Biotechnology*, *61*(5–6), 556–561. https://doi.org/10.1007/s00253-003-1246-2

Lochmatter, S., Gonzalez-Gil, G., & Holliger, C. (2013). Optimized aeration strategies for nitrogen and phosphorus removal with aerobic granular sludge. *Water Research*, *47*(16), 6187–6197. https://doi.org/10.1016/j.watres.2013.07.030

Lotti, T., Kleerebezem, R., Abelleira-Pereira, J. M., Abbas, B., & van Loosdrecht, M. C. M. (2015). Faster through training: The anammox case. *Water Research*, *81*, 261–268. https://doi.org/10.1016/j.watres.2015.06.001

Lotti, T., Kleerebezem, R., Hu, Z., Kartal, B., Jetten, M., & Van Loosdrecht, M. C. M. (2014). Simultaneous partial nitritation and anammox at low temperature with granular sludge. *Water Research*, *66*, 111–121. https://doi.org/10.1016/j.watres.2014.07.047

Lotti, T., Kleerebezem, R., & Loosdrecht, M. C. M. Van. (2015). Effect of Temperature Change on Anammox Activity. *Biotechnology and Bioengineering*, *112*(1), 98–103. https://doi.org/10.1002/bit.25333

Lotti, T., Kleerebezem, R., & van Loosdrecht, M. C. M. (2015). Effect of temperature change on anammox activity. *Biotechnology and Bioengineering*, *112*(1), 98–103. https://doi.org/10.1002/bit.25333

Ma, B., Bao, P., Wei, Y., Zhu, G., Yuan, Z., & Peng, Y. (2015). Suppressing Nitrite-oxidizing Bacteria Growth to Achieve Nitrogen Removal from Domestic Wastewater via Anammox Using Intermittent Aeration with Low Dissolved Oxygen. *Nature Publishing Group*. https://doi.org/10.1038/srep13048

Miller, M. W., DeArmond, J., Elliott, M., Kinyua, M., Kinnear, D., Wett, B., Murthy, S., & Bott, C. B. (2016). Settling and dewatering characteristics of an A-stage activated sludge process

proceeded by shortcut biological nitrogen removal. *International Journal of Water and Wastewater Treatment*, *2*(5), 1–8. https://doi.org/http://dx.doi.org/10.16966/2381-5299.133

Ni, B.-J., Xie, W.-M., Liu, S.-G., Yu, H.-Q., Wang, Y.-Z., Wang, G., & Dai, X.-L. (2009). Granulation of activated sludge in a pilot-scale sequencing batch reactor for the treatment of low-strength municipal wastewater. *Water Research*, *43*(3), 751–761. https://doi.org/10.1016/j.watres.2008.11.009

Peng, Y., & Zhu, G. (2006). Biological nitrogen removal with nitrification and denitrification via nitrite pathway. *Applied Microbiology and Biotechnology*, 15–26. https://doi.org/10.1007/s00253-006-0534-z

Pérez, J., Lotti, T., Kleerebezem, R., Picioreanu, C., & van Loosdrecht, M. C. M. (2014). Outcompeting nitrite-oxidizing bacteria in single-stage nitrogen removal in sewage treatment plants: A model-based study. *Water Research*, *66*, 208–218. https://doi.org/10.1016/J.WATRES.2014.08.028

Peyong, Y. N., Zhou, Y., Abdullah, A. Z., & Vadivelu, V. (2012). The effect of organic loading rates and nitrogenous compounds on the aerobic granules developed using low strength wastewater. *Biochemical Engineering Journal*, *67*, 52–59. https://doi.org/10.1016/J.BEJ.2012.05.009

Philips, S., Laanbroek, H. J., & Verstraete, W. (2002). Origin, causes and effects of increased nitrite concentrations in aquatic environments. In *Reviews in Environmental Science and Biotechnology*. https://doi.org/10.1023/A:1020892826575

Poot, V., Hoekstra, M., Geleijnse, M. A. A., van Loosdrecht, M. C. M., & Pérez, J. (2016). Effects of the residual ammonium concentration on NOB repression during partial nitritation with granular sludge. *Water Research*, *106*, 518–530. https://doi.org/10.1016/j.watres.2016.10.028

Raghoebarsing, A. A., Pol, A., Van De Pas-Schoonen, K. T., Smolders, A. J. P., Ettwig, K. F., Rijpstra, W. I. C., Schouten, S., Sinninghe Damsté, J. S., Op Den Camp, H. J. M., Jetten, M. S. M., & Strous, M. (2006). A microbial consortium couples anaerobic methane oxidation to denitrification. *Nature*, *440*(7086), 918–921. https://doi.org/10.1038/nature04617

Regmi, P., Bunce, R., Miller, M. W., Park, H., Chandran, K., Wett, B., Murthy, S., & Bott, C. B. (2015). Ammonia-based intermittent aeration control optimized for efficient nitrogen removal. *Biotechnology and Bioengineering*. https://doi.org/10.1002/bit.25611

Regmi, P., Miller, M. W., Holgate, B., Bunce, R., Park, H., Chandran, K., Wett, B., Murthy, S., & Bott, C. B. (2014). Control of aeration, aerobic SRT and COD input for mainstream nitritation/denitritation. *Water Research*, *57*, 162–171. https://doi.org/10.1016/j.watres.2014.03.035

Sarma, S. J., Tay, J. H., & Chu, A. (2017). Finding Knowledge Gaps in Aerobic Granulation Technology. In *Trends in Biotechnology* (Vol. 35, Issue 1, pp. 66–78). https://doi.org/10.1016/j.tibtech.2016.07.003

Schloss, P. D., Westcott, S. L., Ryabin, T., Hall, J. R., Hartmann, M., Hollister, E. B., Lesniewski, R. a., Oakley, B. B., Parks, D. H., Robinson, C. J., Sahl, J. W., Stres, B., Thallinger, G. G., Van

Horn, D. J., & Weber, C. F. (2009). Introducing mothur: Open-source, platform-independent, community-supported software for describing and comparing microbial communities. *Applied and Environmental Microbiology*, *75*(23), 7537–7541. https://doi.org/10.1128/AEM.01541-09

Sinha, B., Ajit, A., & Annachhatre, P. (2006). *Partial nitrification—operational parameters and microorganisms involved*. https://doi.org/10.1007/s11157-006-9116-x

Smith, A. L., Skerlos, S. J., & Raskin, L. (2013). Psychrophilic anaerobic membrane bioreactor treatment of domestic wastewater. *Water Research*, *47*, 1655–1665. https://doi.org/10.1016/j.watres.2012.12.028

Smith, A. L., Stadler, L. B., Cao, L., Love, N. G., Raskin, L., & Skerlos, S. J. (2014). Navigating Wastewater Energy Recovery Strategies: A Life Cycle Comparison of Anaerobic Membrane Bioreactor and Conventional Treatment Systems with Anaerobic Digestion. *Environmental Science & Technology*, *48*, 5972–5981. https://doi.org/10.1021/es5006169

Souza, T. S. O., & Foresti, E. (2013). Sulfide-Oxidizing Autotrophic Denitrification: an Evaluation for Nitrogen Removal from Anaerobically Pretreated Domestic Sewage. *Applied Biochemistry and Biotechnology*, *170*(5), 1094–1103. https://doi.org/10.1007/s12010-013-0261-8

Strous, M., Jetten, M. S. M., Heijnen, J. J., & Kuenen, J. G. (1998). The sequencing batch reactor as a powerful tool for the study of slowly growing anaerobic ammonium-oxidizing microorganisms. *Applied Microbiology and Biotechnology*, *50*(1998), 589–596. https://doi.org/10.1007/s002530051340

Szabó, E., Liébana, R., Hermansson, M., Modin, O., Persson, F., & Wilén, B. M. (2017). Microbial population dynamics and ecosystem functions of anoxic/aerobic granular sludge in sequencing batch reactors operated at different organic loading rates. *Frontiers in Microbiology*, *8*(MAY). https://doi.org/10.3389/fmicb.2017.00770

Tao, Y., Gao, D.-W., Fu, Y., Wu, W.-M., & Ren, N.-Q. (2012). Impact of reactor configuration on anammox process start-up: MBR versus SBR. *Bioresource Technology*, *104*, 73–80. https://doi.org/10.1016/j.biortech.2011.10.052

Tay, J. H., Pan, S., He, Y., & Tay, S. T. L. (2004). Effect of organic loading rate on aerobic granulation. I: Reactor performance. *Journal of Environmental Engineering*, *130*(10), 1094–1101. https://doi.org/10.1061/(ASCE)0733-9372(2004)130:10(1094)

Wan, J., Gu, J., Zhao, Q., & Liu, Y. (2016). *COD capture: a feasible option towards energy self-sufficient domestic wastewater treatment*. https://doi.org/10.1038/srep25054

Wett, B., Omari, A., Podmirseg, S. M., Han, M., Akintayo, O., Gómez Brandón, M., Murthy, S., Bott, C., Hell, M., Takács, I., Nyhuis, G., & O'Shaughnessy, M. (2013). Going for mainstream deammonification from bench to full scale for maximized resource efficiency. *Water Science and Technology*, *68*(2), 283–289. https://doi.org/10.2166/wst.2013.150

Wett, B., Podmirseg, S. M., Gómez-Brandón, M., Hell, M., Nyhuis, G., Bott, C., & Murthy, S. (2015). Expanding DEMON Sidestream Deammonification Technology Towards

Mainstream Application. *Water Environment Research*, *87*(12), 2084–2089. https://doi.org/10.2175/106143015X14362865227319

Winkler, M.-K. H., Kleerebezem, R., & van Loosdrecht, M. C. M. (2012). Integration of anammox into the aerobic granular sludge process for main stream wastewater treatment at ambient temperatures. *Water Research*, *46*(1), 136–144. https://doi.org/10.1016/j.watres.2011.10.034

Zhang, C., Zhang, H., & Yang, F. (2015). Diameter control and stability maintenance of aerobic granular sludge in an A/O/A SBR. *Separation and Purification Technology*, *149*, 362–369. https://doi.org/10.1016/j.seppur.2015.06.010

Zhang, L., Narita, Y., Gao, L., Ali, M., Oshiki, M., & Okabe, S. (2017). Maximum specific growth rate of anammox bacteria revisited. *Water Research*, *116*, 296–303. https://doi.org/10.1016/J.WATRES.2017.03.027

Zhou, Y., Zhang, D. Q., Le, M. T., Puah, A. N., Ng, W. J., Qing, D., Minh, Z., & Le, T. (2013). *Energy utilization in sewage treatment-a review with comparisons*. https://doi.org/10.2166/wcc.2013.117

Chapter 4

Long-term stability and performance of an aerobic granular sludge reactor and adaptive sensor-mediated control scheme for nitrogen removal from wastewater

Zerihun A. Bekele[1], Charles B. Bott[2], and Nancy G. Love[1,*]

[1]Department of Civil Engineering and Environmental Engineering, University of Michigan, 1351 Beal Ave, Ann Arbor, MI 48109, USA (Email: *zerualem@umich.edu, nglove@umich.edu*)

[2]Hampton Roads Sanitation District, 1434 Air Rail Ave, Virginia Beach, Virginia 23455, USA (Email: *cbott@hrsd.com*)

Abstract

The long-term stability and performance of an aerobic granular sludge reactor that employed adaptive sensor-mediated control with the aim of nitrogen removal from a dilute mainstream wastewater was studied. The system was studies for 650 days under different influent organic carbon (0-100 mg/L), ammonium (50-60 mg-N/L) and nitrite (0-20 mg-N/L) conditions. A novel sensor-mediated aeration control strategy with adaptive intermittent aeration and ammonium-based aeration control was employed to achieve high nitrogen removal in a single reactor. The granulation extent showed a positive correlation with the organic loading rate, and achieved sufficient granulation at loading rate of (0.2 kg-COD/m^3/day). The system maintained a nitrification rate of 97±1% and achieved total inorganic nitrogen removal of above 89±2%. The results show that using an adaptive aeration control strategy is key to achieving efficient nitrogen

removal from a dilute mainstream wastewater by integrating anammox and heterotrophic denitrification.

4.1. Introduction

To support the efforts of driving water resource recovery facilities towards energy self-sufficiency, novel technologies and processes that are resource and energy efficient are being widely investigated. Towards this effort, aerobic granular sludge reactor (GSR) technology has become a prominent alternative treatment system for both high strength sidestream and low strength mainstream wastewaters. In a GSR system, a granular biomass is developed by subjecting activated sludge flocs to shear force, short settling, feast-famine phases, and other selective pressures. This results in self-aggregation of biomass in to compact, dense and fast settling spherical biofilms as opposed to the conventional activated sludge flocs. As a result, GSR technology requires a smaller footprint by increasing biomass retention capacity and eliminating the need for a separate clarifier, which makes the technology more economical and environmentally sustainable, especially in urban settings.

Individual granules host a bacterial consortium that resides in different redox layers. Consequently, GSR has the potential for simultaneous removal of multiple substrates on an individual granule. This is desirable since a typical wastewater contains at least organic carbon and ammonium nitrogen, which rely upon multiple redox conditions for both to be removed, and avoids multi-redox flow-through treatment units. Due to these attractive characteristics there have been more applications of GSR in the last two decades for medium to high strength wastewater treatment (de Kreuk, Heijnen, et al., 2005; Derlon et al., 2016; Lackner et al., 2014; Yali Liu et al., 2015; Pronk et al., 2015). As a consequence, there is also an interest to using granules for dilute mainstream wastewater. However, granulation and the long-term stability of granules has been reported as a bottleneck slowing broader implementation of the technology (Hamza et al., 2018; Kang & Yuan, 2017; Yang et al., 2004; Yuan et al., 2017). .

Due to the low organic and nitrogen load present in dilute domestic wastewater, granulation and long-term stable operation have been a bottleneck for the application of GSR. Several researchers have identified that developing or sustaining granules for long-term is a challenge below a certain organic or nitrogen loading rates (Sarma & Tay, 2018). Adequate organic loading rate (Szabó et al., 2017), low food to mass (F/M) ratio (Hamza et al., 2018) and lack of sufficient exocellular polymeric substances (EPS) (Yuan et al., 2017) are factors given for poor. More specifically, organic carbon is needed to support the growth of ordinary heterotrophic organisms (OHO), which are also the major source of EPS that is needed for granulation (Luo et al., 2014). To date, the lowest OLR, NLR or OLR plus NLR reported, under which successful granulation has been achieved, are 0.6 kg COD/m^3/day (Ni et al., 2009; Peyong et al., 2012), 1 kg-N/m^3/d (Chen et al., 2019), and 0.2 kg-COD/m^3/day plus 0.1 kg-N/m^3/day (Bekele et al., 2020), respectively. Under these loading rates granules with smaller diameter between 0.4 to 1 mm have been developed.

More recently, novel approaches have been introduced to achieve nitrogen (N) removal through partial nitritation and anaerobic ammonia oxidation (anammox) (PN/A) processes, which realize several advantages over conventional nitrification-denitrification processes. Stoichiometry indicates that, using PN/A reduces oxygen demand by up to 25%, organic carbon by up to 40% and sludge production by up to 75% (Yu Liu et al., 2020). Hence, it is considered a more resource efficient and sustainable biological nitrogen removal approach that drives water recovery facilities towards an energy neutral or net generation. However, successful implementation of PN/A requires use of a robust aeration control strategy to limit competition for resources by other organisms. Specifically, competition for nitrite between anammox, OHOs and nitrite oxidizing bacteria (NOB) is one of the challenges of PN/A in both biofilm and flocculant treatment systems. Furthermore, in the presence of organic carbon, OHOs could easily consume oxygen and prevent ammonia oxidizing bacteria (AOB), which produce nitrite, from performing. Finally, GSR system N-removal performance is strongly influenced by COD:N ratio, which can be hard to control.

To take advantage of the potential benefits of GSR, the challenges of low-strength wastewater deterring its use must be addressed. In our previous work (Bekele et al., 2020) we showed that stable granulation and suppression of NOB can be achieved for low strength wastewater with a COD:N ratio of 2 by applying a proper aeration control strategy. However, we did not achieve N removal beyond 60%. In comparison, Chen et al. (2019) reported 72+10% N removal for a wastewater containing 50mg-N/L and using a treatment system with a short HRT, which is promising. We expect that higher N removal can be achieved and sustained with an improved aeration control strategy. Previously Kishida et al. (2008) and Gao et al., (2011) reported the use of real-time aeration control in GSR using pH and ORP sensors. However, real-time control to support N removal in GSR receiving very low-strength wastewater, such as for effluent from an upstream A-stage carbon capture system, has not been investigated. To that end, a novel sensor mediated control (SMC) scheme with adaptive intermittent aeration was developed based on lessons learned from our previous work and was used to achieve improved N-removal with GSR technology.

We developed a GSR with a novel SMC strategy to optimize aeration and N removal efficiency from a dilute synthetic wastewater with a COD:N ratio up to 2. The system achieved improved performance and long-term operational stability. We further investigated the impact of organic loading on granulation and performance. In addition, we evaluated the effect of operational strategies on the retention of anammox in granules, and maintenance of anammox activity over an extended period. Furthermore, we demonstrated the importance of an adaptive aeration strategy to improve N removal from a dilute mainstream wastewater.

4.2. Methods and Materials

4.2.1. **Reactor setup**

The granular sludge reactor was a closed, glass column reactor with a diameter of 76.2 mm and a working volume of 4.5 L. Aeration was achieved using a glass fine bubble diffuser placed at the bottom of the reactor with a superficial upflow velocity of 1.6 cm/s. The reactor was started with an initial biomass concentration of 5,500 mg-TSS/L, which was obtained by using a seed sludge provided by Hampton Roads Sanitation District's (Norfolk, Virginia, USA) full-scale deammonification (DEMON) reactor. A synthetic feed was used to simulate a dilute mainstream anaerobic digester and contained: VFAs (50% acetate and 50% propionate by COD) ranging from 10 – 100 mg-COD/L; ammonium at 53±8 mg-N/L; dissolved methane at approximately 22 mg-CH_4/L at saturation; and other trace elements. For the details of the media and preparation of procedure refer Zerihun et al. (2020).

For monitoring and controlling, the reactor was equipped with sensors including: an optical dissolved oxygen sensor (WTW; FDO 925; Xylem Inc.); pH meter (accumet® Electrode; Fisher Scientific); and NH_4^+/NO_3^- sensor (IQ SensorNet VARiON® Plus Sensors, Xylem Inc.). The pH was monitored using the pH meter and was maintained between 7.3 ± 0.2 and 8.0 ± 0.2 by dosing $NaHCO_3$ when the pH dropped below 7.3 or aerating when pH surpassed 8.0. The entire experiment was conducted at an ambient temperature between 20 and 23°C.

4.2.2. **Cycle operation**

The reactor was operated with varying total cycle duration ranging from 6 to 8 hrs, depending upon the performance. A cycle started with a 40 min slow feeding stage, followed by a reaction phase that was intermittently aerated with a variable duration of 310 – 430 min, a settling time of 4-10 min, and 4 min of decanting with a volumetric exchange ratio of 50%. During the early phases of operation when nitrite was added to the feed, the initial feed phase remained anoxic,

whereas later when nitrite was removed from the feed and we relied only on reactor-generated nitrite, the feed phase was anaerobic. To avoid confusion, through the dissertation we will refer all non-aerated phases as anaerobic phases. During the anaerobic intermittent aeration periods mixing was done by recirculating the head space gas mixed with dinitrogen gas using a diaphragm pump. During aerobic intermittent aeration periods dry air was mixed in with the dinitrogen and head space gases to achieve aeration. A mass flow controller (MFC) was coupled with a PID controller to control the volume of dry air added to the gas stream to achieve the desired DO setpoint.

4.2.3. **Sensor-mediated control (SMC) strategy**

A novel intermittent aeration strategy with an adaptive aeration time and, hence, total batch cycle time was developed to promote partial nitritation and anammox (PN/A) for efficient N removal and is shown schematically in Figure 4.1. The SMC strategy contains a maximum number of intermittent aeration phases, and both minimum and maximum durations for aerobic and anaerobic phases (Table 4.1). The duration of the aeration phases was controlled by the minimum ammonium residual setpoint, and the maximum duration of the anaerobic phases was controlled by the maximum allowed pH. That is, if the pH crossed the maximum allowed, aeration or settling was initiated. The control scheme allows the system to be adaptive to the dynamic conditions of the reactor, which can vary cycle to cycle. Therefore, the aerobic and anaerobic durations, consequently the total cycle time, were varied in order to meet performance goals. This kind of scheme will be even more relevant for real treatment systems where not only the reactor conditions are dynamic but also the influent is variable. All sensors and pumps were controlled using a program we developed in LabVIEW®.

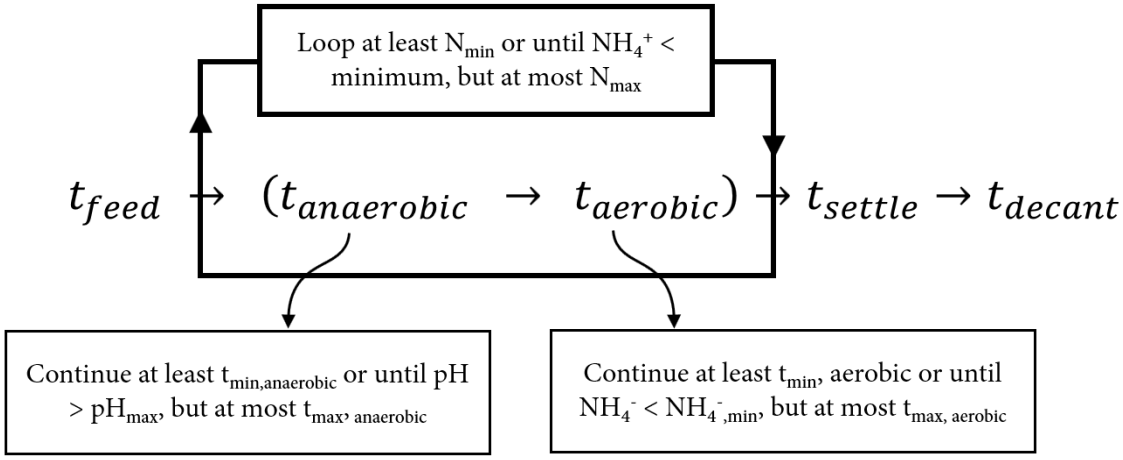

Figure 4.1. The sensor-mediated control scheme with variable aerobic and anaerobic duration controlled by ammonium residual and pH.

Table 4.1. Setting used for the SMC intermittent aeration scheme.

Parameter	Minimum	Maximum	Unit
Number of intermittent cycles	1	6	-
Aerobic duration	5	30	min
Anaerobic duration	30	90	min
Minimum ammonium residual	3	5	mg-N/L
Maximum pH	7.3	8	-

4.2.4. **Long-term operation schedule**

The reactor was operated continuously for 650 days under seven different influent conditions as presented in Table 4.2. The different phases were designed to investigate the impact of organic carbon on granulation, and the impact of the organic carbon (as COD) to N ratio (COD:N) on total inorganic N (TIN) removal performance. The first phase was run for 110 days with ammonium (50 mg-N/L) and nitrite (20 mg-N/L) in the influent to support the retention and further development of anammox bacteria, but without supplemental organic carbon. After the first phase, the organic carbon was gradually increased from 10 to 100 mg-COD/L by Phase 5. Throughout the seven phases, the DO setpoint was kept at 0.3 mg/L and the minimum residual ammonium was maintained at 5 mg-N/L to improve NOB suppression and anammox activity.

Table 4.2: Different phases and operation schedule used for the experiment

Phases	**1**	**2**	**3**	**4**	**5**	**6**	**7**
Operation days	0–110	111–200	201–232	233–300	300–455	455–550	550–650
Influent VFA (mg-COD/L)	0	10	20	80	100	100	100
Influent NO_2^- (mg-N/L)	20	20	20	20	10	0	0
Influent NH_4^+ (mg-N/L)	50	50	50	50	50	60	55
Organic Loading Rate (g-COD/m^3-d)	0	17	34	150	180	200	200
COD:N ratio	0	0.14	0.29	1.14	1.67	1.67	1.82

4.2.5. **Microbial community analysis**

Biomass samples were taken at least once and up to 4 times for each of the seven phases of operation for analyzing the microbial community composition using 16S rRNA gene amplicon sequencing via the Illumina MiSeq platform. The data outputted by the MiSeq analysis was further analyzed using the Mothur MiSeq SOP (Version 1.43.0) (Schloss et al., 2009). The method for DNA extraction and data analysis are outline in Bekele et al. (2020). Final post-processing and visualization of the data were done using a script written in Python which can be found on github.com/zerualem/Sumo-simulation. All MiSeq data have been uploaded to NCBI and can be accessed using the accession number PRJNA549919.

4.2.6. **Modeling and simulation**

As a compliment to the experimental work, a 1-D biofilm granular sludge reactor model was developed with Sumo software (Sumo 19.3.0, Dynamita SARL) to evaluate the relative contribution of anammox and OHO to N removal. The GSR model in Sumo uses a fixed biofilm thickness (or granule radius) with n compartment layers. The first compartment is a variable-volume mixed reactor, while the remaining n-1 layers are spherical granule layers with equal thickness. As depicted in Figure 4.2, the GSR model in Sumo has four main particulate mass balance mechanisms: (1) an internal solids transfer between the biofilm layers described with a diffusion constant and a mass gradient; (2) attachment from the bulk liquid to the biofilm surface

described as a linear function of the bulk TSS concentration; (3) detachment from the biofilm surface to the bulk liquid with a TSS controller that maintains a specified maximum TSS concentration of the reactor; and (4) an internal TSS controller that maintains a uniform TSS concentration among granule layers.

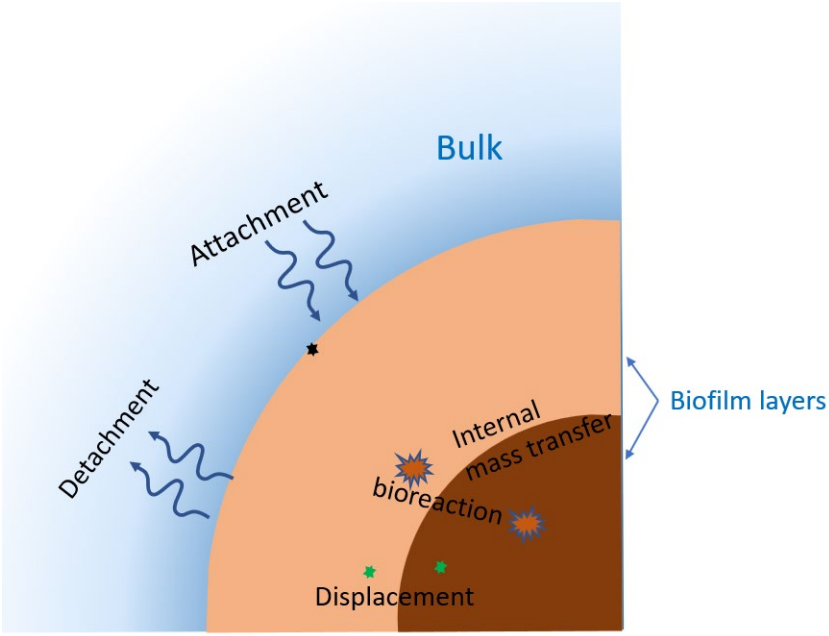

Figure 4.2: Illustration for granules particulate mass balance mechanisms in Sumo.

The biological model includes two-step nitrification, anammox and heterotrophic metabolisms. A biomass concentration of 2,000 mg-TSS/L and a granule diameter of 0.4 mm, which are similar to the last operational phase of the experimental system, were assumed. The simulated condition assumed an influent concentration of 100 mg-COD/L VFA and 50 mg-N/L ammonium. Aeration control was implemented as presented in Section 4.2.3. The stoichiometric and kinetic parameter values used in the simulation are given in Appendix B, Table B-7, and other relevant model parameters are given in Appendix B, Table B-7.

A total of five different single cycle profiles of N species over time were collected during Phase 7 and used to calibrate and validate the model. Three of the profiles were used for calibration (parameter estimation) and two were used for validation. To choose the best model parameters,

the top five parameters obtained from a sensitivity analysis (described in Appendix B, Section 7) were varied using a grid search algorithm we developed in Python while keeping the rest of the model parameters set at their default values. The range of parameters used for the grid search are presented in Appendix B, Table B-6. After conducting a grid search, the best model was chosen with the lowest combined (ammonium, nitrite, and nitrate) standard error of estimate value (Appendix B, Eq. B-2).

4.2.7. **Analytical methods**

Samples were collected from a sample port in the reactor three times a week (with a few exceptions) after settling. Samples were analyzed for ammonium (Standard Method [SM] Sec. 4500-NH3 F), nitrite (SM Sec. 4500-NO_2 – B), nitrate (SM Sec. 4110 B), and methane (SM 2720, 6211, and 6010). In addition, cross-cycle sampling was done over a single operating cycle to obtain profiles of soluble N species that were used for model calibration, as described in Section 4.2.6. Additionally, in situ batch activity tests were conducted to determine nitrification and anammox activities, as described in Appendix A Section 13. The physical characteristics of granules, including diameter, density, and sludge volume index (both SVI_5 and SVI_{30}) were monitored as described in Appendix A, Section 11. All deviation values that are given are at a 95% confidence interval from a t-test distribution.

4.3. Results

4.3.1. **Biomass characteristics across all Phases**

4.3.1.1. Impact of organic loading on granule development and community composition

During Phase 1, we operated the reactor with no VFA, an ammonium load of 0.11 kg-N/m^3/day (NH_4^+ + NO_2^-), and a low DO setpoint (~0.3 mg/L) to facilitate the retention of anammox (AMX). Under these conditions, the specific activity of AMX (SAA), which was 0.194 g-N/g-VSS/day initially, declined slightly to 0.167 g-N/g-VSS/day by the end of Phase 1. This range of SAA values is higher than what was measured during our pervious experiment (Chapter 3,

Bekele et al., 2020). At the same time, the genome-based community analysis showed that the relative abundance of AMX also declined slightly from 15.2 to 11.8% of the total sequenced bacterial community between the start and end of Phase 1. Furthermore, granulation (diameter > 0.2 mm) was not observed during Phase 1 (Figure 4.3b). Starting with Phase 2, we increased the OLR to 0.02 kg COD/m^3/day with VFA addition and assumed this gradual increase would support OHOs growth while minimizing loss of AMX. This loading condition lasted 91 days and generated a small fraction of granules (6% by mass) that had an average diameter of 0.25±0.03 mm. During Phase 3 (31 days), the OLR was doubled to 0.04 kg COD/m^3/day and resulted in both a concomitant doubling of the granule mass fraction (12% by mass) and an increased average granule diameter to 0.31±0.03mm. As shown in Figure 4.3, the gradual increase in OLR to a maximum load of 0.2 kg COD/m^3/day during Phase 6 resulted in a step-wise increase in granule size and fraction to an average diameter of 0.43 $\pm$ 0.03 mm and a granule fraction above 80% by mass. We saw other indications of granule maturation in Phase 6, such as an SVI_5:SVI_{30} ratio of 1.06$\pm$0.01 (Appendix B, Figure B-2). Collectively, these results suggest that a minimum OLR of 0.2 kg COD/m^3/day is needed to initiate sufficient granulation (i.e., greater than 80% granules by mass) at a constant NLR of 0.12 kg-N/m^3/day (de Kreuk, McSwain, et al., 2005).

4.3.1.2. Biomass physical characteristics

Settling time decreased as OLR increased and granules formed. Ultimately, settling time declined from 20 to 5 minutes across the seven phases while the overall biomass concentration initially declined (due to washout after inoculation), then increased to a stable average concentration of 2,013 ± 63 mg TSS/L by Phase 7 (See Appendix B, Figures B-1 and B-4). As granules formed and became a larger fraction of the total biomass (Figure 4.3), the overall SRT of the flocculant biomass that left with the decant was initially 14±2.4 days in Phase one and became 11.4±0.8 days in Phase 7. The SRT of the granular biomass is hard to estimate but is presumed to be much larger, which is necessary to retain slow growing bacteria such as X_{ANX}. To further characterize settleability and granulation, we estimated SVI_{5min} and SVI_{30min} as well as their ratio. The SVI_{5min} (39±4 mL/g) and SVI_{30min} (36±3 mL/g) ratio in Phase 1 was 1.08$\pm$0.22

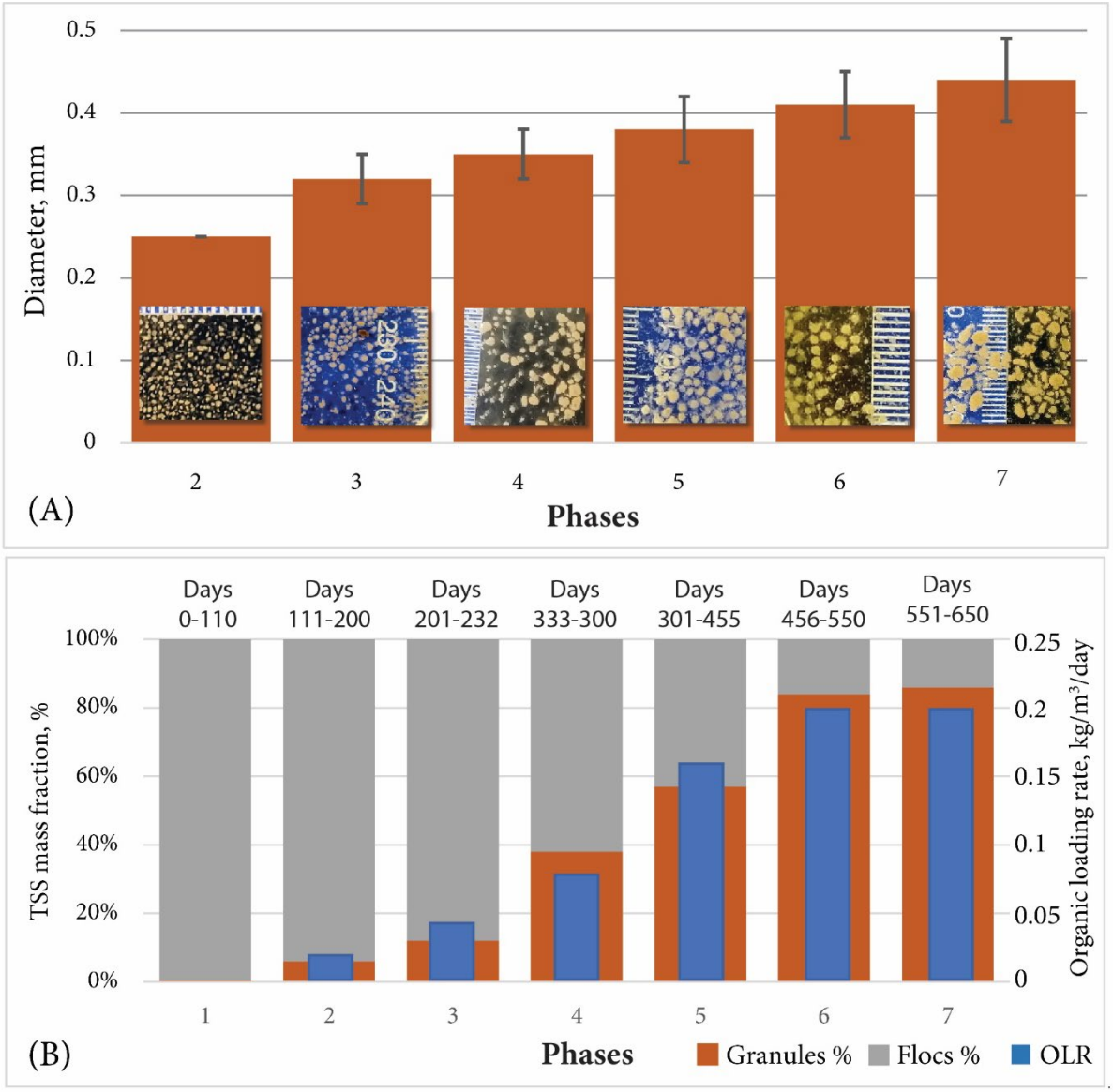

Figure 4.3. (A) Average granule diameter across phases. (B) TSS mass fraction of granules vs flocs from Phase 1 through Phase 7 and the corresponding organic loading rate. In Figure A, the demarcation scale shown on the images is in mm units.

and were largely influenced by the full-scale inoculum. These values slowly increased and remained between 60 mL/g and 80 mL/g for Phases 2 through 5, and had an average SVI_{5min}:SVI_{30min} ratio of 1.16±0.08. The average ratio dropped during the last two phases to 1.05±0.02, which is similar to the ratio of the inoculum and indicates a higher extent of granulation.

4.3.2. **Microbial dynamics across all Phases**

Based on whole community 16S rRNA sequencing analysis across phases and under different operational strategies, the microbial community composition changed significantly from the composition of the original inoculum (Figure 4.4). The top classified phyla present in the inoculum with relative abundance > 1% were (in order from most dominant to least dominant): Proteobacteria (21.9%), Planctomycetes(20.0%), *Chloroflexi* (10.8%), *Ingavibacteria* (9.6%), *Acidobacteria* (7.8%), *Bacteroidetes* (3.6%), Actinobacteria (3.1%), Nitrospirae (2.2%), and *Verrucomicrobia* (1.3%). By Phase 7, the microbial composition changed significantly so that the top Phyla were: Proteobacteria (38.9%), Bacteroidetes (16.6%), *Verrucomicrobia* (11.3%), Planctomycetes (7.9%), *Chloroflexi* (6.5%), and *Ingavibacteria* (3.6%). The dominant OTUs identified as Planctomycetes were mainly comprised of the anammox genera (75%) throughout all phases. The number of dominant ($\geq$ 1%) OTUs declined from 9 to 6 between inoculation and Phase 7. Proteobacteria remained the most dominant phyla and is the most common phyla in wastewater treatment plants (Wu et al., 2019). All six phyla that were dominant in Phase 7 were also present among the most dominant OTUs in the inoculum. Importantly, Planctomycetes represented a smaller fraction of the population but were still dominant, and Nitrospirae, which includes NOB and was dominant in the inoculum, had a relative abundance of 0.01% in the biomass from Phase 7. This shift is reflective of successful out-selection of the taxa.

As presented in Figure 4.4b, the relative abundance of the ammonia oxidizing Proteobacteria Nitrosomonadales (including genus *Nitrosomonas*) declined from 5.0% at the end of Phase 1 to 2.3% by the end of Phase 7. At the same time, the relative abundance of the nitrite-oxidizing bacteria Nitrospirales (including genus *Nitrospira*) was 2.3% in the inoculum but effectively washed out by Phase 7. The anammox Planctomycetes (including the genus *Candidatus Brocadiales*) significantly declined from a relative abundance of 13.6% in Phase 1 to 3.9% in Phase 2, however, starting in Phase 5 it recovered and reached a relative abundance of 7.9% by the end of Phase 7. Collectively, the outcomes shown in Figure 4.4 suggest that both OHOs and

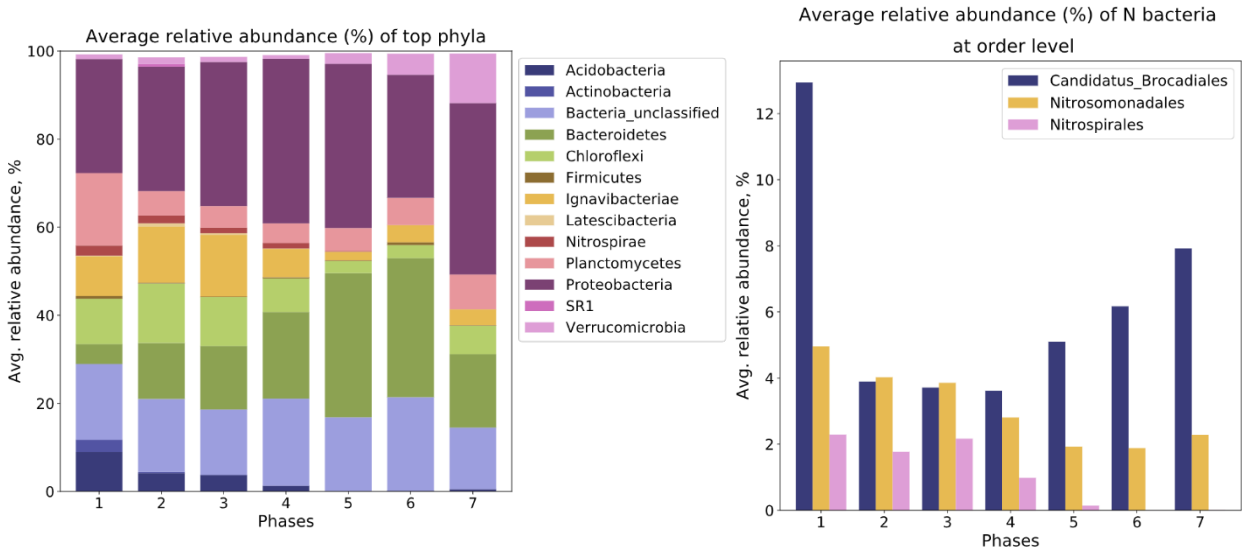

Figure 4.4. (a) Relative abundances (%) of most dominant (>1%) OTUs at the phylum level across different operating phases. (b) Average percent relative abundance of the Order of microorganisms involved with nitrogen transformation for each Phase.

anammox participated in TIN removal, and by the end of the experimental run had minimal competition with NOB for nitrite that was internally generated by AOB.

4.3.3. **Dynamic aeration strategy and nitrogen removal performance**

In contrast to our prior work (Chapter 3; Bekele et al., 2020), the SMC strategy employed with this experiment allowed flexible intermittent aeration and variable aeration cycle length. The intermittent aeration periods depended heavily on the influent condition, which was influenced by the quality of residual effluent that reflected the reactor's performance during the prior cycle. At the beginning of each operational phase, the intermittent aeration setting, characterized as aerobic and anaerobic duration and the number of intermittent cycles, was determined based on previous research work and simulation. The settings were gradually adjusted automatically within each phase via the SMC to ensure that the desired residual ammonium was maintained, and the desired degree of nitrification was achieved by the end of the last aerobic cycle. Using this kind of adaptive aeration strategy allowed us to move toward stable operating conditions that

improved both aeration efficiency and nitrogen removal, two performance goals that are often in tension over large segments of the potential operating range.

4.3.4. **Nitrogen removal performance**

Nitrification was established during the early phases while TIN removal peaked at slightly above 90% during the last two phases of the reactor's operation. Nitrification fluctuated widely during the first phase as the inoculum was acclimating to the reactor environment; however, from Phase 2 until Phase 7, more than 90% of the ammonium in the feed was nitrified (Figure 4.5a). In contrast, TIN removal varied over time, eventually peaking during Phase 7, and was positively correlated with COD:N ratio. During the first three phases of operation when the influent COD:N ratio was low (<0.3), the average TIN removal was between 50 and 60%. The cross-cycle profile data taken during these phases (Appendix B, Table B-2) indicate a steady consumption of nitrite and ammonium during the anaerobic phases, while nitrate increased. For example, nitrite decreased from ~20 mg-N/L in the influent (when it was supplemented) to 1.1±0.6 mg-N/L in the effluent during these phases, while ammonium decreased from 47.8±2.2 to 6±1. At the same time, effluent nitrate averaged 20±2 mg-N/L, yielding an average TIN removal over the three phases of 54.7±3%. Collectively, these measurements support the possibility that a substantial fraction of TIN removal occurred via a metabolic process driven predominantly by nitrite as electron acceptor. In addition, SAA averaged 0.17±01 mg-N/mg-VSS/d during these phases (Appendix B, Figure B-11). These results and the fact that the influent had a low COD:N ratio indicate that much of the TIN removal occurred via anammox. When the COD:N ratio increased to 1.14 starting in Phase 4, the average TIN removal further increased to 75±5%, while the effluent nitrate decreased to 9.3±4.0 mg-N/L and the effluent nitrite doubled while remaining low at 2.4±1.1 mg-N/L. The SAA was 0.105 g-N/g-VSS/d. Hence, the increase in the influent COD:N ratio appeared to drive the observed improvement in TIN removal.

Phase 5 reflected a transition, when the influent nitrite was decreased to 10 mg-N/L, OLR was increased to 0.2 kg-COD/m^3/day, and COD:N was 1.67. During this phase, the TIN removal varied from ~50% at the start of the phase to ~75% at the end (Appendix B, Fig B-6). During Phases 6 and 7 when external nitrite supplementation ended and COD:N was between 1.67 and 1.82, TIN removal gradually increased and stabilized at an average removal rate of 89±2 % and effluent TIN of 6.2±0.6 mg-N/L in Phase 7. In line with this, the anammox SAA gradually increased to 0.139 g-N/g-VSS/day by the end of Phase 7. The reactor performance was most stable during the last two phases that occurred over 195 days, when the influent NLR was ~0.12 kg-N/m^3/day, OLR was ~0.2 kg-COD/m^3/day, COD:N was 1.82, and granules constituted more than 80% of the biomass. This performance is substantially better than our prior work at a COD:N of 2 (Chapter 3, Bekele et al., 2020) when we used SMC but maintained defined aeration and anaerobic cycle lengths. Hence, we were able to achieve high N removal in a granular sludge system by using an adaptive SMC scheme that allowed the aeration and cycle lengths to vary based on performance within any given cycle.

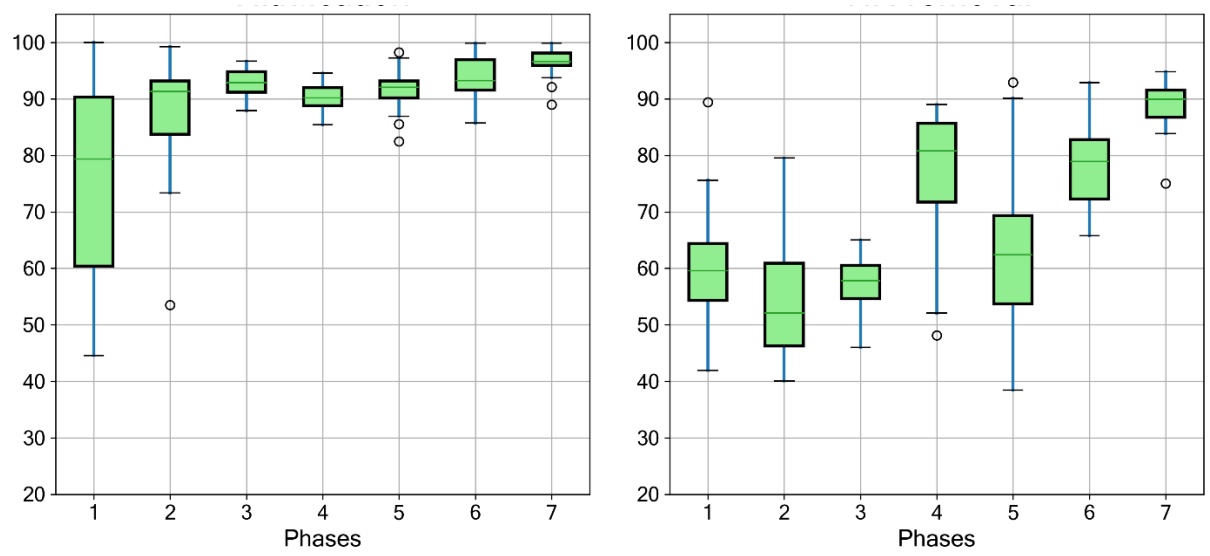

Figure 4.5. Box plots showing (a) nitrification efficiency (%). (b) total inorganic nitrogen (TIN) removal efficiency (%) across the different phases.

4.3.5. **Modeling results**

4.3.5.1. Sensitivity analysis and calibration

After conducting a global sensitivity analysis with 18 model parameters, the sensitivity indices were computed for ammonium, nitrite, and nitrate. The values of the sensitivity indices indicate the average overall effect the parameters have on the given state variables (Appendix B, Figure B-13). From this, the top six parameters with the highest combined influence on ammonium, nitrite, and nitrate were chosen for further calibration. These parameters included: maximum specific growth rate of AOB ($\mu_{max,AOB}$); OHO decay rate (b_{OHO}); oxygen half saturation of AOB ($k_{O2,AOB}$); maximum specific growth rate of AMX ($\mu_{max,AMX}$); maximum specific growth rate of OHO ($\mu_{max,OHO}$); and rate of hydrolysis (q_{HYD}). All identified model parameters except q_{HYD} are normally expected to be outcomes of sensitivity and calibration analysis. The reason q_{HYD} was part of the sensitivity result was due to the fact that the hydrolysis model in the Sumo version used (19.3.0) was calibrated for an anaerobic digestor, but this is expected to be corrected in future Sumo versions. Consequently, future work will include further refinement in model calibration. For purposes of this dissertation, we show the calibrated model as developed and include the calibrated value for q_{HYD}.

These model parameters were calibrated using three different cross-cycle profiles of inorganic N chemical species obtained during Phase 7, and the ranges of the parameters used for the calibration are presented in Appendix A, Table A-6. The parameter values that yielded the lowest combined standard error are presented in Table 4.3. These parameter values were then used for model validation, which was done using two additional cross cycle profiles of inorganic N species obtained during Phase 7. The results of both the calibration and validation are presented in Appendix B, Figures B-14 through B-15.

Table 4.3. Values of the most sensitive parameters with the lowest standard error.

Parameters	$\mu_{max,AOB}$	$k_{O2,AOB}$	$\mu_{max,OHO}$	$\mu_{max,AMX}$	b_{OHO}	q_{HYD}
Unit	per day	mg-O_2/L	per day	per day	per day	per day
Values	0.7	0.25	6.0	0.12	0.45	0.09

4.3.6. **N-removal pathways**

The calibrated and validated model was used to analyze the N-removal pathways among four microbial groups—AOB, NOB, OHO and AMX. From this, the utilization and production rates for nitrite, nitrate, ammonium, and nitrogen gas were obtained, and the fraction of TIN removal within granule layers by OHO versus AMX was determined (Figure 4.6). Based on this analysis, OHO and AMX contributed 42% and 58% to TIN-removal, respectively. While OHOs removed N mostly in the outer layer, AMX also made its greatest contributions to TIN removal via the outer layers. When we look at the rate of N_2 production for AMX, the highest rate (141± 24 mg-N/L/hr) occurred in the inner most layer and decreased to 45±7 mg-N/L/hr radially toward the outer layer (Appendix B, Figure B-14). In contrast for OHOs, the rate of N_2 production decreased radially from the outer layer (85±42 mg-N/L/hr) to the inner layer (10±1 mg-N/L/hr). In addition, 60% of OHO-driven TIN removal occurred during the anaerobic feed phase and the first anaerobic stages, while for AMX almost all N removal occurred after the first aerobic stage.

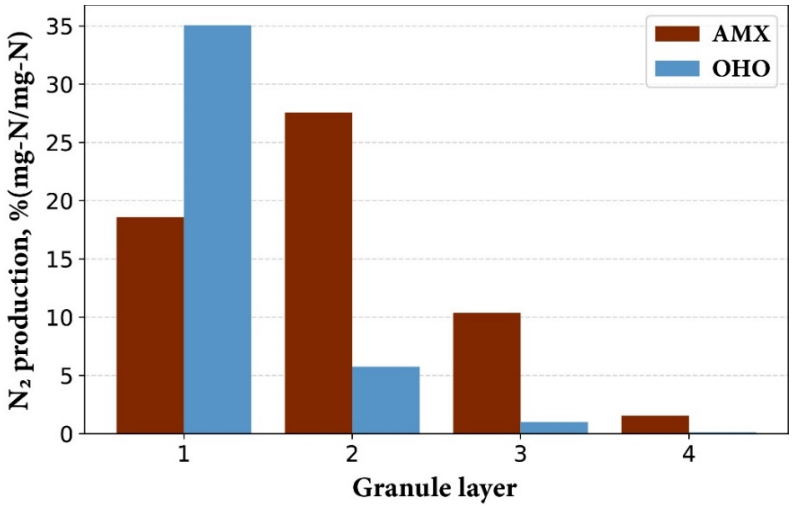

Figure 4.6. Production of N_2 by OHO and AMX in granule layers for a single cycle. Layer 1 is closest to the bulk liquid and layer 4 is the center of the granule. The percentage calculation is given relative to the total N_2 production per cycle.

4.4. Discussion

4.4.1. **Minimum organic loading rate is needed for sufficient granulation**

Operating the reactor under different low OLRs with the same NLR indicated that a minimum OLR was needed to develop a predominantly granular sludge. Once the OLR reached 0.2 kg-COD/m^3/day, the biomass existed predominantly in granular form (>80% by mass) over more than 150 days. Furthermore, our results show a positive correlation between OLR and granulation (Appendix B, Figure B-3). The presence of organic substrate promotes the growth of OHOs, which contributes a higher amount of EPS-producing biomass. Others have reported that heterotrophic organisms play a major role in granule formation in aerobic granular systems as they are known to be the major generators of EPS, which is an important constituent of granule structure (Luo et al., 2014; Peyong et al., 2012; Zhang et al., 2011). Peyong et al. (2012) found that lowering the OLR to 0.13 kg-COD/m^3/day resulted in granule disintegration and biomass washout from their laboratory-scale system. In line with this, we conducted a long-term microbial analysis (Figures 4.3 and B-9 in Appendix B) that shows the consistent presence and development of a strong OHO community. Luo et al., (2014) found also that low COD:N ratio

(<2) could impact the integrity of granules as a result of lower EPS generation. Our results suggest that a higher organic load and presence of a significant and stable OHO population is important for supporting granulation in wastewater with a low nitrogen load.

4.4.2. **Anammox biomass and activity was sustained**

Although the fraction of the microbial community comprised of AMX declined from the inoculum (Candidadus Brocadiales 12.4-13.6% to 8%), its relative percent abundance and specific activity were maintained throughout the seven phases of operation. We attribute this success in part to the adaptive SMC strategy, which is designed to promote PN/A by automatically adjusting the anaerobic: duration based on in-cycle performance. During Phase 1, the reactor was fed only ammonium and nitrite and had a high anaerobic to aerobic duration fraction of 9.5±1.6 (Appendix B, Figure B-12), which was done to retain anammox activity during startup. The initial AMX relative abundance in the inoculated reactor measured at the genus level as Candidatus Brocadiales was 13% (Appendix B, Figure B-10). This dominant composition was mostly maintained through Phase 1 with the lowest measured relative abundance being 11.5%. However, during Phase 2, ammonium and nitrite loading was constant while VFA loading was increased from 0 to 0.02 kg-COD/m^3/day. Furthermore, the anaerobic to aerobic ratio was gradually reduced to 7.5±0.3 to insure sufficient ammonium oxidation by the end of each cycle. Consequently, the anammox population declined significantly to an average relative abundance of 3.9±1.4%.

The SMC strategy helped to retain AMX and to improve granulation. During Phases 3 and 4, the COD:N was increased to 1.14 while the aeration strategy was adjusted to avoid any further loss of AMX. The adjustment in the control strategy was automated through the SMC, which increased the aerobic time to achieve an anaerobic:aerobic duration ratio of 5.2 by the end of Phase 4. This increased nitritation so that there was enough nitrite for anammox consumption. As a result, the anammox relative abundance remained stable during Phases 3 and 4 (3.6±0.6%), and TIN

removal improved to 76±5 percent (Figure 4.4b). Starting with Phase 5, we stopped feeding nitrite while the VFA loading was increased to 0.20±0.01 kg-COD/m^3/day throughout the remaining phases, yielding a COD:N of 1.67. In response, the SMC system automatically reduced the anaerobic to aerobic ratio to 3 to maintain nitritation. Consequently, similar to what was observed in the previous phases, the AMX relative abundance and SAA increased. At the same time, a significant fraction of the biomass was converted to granular biomass (Figure 4.3b). We believe that the increased aerobic fraction and OLR contributed to granulation. The observation that a higher aerobic fraction improved granulation and granule stability has been previously reported (Mosquera-Corral et al., 2005; Rollemberg et al., 2020). On the other hand, too much aeration will adversely affect N-removal performance. Hence, it can be concluded that an optimum aeration is needed that does not compromise granule stability and N-removal performance. In this study, we moved toward this operating condition by employing an adaptive intermittent aeration scheme using a SMC, which prioritized N-removal performance.

Microbial community changes were consistent with the observed improvement in TIN removal performance. AMX relative abundance decreased after inoculation and after the initial granulation phases; however, it returned to 7.9% in the last phase of operation. This anammox SAA is comparable with what was obtained in (Bekele et al., 2020). In addition, samples taken during Phase 5, 6, and 7, when granules and flocs were separated using a 0.2 mm sieve and the microbial community structure was analyzed separately indicate that granules had a higher relative abundance of anammox than flocs (Appendix B, Figure B-7 through B-9). Hence, since granules made up the majority of biomass during those phases, it is reasonable to conclude that the anammox population was stably maintained.

Overall, these results indicate that our granules contained a consortium of key microorganisms. Some of these microorganisms played a major role in initial granule formation while others supported the development of mature and stable granules. In parallel, the microbial community structure in the reactor shifted to a bacterial community that is specialized in nitrification and

denitrification, which allowed individual granules to perform multiple metabolisms. Hence, the microbial dynamics observed in our system clearly indicates a significant shift both in the community structure and function as a result of the adaptive SMC strategy implemented across the different phases for the given influent composition.

4.4.3. **High N removal was achieved using adaptive SMC**

The results presented in Figure 4.4 suggest that GSR with real-time SMC shows promise for use with mainstream N removal when treating low strength wastewater. The techniques used in this research resulted not only in higher N removal, but also in the development of a stable granular biomass, which has not been successful demonstrated previously with low strength wastewater. The highest N removal reported using low strength (<2 kg-COD/m^3/day) wastewater was ~90% by Liu et al., (2007). However, their experiment was only performed for 22 days and with a COD:N of 4, higher than what was used in our research. Chen et al. (2019) reported an average of 72% N removal using a higher NLR of 2.4 kg-N/m^3/day but with no organic carbon (COD:N=0). In the present study, besides performance improvements, the use of adaptive SMC to improve the timing of intermittent aeration by automatically adjusting cycle length is a novel approach that can help to increase process stability and reduce aeration expense.

The adaptive aeration control strategy applied in this work is a promising method to achieve N-removal for pre-treated, dilute mainstream wastewater. This improved aeration strategy is one of the key differences between the previous work, where N-removal peaked at 60%, and this work where the N-removal was 89±2% during the last operational phase, which lasted 100 days (Figure 4.4b). Our previous study indicated that suppression of NOB and partial nitritation can be achieved with a low DO setpoint and intermittent aeration coupled with ammonium residual control. However, the limited N-removal called for more aggressive control of the intermittent aeration. Hence, controlling the individual aerobic and anaerobic durations with ammonium and pH-based aeration control was evaluated in this work. Previously, (Kishida et al., 2008) used pH

to detect end of nitrification and (Gao et al., 2011) used pH and DO to detect nitrification. However, these approaches would not be effective for low strength wastewater because: (1) the signal to indicate the end of nitrification when a low DO setpoint is used is unclear; (2) in fact, our goal was not to have complete nitrification but, rather, it was to achieve partial nitritation; and (3) for NOB suppression short aerobic durations are suggested instead of long aerobic duration.

The aerobic duration increased in response to the reactor's operational conditions. The total anaerobic to aerobic duration ratio decreased from 9.5 in Phase 1 to 3 in Phase 7. The influent in the earlier phases contained nitrite, hence less aerobic time was needed to achieve partial nitritation. However, once nitrite was removed from the influent and VFA was increased in the influent, more aerobic duration was needed to achieve partial nitritation. In our previous experimental result, where we used a fixed intermittent aeration setting, the aerobic fraction was ~0.57 (Chapter 3). However, in the current work we were able to reduce the aerobic fraction to 0.33 at the same time achieving higher TIN removal with the use of an adaptive SMC. This result highlights the potential aeration expense saving that can be achieved using such kind of adaptive aeration control.

In addition to aeration demand for partial nitritation, increased aeration duration could be one factor for improved granulation in our system. The impact of aerobic fraction on granulation was studied by Rollemberg et al. (2020) who observed that a minimum of 55% of aerobic fraction is needed to obtain stable granules in their system. This % value is much higher than what was observed in the system reported here, which had an aerobic fraction of 33% during Phase 7. Ultimately, the % of aerobic fraction will vary based on nitritation needs, nitrogen removal needs, and granulation.

4.4.4. **Both heterotrophic denitrification and anammox contributed to N removal**

As was suggested in our previous work, both anammox and OHOs contributed to N-removal and the result from the modelling is consistent with this hypothesis. The modelling results suggest that anammox is the major contributor for N-removal in the system with up to 62% contribution, indicating a successful PN/A was achieved in the system. Furthermore, the operational strategy allowed the use of VFA for N-removal instead of its aerobic oxidation, which means reduced aeration expense and maximized resource utilization. As a result, the integration of OHO and AMX resulted in higher N-removal during this study. Achieving N-removal with PN/A coupled simultaneously with OHO-driven denitrification is desirable for A-stage effluents, which contain some organic carbon that can be used to achieve denitrification using nitrate produced from PN/A. Thus, coupling PN/A and heterotrophic denitrification will increase the overall N-removal in the system in addition to what can be achieved by only using PN/A, as shown in this work.

4.5. Conclusions

To achieve high N-removal in a cost effective manner with lower aeration expense and no external carbon sources, incorporating PN/A and heterotrophic denitrification is important. This is especially true because the COD:N ratio in pre-treated wastewaters is too low to achieve N-removal using the conventional nitrification-heterotrophic denitrification path. This work showed that higher N-removal can be achieved in a single GSR using an adaptive SMC scheme, which is designed to have an adaptive intermittent aeration period controlled with ammonium-based aeration control. With this strategy it was possible to integrate both anammox and heterotrophic denitrification. Moreover, we showed that organic carbon was instrumental both to achieve granulation and improved N-removal. In addition, such a strategy can be automated and is likely to be especially valuable when implemented in real wastewater where the influent composition is dynamic.

4.6. References

Bekele, Z. A., Delgado Vela, J., Bott, C. B., & Love, N. G. (2020). Sensor-mediated granular sludge reactor for nitrogen removal and reduced aeration demand using a dilute wastewater. *Water Environment Research*, 1–11. https://doi.org/10.1002/wer.1296

Chen, R., Ji, J., Chen, Y., Takemura, Y., Liu, Y., Kubota, K., Ma, H., & Li, Y. Y. (2019). Successful operation performance and syntrophic micro-granule in partial nitritation and anammox reactor treating low-strength ammonia wastewater. *Water Research*, *155*, 288–299. https://doi.org/10.1016/j.watres.2019.02.041

de Kreuk, M. K., Heijnen, J. J., & van Loosdrecht, M. C. M. (2005). Simultaneous COD, nitrogen, and phosphate removal by aerobic granular sludge. *Biotechnology and Bioengineering*, *90*(6), 761–769. https://doi.org/10.1002/bit.20470

de Kreuk, M. K., McSwain, B. S., Bathe, S., Tay, S. T.-L., & N., S. (2005). Discussion outcomes. In *Aerobic granular sludge* (pp. 155–169). IWA Publishing.

Derlon, N., Wagner, J., da Costa, R. H. R., & Morgenroth, E. (2016). Formation of aerobic granules for the treatment of real and low-strength municipal wastewater using a sequencing batch reactor operated at constant volume. *Water Research*, *105*, 341–350. https://doi.org/10.1016/j.watres.2016.09.007

Gao, D., Yuan, X., Liang, H., & Wu, W. M. (2011). Comparison of biological removal via nitrite with real-time control using aerobic granular sludge and flocculent activated sludge. *Applied Microbiology and Biotechnology*, *89*(5), 1645–1652. https://doi.org/10.1007/s00253-010-2950-3

Hamza, R. A., Sheng, Z., Iorhemen, O. T., Zaghloul, M. S., & Tay, J. H. (2018). Impact of food-to-microorganisms ratio on the stability of aerobic granular sludge treating high-strength organic wastewater. *Water Research*, *147*, 287–298. https://doi.org/10.1016/J.WATRES.2018.09.061

Kang, A. J., & Yuan, Q. (2017). *Long-term stability and nutrient removal efficiency of aerobic granules at low organic loads*. https://doi.org/10.1016/j.biortech.2017.03.057

Kishida, N., Tsuneda, S., Sakakibara, Y., Kim, J. H., & Sudo, R. (2008). Real-time control strategy for simultaneous nitrogen and phosphorus removal using aerobic granular sludge. *Water Science and Technology*, *58*(2), 445–450. https://doi.org/10.2166/wst.2008.410

Lackner, S., Gilbert, E. M., Vlaeminck, S. E., Joss, A., Horn, H., & van Loosdrecht, M. C. M. (2014). Full-scale partial nitritation/anammox experiences – An application survey. *Water Research*, *55*, 292–303. https://doi.org/10.1016/J.WATRES.2014.02.032

Liu, Y.-Q., Moy, B. Y.-P., & Tay, J.-H. (2007). COD removal and nitrification of low-strength domestic wastewater in aerobic granular sludge sequencing batch reactors. *Enzyme and Microbial Technology*, *42*(1), 23–28. https://doi.org/10.1016/j.enzmictec.2007.07.020

Liu, Yali, Kang, X., Li, X., & Yuan, Y. (2015). Performance of aerobic granular sludge in a sequencing batch bioreactor for slaughterhouse wastewater treatment. *Bioresource Technology*, *190*, 487–491. https://doi.org/10.1016/j.biortech.2015.03.008

Liu, Yu, Gu, J., & Zhang, M. (2020). Approaches to energy and resource recovery from municipal wastewater. In *A-B Processes: Towards Energy Self-sufficient Municipal Wastewater Treatment* (pp. 29–67). IWA Publishing. https://doi.org/10.2166/9781789060089_0029

Luo, J., Hao, T., Wei, L., Mackey, H. R., Lin, Z., & Chen, G.-H. (2014). Impact of influent COD/N ratio on disintegration of aerobic granular sludge. *Water Research*, *62*, 127–135. https://doi.org/10.1016/j.watres.2014.05.037

Mosquera-Corral, A., de Kreuk, M. K., Heijnen, J. J., & van Loosdrecht, M. C. M. (2005). Effects of oxygen concentration on N-removal in an aerobic granular sludge reactor. *Water Research*, *39*(12), 2676–2686. https://doi.org/10.1016/j.watres.2005.04.065

Ni, B.-J., Xie, W.-M., Liu, S.-G., Yu, H.-Q., Wang, Y.-Z., Wang, G., & Dai, X.-L. (2009). Granulation of activated sludge in a pilot-scale sequencing batch reactor for the treatment of low-strength municipal wastewater. *Water Research*, *43*(3), 751–761. https://doi.org/10.1016/j.watres.2008.11.009

Peyong, Y. N., Zhou, Y., Abdullah, A. Z., & Vadivelu, V. (2012). The effect of organic loading rates and nitrogenous compounds on the aerobic granules developed using low strength wastewater. *Biochemical Engineering Journal*, *67*, 52–59. https://doi.org/10.1016/j.bej.2012.05.009

Pronk, M., de Kreuk, M. K., de Bruin, B., Kamminga, P., Kleerebezem, R., & van Loosdrecht, M. C. M. (2015). Full scale performance of the aerobic granular sludge process for sewage treatment. *Water Research*, *84*, 207–217. https://doi.org/10.1016/j.watres.2015.07.011

Rollemberg, S. L. de S., Ferreira, T. J. T., Firmino, P. I. M., & dos Santos, A. B. (2020). Impact of cycle type on aerobic granular sludge formation, stability, removal mechanisms and system performance. *Journal of Environmental Management*, *256*, 109970. https://doi.org/10.1016/j.jenvman.2019.109970

Sarma, S. J., & Tay, J. H. (2018). Aerobic granulation for future wastewater treatment technology: challenges ahead. *Environ. Sci.: Water Res. Technol*, *4*(9). https://doi.org/10.1039/c7ew00148g

Szabó, E., Liébana, R., Hermansson, M., Modin, O., Persson, F., & Wilén, B. M. (2017). Microbial population dynamics and ecosystem functions of anoxic/aerobic granular sludge in sequencing batch reactors operated at different organic loading rates. *Frontiers in Microbiology*, *8*(MAY). https://doi.org/10.3389/fmicb.2017.00770

Wu, L., Ning, D., Zhang, B., Li, Y., Zhang, P., Shan, X., Zhang, Q., Brown, M., Li, Z., Van Nostrand, J. D., Ling, F., Xiao, N., Zhang, Y., Vierheilig, J., Wells, G. F., Yang, Y., Deng, Y., Tu, Q., Wang, A., … Zhou, H. (2019). Global diversity and biogeography of bacterial communities in wastewater treatment plants. *Nature Microbiology*, *4*(7), 1183–1195. https://doi.org/10.1038/s41564-019-0426-5

Yang, S. F., Liu, Q. S., Tay, J. H., & Liu, Y. (2004). Growth kinetics of aerobic granules developed in sequencing batch reactors. *Letters in Applied Microbiology*, *38*(2), 106–112. https://doi.org/10.1111/j.1472-765X.2003.01452.x

Yuan, S., Gao, M., Zhu, F., Afzal, M. Z., Wang, Y. K., Xu, H., Wang, M., Wang, S. G., & Wang, X. H. (2017). Disintegration of aerobic granules during prolonged operation. *Environmental Science: Water Research and Technology*, *3*(4), 757–766. https://doi.org/10.1039/c7ew00072c

Zhang, H., Dong, F., Jiang, T., Wei, Y., Wang, T., & Yang, F. (2011). Aerobic granulation with low strength wastewater at low aeration rate in A/O/A SBR reactor. *Enzyme and Microbial Technology*, *49*(2), 215–222. https://doi.org/10.1016/J.ENZMICTEC.2011.05.006

Chapter 5

Simulation based evaluation of various feed conditions on the nitrogen removal performance of an aerobic granular sludge reactor with sensor-mediated control

Abstract

To advance wide adaption of aerobic granular sludge reactor (GSR) as a mainstream nitrogen removal alternative, process optimization, stable operation, and efficiency under different influent conditions are needed. To that end, the potential of an experimentally evaluated GSR with a sensor mediate control (SMC) was investigated using simulation to achieve N-removal as a B-stage mainstream system. A biofilm model tailored to a GSR bioreactor implemented as a sequencing batch reactor with intermittent aeration control was used to evaluate the impact of varying influent conditions (VFA from 0 to 200 mg-COD/L, ammonium from 25 to 150 mg-N/L), granule diameters (0.2 to 0.8 mm), and DO setpoints on overall total inorganic nitrogen (TIN) removal. The results show that the system can achieve nitrogen removal above 90% under a range of different influent conditions, suggesting that the GSR system with an SMC strategy increases the flexibility of the system. The results also indicate that there is an optimum COD:N ratio for a given influent ammonium, which decreased as influent ammonium increased. In addition, a lower DO setpoint is preferred to achieve high nitrogen removal, which is desirable if reduced aeration is to be achieved. The simulation results presented here reflect a preliminary effort toward understanding the conditions that upstream A-stage systems need to meet in order to support using GSR B-stage systems to their fullest potential.

5.1. Introduction

For current water resource recovery facilities (WRRFs), achieving sustainability using resource and energy efficient engineering solutions is paramount. For mainstream wastewater, the A-B process fits into this paradigm by promising carbon capture in the A-stage for energy production, and nutrient removal (mainly nitrogen) in the B-stage. Commonly used A-stage systems include high rate activated sludge (HRAS) and chemically enhanced primary treatment (CEPT); an evolving A-stage technology is the anaerobic membrane biofilm reactor (anMBR). The B-stage may include a range of options, including membrane biofilm reactors and aerobic granular sludge reactors (Y. Liu et al., 2020). An aerobic granular sludge reactor (GSR) is one of the B-stage technologies that is gaining significant attention over the last two decades because of it high solids retention capacity, resource efficiency and smaller foot print (Y. Liu & Tay, 2004). Both the A-stage and B-stage systems have been studied extensively; however, to successfully integrate the two stages and achieve maximum energy efficiency from the entire process presents several challenges (McCarty, 2018). One main challenge is controlling effluent composition leaving the A-stage in such a way that it is suitable for the downstream B-stage (Miller et al., 2012). Furthermore, it is necessary to operate B-stage systems in a way that it can use the substrates efficiently and minimize energy expense spent for nitrogen (N) removal. Therefore, it is important to develop a robust real-time operational control strategy that can adapt to a variable influent quality at the same time to efficiently use substrates for N removal.

Among the commonly used aeration control techniques is a combination of fixed DO setpoint, intermittent aeration, and ammonium-based aeration control (Claros et al., 2012; Kim et al., 2004; Regmi et al., 2015; Saxena et al., 2019). Most of these are applied at a specific influent condition or by using a fixed control setting. However, in a real wastewater system the composition of the wastewater typically fluctuates and, as a result, the use of a fixed aeration control strategy will be ineffective. For instance, Schraa et al., (2020) did a full plant model-based assessment on the effectiveness of a real-time control strategy on a partial nitritation/anammox

(PN/A)- based biofilm system using a different control strategy than that used in this dissertation. They showed that a constant DO setpoint did not meet N-removal requirements due to the dynamic nature of the influent wastewater. Specific to the aerobic GSR technology, few studies have been done to develop a real-time control strategy that is applicable for optimizing N removal. For instance, Kishida et al. (2008) used a fixed DO setpoint and controlled the aerobic duration using dissolved oxygen (DO), pH and electric conductivity (EC) to achieve N and phosphorus removal. Gao et al. (2011) controlled the aerobic and anaerobic duration using DO, pH, and oxidation reduction potential (ORP) to detect the end of nitrification and denitrification. However, studies have not been reported that evaluated the performance of an aerobic GSR coupled with real-time aeration control in handling different influent composition.

To achieve N-removal in a B-stage system, PN/A is an ideal biological process because it has the potential to reduce aeration demand, eliminate the requirement for internal or exogenous carbon, and lower excess biomass. Applying PN/A in an aerobic GSR promises an ideal energy and resource efficient alternative. However, successful implementation of this novel technology in a mainstream condition remains a challenge (Nsenga Kumwimba et al. 2020) due to the fact that several conditions have to be met to efficiently remove nitrogen. Those conditions may include some or all of the following: an appropriate COD:N ratio, stable granulation, sustained anammox activity, and out-competition of undesired organisms such as nitrite oxidizing bacteria (NOB) (Franca et al., 2018; Nancharaiah & Sarvajith, 2019; Sarma & Tay, 2018). Hence, complex systems such as PN/A within an aerobic GSR require a robust process control approach that creates the right operational conditions to match influent conditions for sustaining N removal.

In this chapter, the impact of influent composition and aeration control strategy on N removal performance in an aerobic GSR and the overall composition of the granular biomass are evaluated through a simulation-based preliminary study. This chapter expands upon the experimental work presented in Chapter 4 and uses the same model form (but not the same calibrated version) and implements the SMC conditions to expand upon the influent

composition and aeration strategies that are tested via simulation. We believe this approach can serve as a proof of concept to show the practical potential of a robust sensor-mediated control strategy, and to highlight which B-stage influent composition is most amenable to treatment with the designated aerobic GSR system.

5.2. Methods and materials

5.2.1. Granular sequencing batch reactor model

A model including a granular sludge batch reactor managed by a sensor-mediated control strategy was developed based on the experimentally evaluated system in Chapter 4 using Sumo software (Version 19.3.0, Dynamita SARL). The GSR in Sumo is a fill and draw reactor with a one-dimensional fixed thickness biofilm and a variable volume completely mixed compartment. Hence, the granule size and volume are assumed to remain constant. The total biomass concentration is assumed to have a maximum target concentration, but not a lower limit, which means that any excess biomass will be wasted to maintain the specified target TSS concentration. The GSR in SUMO is modeled with n layers, with the first layer as a completely mixed variable volume compartment, and the remaining n-1 layers as granular biofilm layers with equal thickness (i.e., layer thickness = radius/(n-1)). For this work, the model included 5 layers: a bulk compartment and 4 biofilm layers. The number of biofilm layers was chosen by considering the minimum required to capture the expected biomass distribution of the four active bacterial groups (i.e., OHO, AOB, NOB, and AMX) and to minimize the computation time needed to run each simulation. The biological model includes kinetic and stoichiometric expressions for: two-step nitrification via AOB and NOB; anammox (AMX); and heterotrophic denitrification (via OHOs).

The reactor was modelled and calibrated based on the experimental results presented in Chapter 4. The version of the model used in this Chapter is slightly different from that used in Chapter 4 due the model version changes in Sumo, but the relative trends in the results are assumed to be

valid. The new parameter set used in this work that are different from what was used in Chapter 4 are present in Appendix C, Table C-1. The experimental reactor was evaluated using a low-strength A-stage effluent wastewater with an average organic loading rate (OLR) of 0.2 kg-COD/m^3/d and a nitrogen loading rate (NLR) of 0.1 kg-N/m^3/d. Additional details on this work can be found in Chapter 4. The reactor in Chapter 4 had an average total suspended solids (TSS) concentration of 2,000 mg/L during its last stable phase of operation. The volume of the reactor used in the simulation model was 500 L with an exchange ratio of 50%.

The lab scale reactor was operated using an SMC strategy that had dynamic intermittent aeration controlled by residual ammonium, DO setpoint and pH as described in Section 4.2.3. As a result, depending on the influent condition and the state of the reactor, each intermittent phase duration was automatically adjusted. The same aeration control strategy was also implemented in the simulations to evaluate its impact on the overall performance of the system.

5.2.2. Simulation scenarios

To evaluate the applicability of the GSR system coupled with SMC as a B-stage N removal option, different scenarios combining influent composition and operational parameters were used (Table 5.1) The range of concentrations used were based on what is typically found in effluents from example A-stage technologies, such as CEPT, AnMBR, or HRAS. Although we used a maximum biomass concentration of 2,000 mg-TSS/L based on our experimental work from Chapter 4, the TSS concentration is expected to be different across different runs depending upon the influent composition and the operational conditions.

Since the granule's diameter depends on both influent composition and operating conditions, different granule sizes were simulated for each influent condition rather than using a fixed size. As a result, the impact of different granule sizes on the performance of the GSR was evaluated from the simulation results. Hence, four different granules sizes in the range of 0.2 to 0.8 mm were selected for analysis based on both what was observed from our experimental results and

based on the literature for low strength wastewater (Derlon et al., 2016; Hamza et al., 2018; Ni et al., 2009; Xu et al., 2012).

All possible combinations of selected values were evaluated by simulation. The input conditions that varied included: six influent VFA concentrations, four ammonium concentrations, and four granule diameters (a total of 96 possible combinations). These were paired with 24 different aeration control conditions (four DO setpoints, four maximum aerobic duration times, and four maximum anaerobic duration times). This gives a total of 6,144 simulation scenarios. Each simulation was run until a steady-state condition was obtained, which occurred when the active biomass concentrations reached steady-state. A Python script was written to connect with Sumo and automate the simulation process.

Table 5.1: Model simulation scenario for different influent conditions and operation parameters

Parameter	min	max	unit	Selected Values for simulation
VFA (soluble COD)	0	200	mg-COD/L	0, 25, 50, 100, 150, and 200
NH_4^+	25	100	mg-N/L	25, 50, 75, and 100
DO setpoint	0.1	0.75	mg-O_2/L	0.1, 0.3, 0.5, and 0.75
granules size	0.2	0.8	mm	0.2, 0.4, 0.6, and 0.8
max aerobic duration	15	60	min	15, 30, 45, and 60
max anaerobic duration	30	120	min	30, 60, 90, and 120

5.3. Results

5.3.1. **Effect of COD:N ratio on N-removal performance**

Figure 5.1. shows the best TIN removal efficiency achieved for a given influent VFA and NH_4^+ concentration, out of the 24 aeration operation conditions for the four different granule diameters. The first peak TIN removal efficiency occurred at or below a COD:N ratio of 1 when NH_4^+ is above 25 mg-N/L, and the peak COD:N ratio increased as the influent NH_4^+ concentration increased for all granule diameters. When the influent NH_4^+ was 25 mg-N/L, the peak percent TIN removal occurred at (for diameter = 0.2 mm) or greater than (for all other diameters) a COD:N ratio of 2. Also, as the COD:N ratio increased, the TIN removal efficiency

dropped sharply for NH_4^+ concentrations above 25 mg-N/L. This coincided with Figure 5.2, which shows the percent TIN removal decreasing as the influent VFA concentration increased above 100 mg-COD/L and at COD:N ratios ranging from 1.5 to 6. These results indicate that the GSR is best suited to handle a lower VFA load (< 150 mg-COD/L) across the range of ammonium simulated. Furthermore, the results show that granule diameter does not influence percent TIN removal at most COD:N ratios when the granule diameter is above 0.2 mm; at or below 0.2 mm, TIN removal performance typically lags relative to the other simulated diameters (Appendix C, Figure C-1).

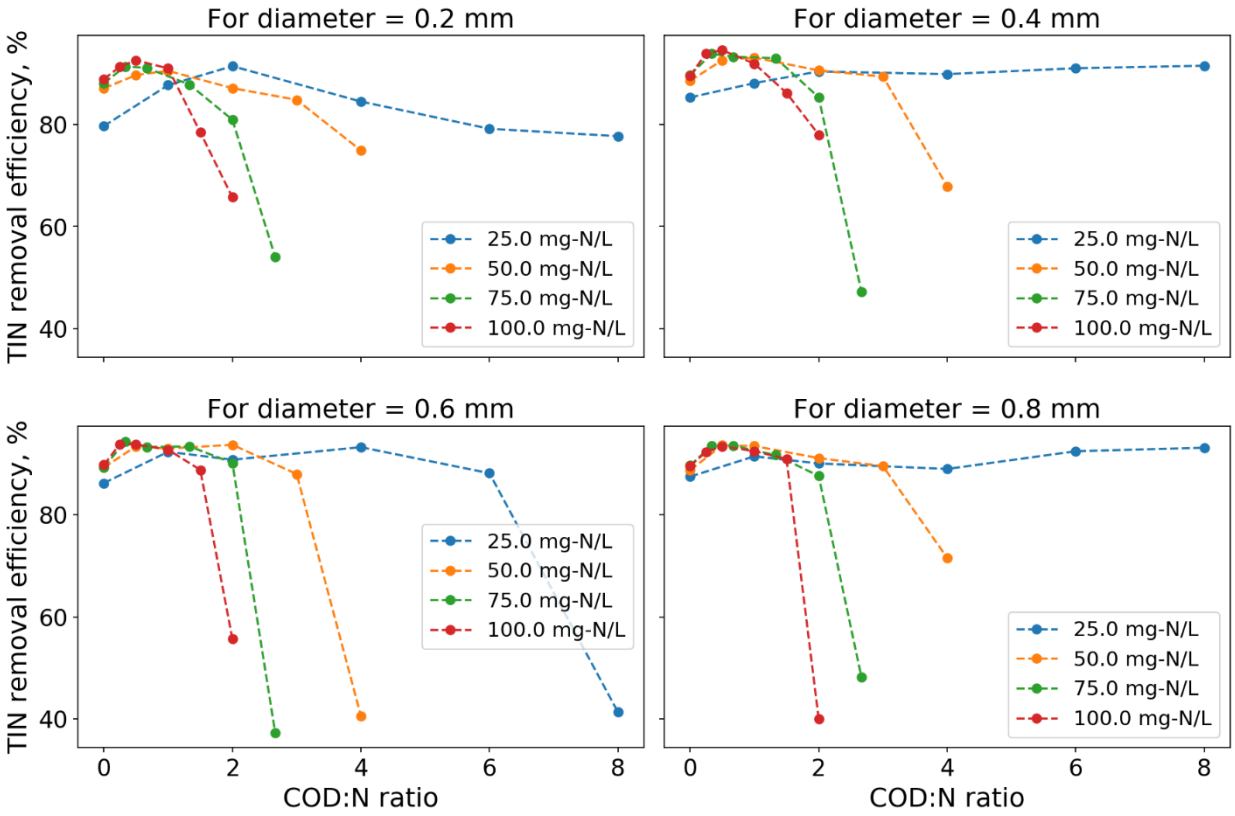

Figure 5.1: COD:N ratio vs TIN removal efficiency across different granule diameters. The lines represent a regression curve for each influent NH_4^+ to indicate the general trend observed in each category. Each point in the figure represent one combination of influent VFA and NH_4^+, and a diameter (totally 96 combinations).

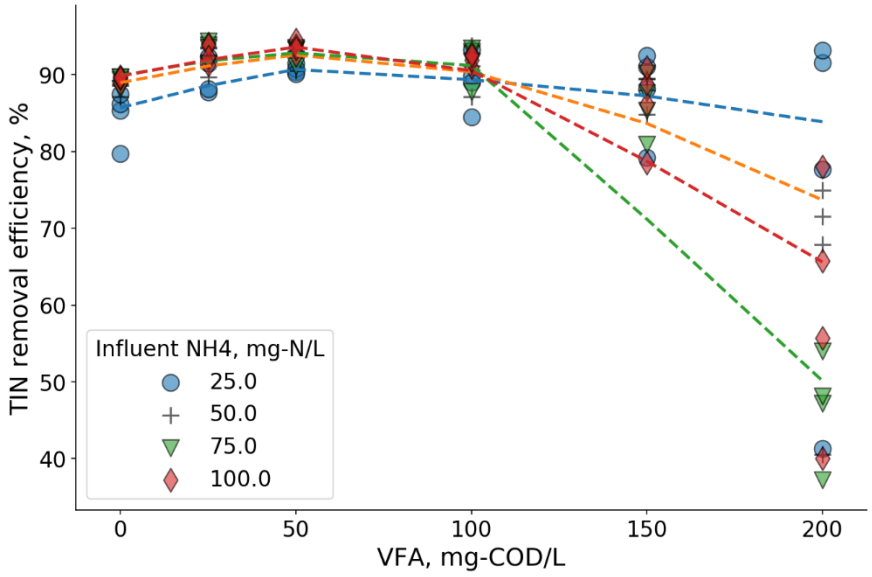

Figure 5.2: Influent VFA vs TIN removal efficiency for all granule diameters and all DO setpoints. The lines represent a regression curve for each influent NH_4^+ to indicate the general trend observed in each category. Each point in the figure represent one combination of influent VFA, NH_4^+, DO setpoint, and diameter (in total, 96 combinations).

5.3.2. Effect of influent VFA load on total cycle time

Figure 5.3 shows that long cycle times and longer anaerobic times are needed to maximize TIN removal with the SMC scheme when the influent contains higher (>150 mg-COD/L) VFA concentrations. However, these longer maximum anaerobic times (>90 min) also corresponded with dramatically lower TIN removal efficiency. There are several possible drivers of this. Higher VFA gives OHOs a competitive advantage for resources in common with AOBs (O_2, NH_4^+), possibly driving down DO quickly during aerobic phases that minimizes nitrite formation and maximizes anaerobic phase time. Furthermore, if more NH_4^+ is consumed to support OHO growth, less remains for AMX to convert to N_2. These observations are consistent with the information conveyed by Figure 5.4, which shows that the model predicts a lower anaerobic time is needed for efficient TIN removal when the influent contains more ammonium that would offset the inordinate NH_4^+ consumption by OHOs and yield more nitrite for denitritation by both AMX and OHO. Further simulations are needed to refine these observations and determine if other parameter outputs are consistent with this interpretation.

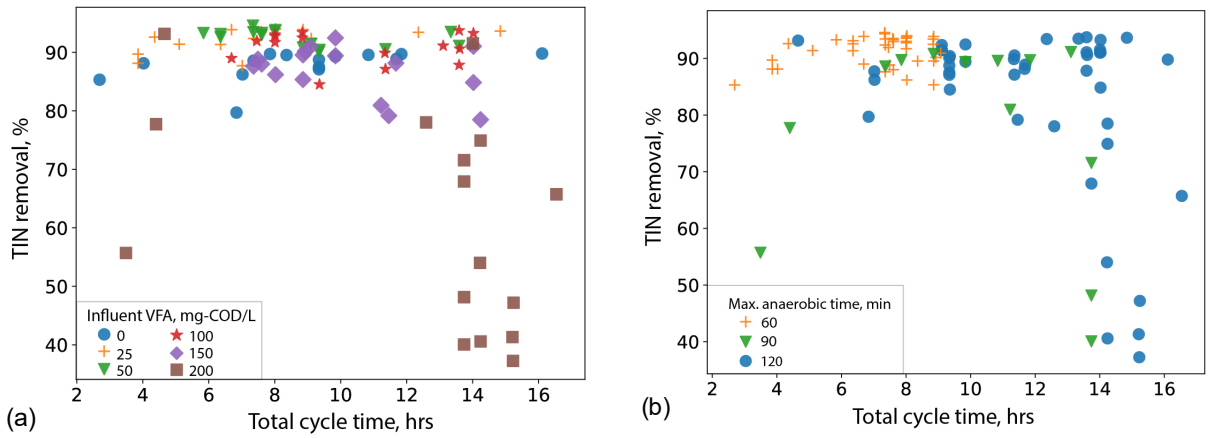

Figure 5.3: Total cycle time vs the best TIN removal efficiency achieved. The points on the figure are for all granule diameters and influent VFA and ammonium input conditions (a total of 96 input conditions) (a) points are colored with influent VFA concentration, (b) points are colored with maximum anaerobic time setting selected based on the best TIN removal efficiency.

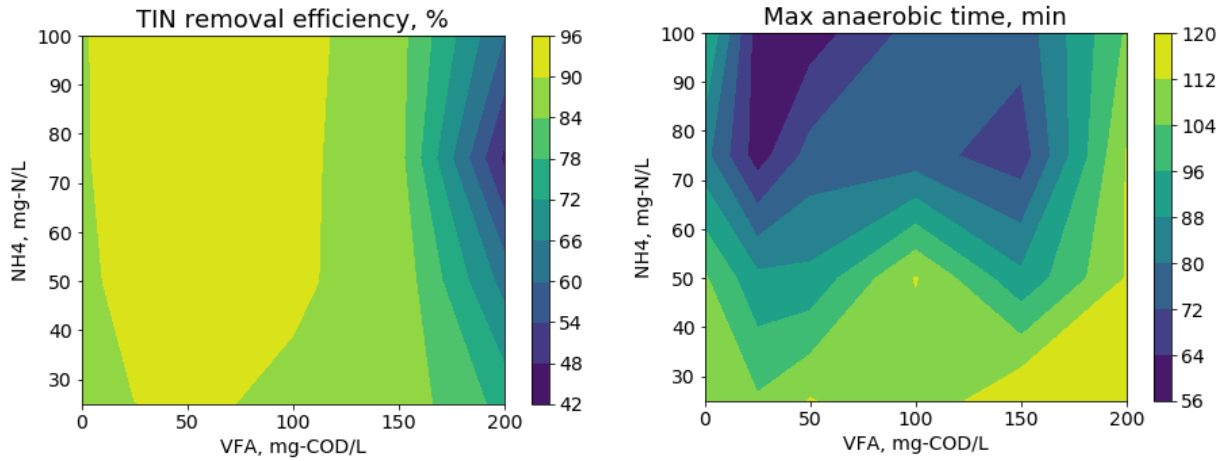

Figure 5.4: Comparing TIN removal efficiency and maximum anaerobic time setting required for the different influent VFA and NH_4^+ concentrations for all granule diameters.

5.3.3. **Impact of DO setpoint on N removal**

Generally, a lower DO setpoint was preferred across different granule sizes for a given influent VFA and ammonium load. As presented in Figure 5.5, a lower DO setpoint resulted in the highest TIN removal efficiency, especially when the granule diameter was less than 0.5 mm. As the granule size increased, there is a minor shift towards higher DO setpoints; however, the lower DO setpoint was still dominant. The reason a higher DO setpoint was preferred for a larger granule diameter can be explained by the need to overcome diffusion limitations in the inner

core of granules. For the lower DO setpoints (≤0.4 mg-DO/L), the total aerobic time needed generally increased, while the higher DO setpoints (> 0.4 mg-DO/L) had similar total aerobic times across different granule diameters (Figure 5.6). On the other hand, higher DO setpoint decreased the total cycle time for a given input condition while the TIN removal efficiency decreased (Appendix C, Figure C-5). This indicates that the choice of DO setpoint depends on the offset between HRT and TIN removal efficiency.

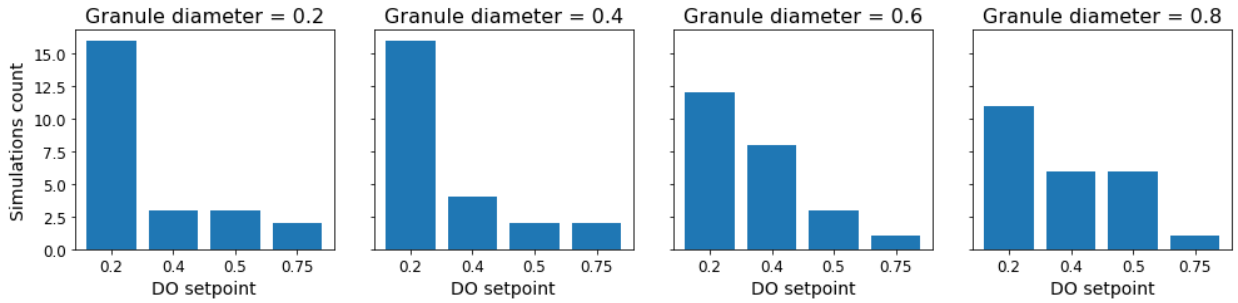

Figure 5.5: Number of best simulations (with the highest TIN efficiency for all influent VFA and ammonium combinations) for each DO setpoint across different granule sizes.

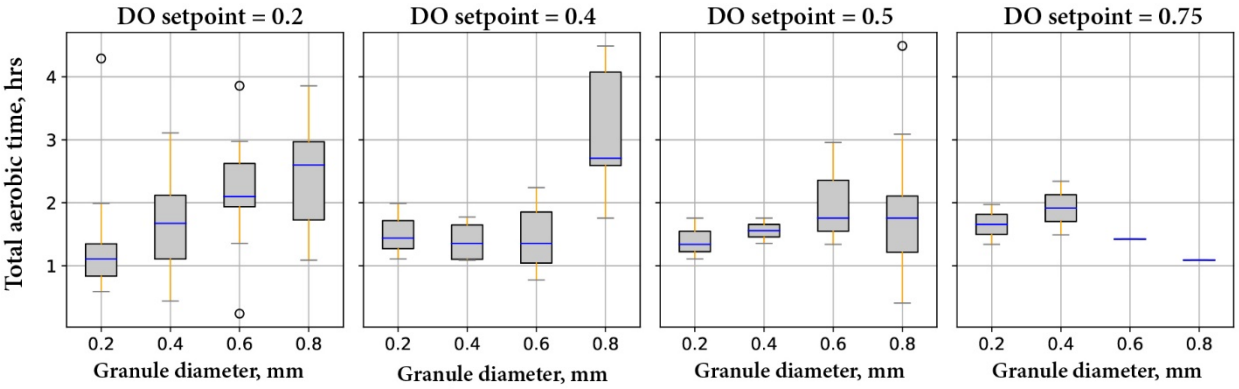

Figure 5.6: Total aerobic time required for different DO setpoints and granule diameters to achieve the highest TIN efficiency for all influent VFA and ammonium combinations.

5.3.4. **Impact of granule diameter choice**

The choice of granule diameter is expected to impact the overall performance and other characteristics of the reactor as it influences diffusion and microbial distribution inside the granule layers. Figure 5.7 presents the overall TIN removal efficiency for different granule sizes and different influent concentrations when the maximum aerobic duration per aerobic sequence

is equal to 30 min and the maximum anaerobic duration per anaerobic sequence is equal to 60 min. As shown, the TIN removal increases with an increase in granule size. A similar trend is also observed with different intermittent aeration settings (See Appendix C, Figure C-2). However, as shown in Figure 5.6 at a lower DO setpoints a larger granule size has the impact of increasing the total aerobic time needed to achieve the highest possible TIN-removal efficiency.

5.3.5. **Biomass characteristics**

Depending on the influent composition and operation conditions, the steady-state microbial composition of the reactor is expected to vary. Figure 5.8 presents the average active biomass concentration per granular volume for different influent VFA and ammonium compositions. As shown, the influent composition has a strong effect on the final community composition. For instance, higher influent VFA significantly reduced the concentration of AMX, AOB, and NOB while OHO increased (paired t-test, p-values < 0.05). On the other hand, increased influent NH_4^+, in turn, increased the concentration of AMX and AOB, but decreased the concentration of OHO and NOB. The increase in DO setpoint to 0.75 mg/L increased the NOB concentration, while larger granule size favored the retention of AMX and reduction of AOB and NOB (Figure 5.9). In general, the microbial groups most affected by influent composition, granule diameter, and DO setpoint were AMX and AOB.

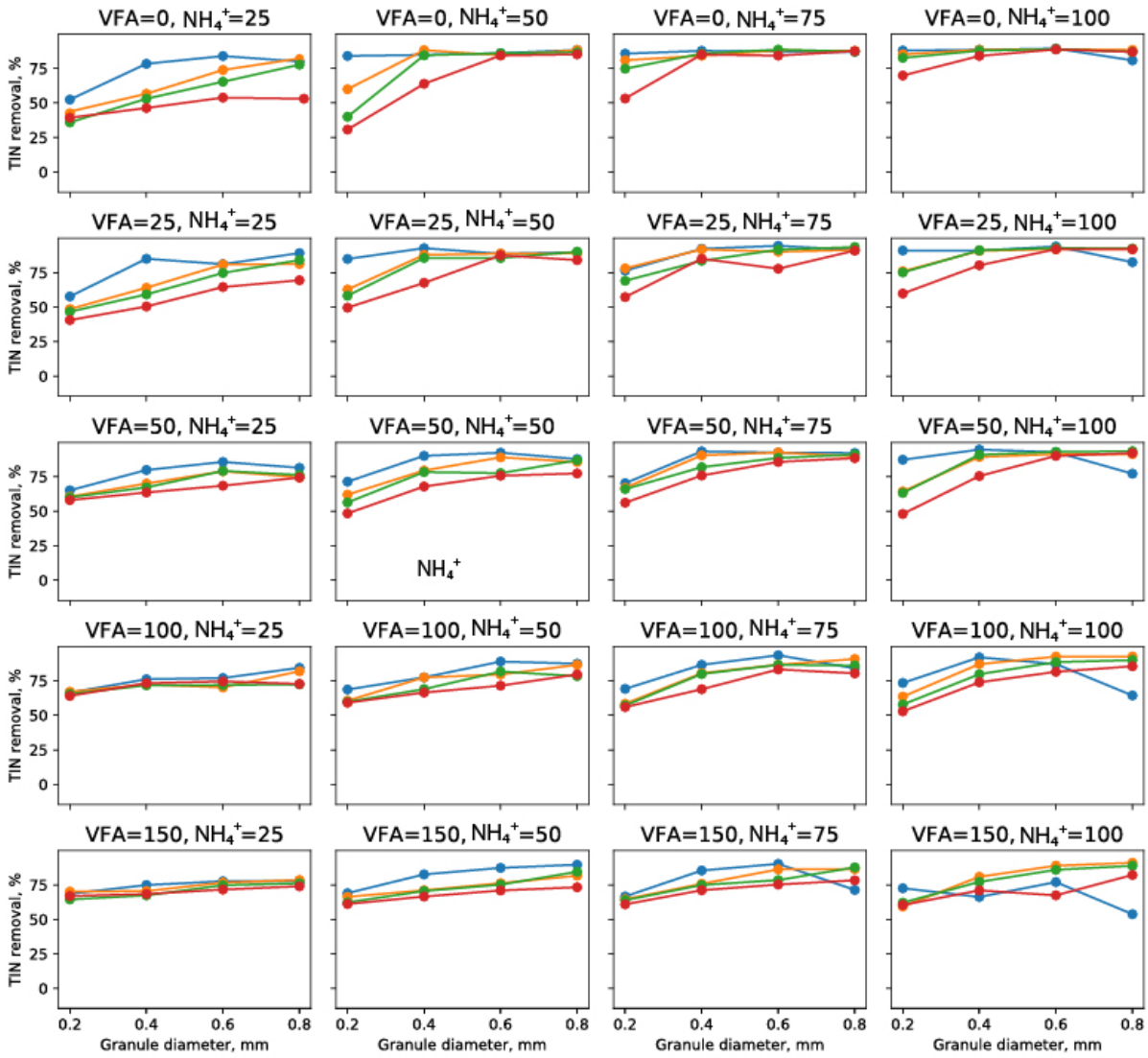

Figure 5.7: TIN removal efficiency vs granule diameter for different influent VFA and ammonium combinations, and for max. aerobic time = 30 and max. anaerobic time=60 mins. The four different line represent the different DO setpoints (blue: 0.2 mg/L, orange: 0.4 mg/L, green: 0.5 mg/L, and red:0.75 mg/L)

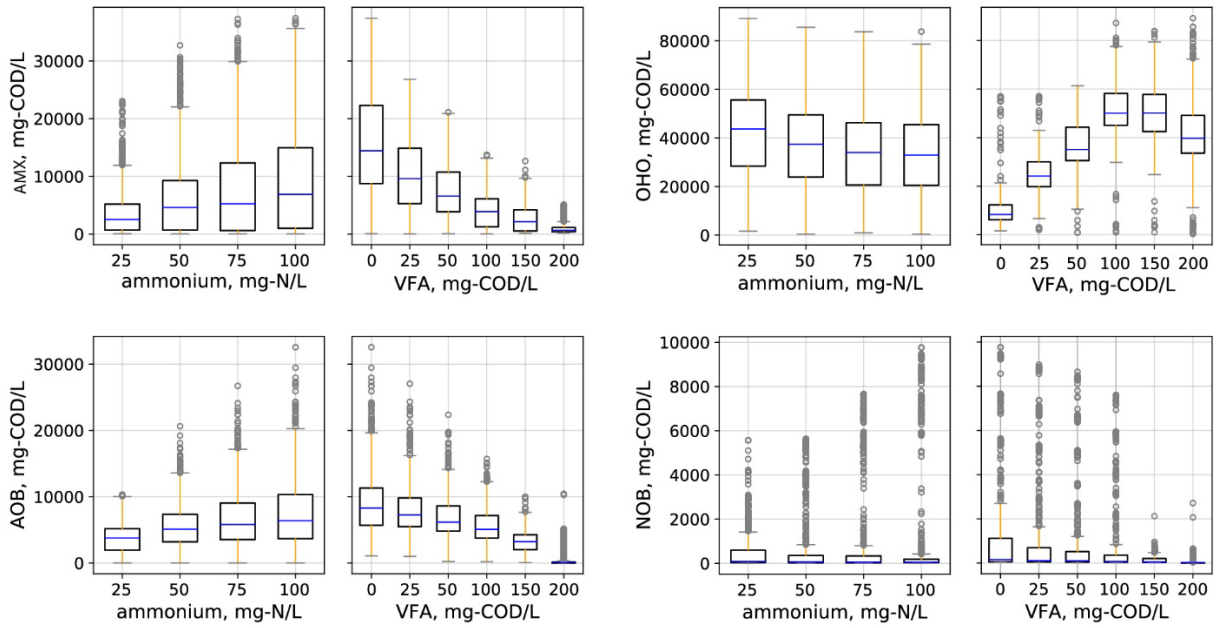

Figure 5.8: The steady-state average concentrations of AMX, OHO, AOB, and NOB for different influent VFA and ammonium concentrations. The concentrations are given per volume of the granules. The figure is generated using all simulation results grouped as per the x-axis shown on each figure.

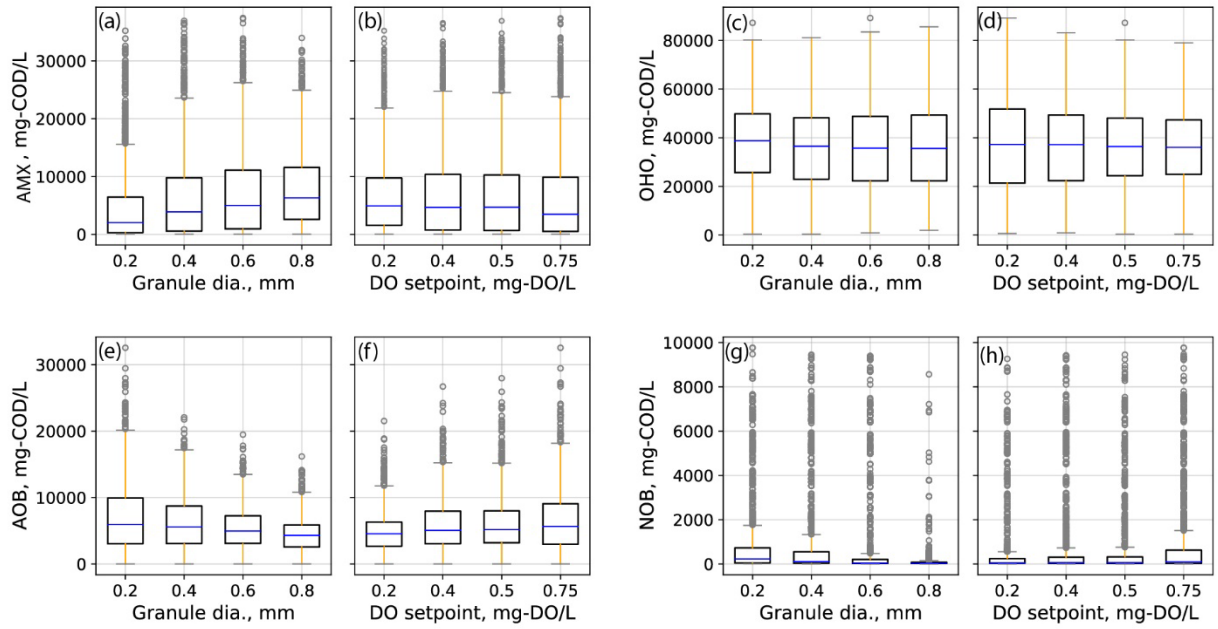

Figure 5.9: The steady-state average concentrations of AMX, OHO, AOB, and NOB for different DO setpoints and granule diameter. The concentrations are given per volume of the granules. The figure is generated using all simulation results grouped as per the x-axis shown on each figure.

5.3.6. **Effect of steady-state biomass concentration**

As indicated in the methods, Sumo's GSR model maintains the target TSS in the reactor by controlling the detachment rate. The simulation results presented above are done with a target TSS of 2,000 mg/L (per total reactor volume including the bulk and biofilm) based on what was measured in the lab scale reactor and its specific influent composition and operational settings (Chapter 4). However, it is expected that the steady state TSS in the reactor will depend on the influent strength and operational conditions. Other have shown that high inert mass in the granule core can compromise the integrity of the granules, which will lead to the disintegration of granules (Y.-Q. Liu et al., 2005; Yuan et al., 2017; Zheng et al., 2006). Hence, the active biomass can be a good proxy for the health of granules. As such, a higher influent load is expected to yield a higher active biomass, but it also depends on the operational conditions, such as DO setpoint, aerobic and anaerobic duration, total cycle time, SRT, and so forth.

Figure 5.10 presents the distribution of average active biomass concentration for all simulations obtained at the end of the simulation time. All the simulations had an initial active biomass concentration of ~52,700 mg-TSS/L (per granule biofilm volume) (52.7% of the total granule mass). The result in Figure 5.10 indicates that as the influent VFA concentration increased, the average active biomass also increased to a point; therefore, the model indicates that healthy granules are likely in the system as VFA approaches 100 mg-COD/L. Beyond 100 mg-COD/L, however, the active biomass started to decrease. This shift in the active biomass could be due to other operational conditions and the maximum TSS target set in the model, and deserves further evaluation to understand the conditions under which it would actually occur.

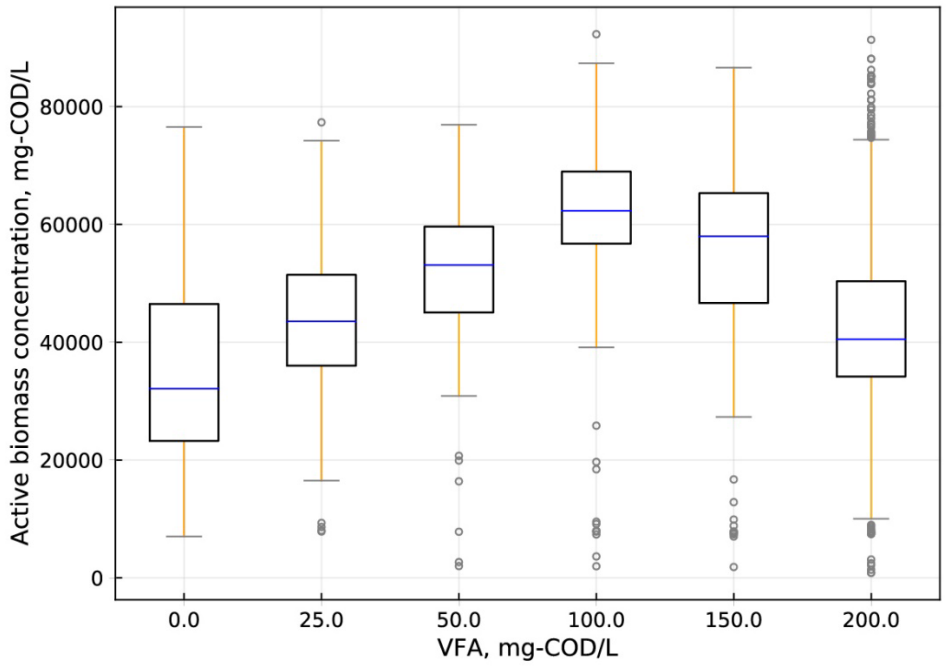

Figure 5.10: Boxplot of active biomass distribution vs influent VFA. Paired t-test p-values between the different groups are all well below 0.05, indicating a significant difference. The figure is generated using all simulation results grouped by VFA concentration in the feed.

5.4. Discussion

5.4.1. Influent VFA influences TIN removal performance and granule stability

The results indicate that the influent VFA concentration strongly influences the overall TIN removal performance and the biomass characteristics of granules. In terms of performance, higher N-removal was achieved when the influent VFA was below 100 mg-COD/L, irrespective of influent ammonium concentration when NH_4^+ was 50 mg/-N/L or higher (Figure 5.2). On the other hand, VFA concentrations below 100 mg-COD/L had a negative impact on the active biomass fraction (Figure 5.10), which means the granules carry more inert particulate material that can ultimately lead to granule disintegration (Peyong et al., 2012). As a result, the disintegrated granules could easily be washed out of the system, causing loss of biomass that ultimately affects reactor performance (Luo et al., 2014). On the other hand, low influent VFA could also mean longer time to granulation or an inability to develop granules. Indeed, we saw poor granulation when the influent VFA concentration was below 100 mg-COD/L in the

experimental system (Chapter 4). Furthermore, the GSR underperformed when the VFA was <100mg-COD/L and at an influent NH_4^+ concentration of 25 mg-N/L. In contrast, TIN removal deteriorated substantially when $NH_4^+ \geq 50$ mg-N/L and VFA $\geq$ 100 mg-COD/L. It also deteriorated in two of the four simulation cases when $NH_4^+ = 25$ mg-N/L, and reasons for this variability need to be further evaluated. One possible reason for the deterioration of TIN removal at higher VFA concentrations is that higher organic loading promoted more OHOs (Figure 5.8), which can out-compete other slower growing organisms both for resources and space in the granular biofilm (Mozumder et al., 2014).

TIN removal performance increased with increasing granule diameter, but the degree of this effect declined as VFA concentrations increased (Figure 5.7). At the same time, the effect of granule diameter decreased as NH_4^+ concentration increased for a given VFA concentration; that is, as the COD:N ratio decreased, the impact of granule diameter on TIN removal performance decreased. Therefore, any influence of granule size on performance is likely due to factors beyond just feed VFA concentration or COD:N ratio. We know from basic stoichiometry that larger VFA loads yield more biomass (as shown for OHOs in Figure 5.8) and will produce larger granules if we assume all biomass formed exists as granules. This, in turn, provides a larger anaerobic niche that supports growth of AMX (also shown in Figure 5.8). Therefore, VFA's effect on TIN removal is as a contributor, but not the sole effect. It is also true that a larger ammonium load supports greater AMX growth (Figure 5.8). More refined simulations and defined experiments are needed to improve our understanding of these effects.

The simulation results reveal that when the influent VFA was > 100 mg-COD/L, a range of factors reduced TIN removal efficiency, increased cycle time, and reduced active biomass. This result is specific to the scenario simulated, where the system had high specific organic load (kg COD/kg VSS). Under these conditions, much of the aeration will be consumed for oxidation of organic carbon, which limits nitrification. Since the sensor-mediated control scheme is designed to increase N-removal, a longer anaerobic time was required for these simulated conditions

(Figure 5.3b and 5.4b), and the overall cycle time was much longer. It is noteworthy that the model has a limitation on the maximum TSS; hence, any excess biomass produced was washed out of the system. As a result, granule size and biomass concentration did not increase during the simulation. This means that the reactor had less active biomass since SUMO directs much of the detachment to the granules outer layer where there is more active biomass. All in all, our simulation strongly indicates that the preferred VFA concentration is < 100 mg-COD/L with a COD:N ratio between 1-2. Given that the system operates best at a low COD:N ratio makes this design suitable as a B-stage TIN removal system that is coupled with an upstream A-stage system that is designed to remove most of the carbon. This pairing ultimately reduces the COD:N ratio coming into the B-stage (Delgado Vela et al., 2015). In addition, as was reported in Chapter 4, it is desirable to integrate anammox and heterotrophic denitrification to gain improved N-removal in the system (Cao et al., 2020). Consequently, our system overcomes the lack of sufficient carbon for heterotrophic denitrification by also supporting PN/A.

The poor performance at higher VFA concentrations may have been due, in part, to the maximum TSS target value set during the simulation. Assuming all other parameters remain unchanged, the removal capacity of the reactor is determined by the biomass retained in the system. Thus, the TSS concentration of 2,000 mg/L used in this simulation set the maximum system capacity. To investigate if a higher TSS would shift the area of acceptable TIN removal performance, we conducted a simulation for an influent VFA concentration of 150 mg-COD/L and ammonium concentration of 75 mg-N/L with a target TSS of 3,000 mg/L. The result indicates that with 3,000 mg/L TSS, we get higher TIN removal efficiency, OLR, and NLR for all granule diameters (Appendix C, Figure C-6). This means that we can increase the capacity of the system to remove TIN by increasing biomass retention. Future simulations need to consider adjusting the TSS setpoint in accordance with the VFA applied.

5.4.2. Low DO setpoint and higher anaerobic time are required for higher N-removal

When we consider the highest TIN removal achieved over all influent compositions and granule diameters simulated, the majority of them were achieved with a low DO setpoint <0.4 mg-DO/L, and a high anaerobic duration (90 and 120 min) (Figures 5.5 and 5.3b). This is expected since the SMC system is designed to promote partial nitritation and anammox (PN/A). As such, a lower DO setpoint and longer anaerobic time creates more time for the anammox process to occur within the granules. This is also consistent with our previous findings (Bekele et al., 2020 and Chapter 3). More anaerobic time is especially important with smaller granules and with higher organic carbon so that anammox activity can be maintained and nitritation can be limited. In smaller diameter granules, oxygen can penetrate toward the center of the granule if the DO setpoint is too high or OLR rate is too low (Li et al., 2008); either will limit anammox activity. On the other hand, the results also show that the DO setpoint did not have a significant impact on the microbial community composition (Figure 5.9). This could be because the intermittent aeration setting has higher anaerobic duration than aerobic duration, except in one scenario. This was done based on the results observed in Chapter 4, where in all cases a lower aerobic time than anaerobic time was needed to achieve N-removal. This indicates that, generally, our system can operate at a lower aeration expense than other similar systems where more aerobic time was needed to achieve N-removal (Lochmatter et al., 2013). It is important to note that a shorter anaerobic time produced less variability in the TIN removal efficiency; further simulations may help to determine how to reduce variability when using longer anaerobic times.

5.4.3. Using a DO setpoint supports NOB repression

Using a DO setpoint allowed ammonia oxidizing bacteria to be dominant and subjected nitrite oxidizing bacteria to a small fraction of the microbial population (Figure 5.9). The impact of small changes in DO setpoint between 0.2 and 0.4 mg/L have the largest impact on AOB concentration. This is consistent with the experimental system described in Chapter 4, where a DO setpoint of 0.3 mg/L was used to achieve NOB repression.

5.4.4. Simulations support use of a Sensor-Mediated Control strategy to achieve flexibility to treat a wider influent composition

Simulations show that the AGS achieved high TIN removal efficiency for a wide range of influent VFA and ammonium compositions and granule diameters. The system was able to reliably handle an influent VFA concentration up to 150 mg-COD/L and at most a COD:N ratio of 2 to achieve a TIN removal efficiency of > 80% and reaching up to 94% for all influent NH_4^+ concentrations simulated (Appendix C, Figure C-3). Moreover, the maximum COD:N ratio that can be handled by the system depended on the influent ammonium concentration regardless of granule diameter (Figure 5.1) but can vary much depending upon DO setpoint (Figure 5.5). The results also indicate that to achieve sufficient N-removal for some of the input conditions it takes a very long cycle time or HRT, which is not desirable from a practical perspective. Hence, if we ignore those simulations resulting in a total cycle time of 12 hrs, the system can handle an OLR of up to 0.2 kg-COD/m^3/day (Appendix C, Figure C-4). These results highlight the importance of having an adaptive SMC strategy with flexible intermittent aeration to handle variable inputs from A-stage technologies that will produce effluents with variable composition.

5.5. Conclusion

Using simulation, we showed that a GSR with an SMC can treat a range of influent conditions and potentially yield a sufficient TIN removal. Using a real-time control strategy with a DO setpoint, ammonium-based aeration, and an adaptive intermittent aeration rather than using fixed aeration settings, the reactor was able to handle a fairly broad range of influent conditions. Such an adaptive aeration control strategy offers the advantage of achieving desired treatment goals while at the same time using resources efficiently. The simulations conducted for this initial analysis serve as a starting point for a more robust simulation effort to further evaluate GSR and SMC-linked operations to enhance TIN removal across a range of A-B treatment system configurations.

5.6. References

Bekele, Z. A., Delgado Vela, J., Bott, C. B., & Love, N. G. (2020). Sensor-mediated granular sludge reactor for nitrogen removal and reduced aeration demand using a dilute wastewater. *Water Environment Research*, 1–11. https://doi.org/10.1002/wer.1296

Cao, S., Du, R., & Zhou, Y. (2020). Coupling anammox with heterotrophic denitrification for enhanced nitrogen removal: A review. *Critical Reviews in Environmental Science and Technology*, *0*(0), 1–34. https://doi.org/10.1080/10643389.2020.1778394

Claros, J., Serralta, J., Seco, A., Ferrer, J., & Aguado, D. (2012). Real-time control strategy for nitrogen removal via nitrite in a SHARON reactor using pH and ORP sensors. *Process Biochemistry*. https://doi.org/10.1016/j.procbio.2012.05.020

Delgado Vela, J., Stadler, L. B., Martin, K. J., Raskin, L., Bott, C. B., & Love, N. G. (2015). Prospects for Biological Nitrogen Removal from Anaerobic Effluents during Mainstream Wastewater Treatment. *Environmental Science & Technology Letters*, *2*(9), 234–244. https://doi.org/10.1021/acs.estlett.5b00191

Derlon, N., Wagner, J., da Costa, R. H. R., & Morgenroth, E. (2016). Formation of aerobic granules for the treatment of real and low-strength municipal wastewater using a sequencing batch reactor operated at constant volume. *Water Research*, *105*, 341–350. https://doi.org/10.1016/j.watres.2016.09.007

Franca, R. D. G., Pinheiro, H. M., van Loosdrecht, M. C. M., & Lourenço, N. D. (2018). Stability of aerobic granules during long-term bioreactor operation. *Biotechnology Advances*, *36*(1), 228–246. https://doi.org/10.1016/J.BIOTECHADV.2017.11.005

Gao, D., Yuan, X., Liang, H., & Wu, W. M. (2011). Comparison of biological removal via nitrite with real-time control using aerobic granular sludge and flocculent activated sludge. *Applied Microbiology and Biotechnology*, *89*(5), 1645–1652. https://doi.org/10.1007/s00253-010-2950-3

Hamza, R. A., Sheng, Z., Iorhemen, O. T., Zaghloul, M. S., & Tay, J. H. (2018). Impact of food-to-microorganisms ratio on the stability of aerobic granular sludge treating high-strength organic wastewater. *Water Research*, *147*, 287–298. https://doi.org/10.1016/J.WATRES.2018.09.061

Kim, J. H., Chen, M., Kishida, N., & Sudo, R. (2004). Integrated real-time control strategy for nitrogen removal in swine wastewater treatment using sequencing batch reactors. *Water Research*. https://doi.org/10.1016/j.watres.2004.05.006

Kishida, N., Tsuneda, S., Sakakibara, Y., Kim, J. H., & Sudo, R. (2008). Real-time control strategy for simultaneous nitrogen and phosphorus removal using aerobic granular sludge. *Water Science and Technology*, *58*(2), 445–450. https://doi.org/10.2166/wst.2008.410

Li, Y., Liu, Y., Shen, L., & Chen, F. (2008). DO diffusion profile in aerobic granule and its microbiological implications. *Enzyme and Microbial Technology*, *43*(4–5), 349–354. https://doi.org/10.1016/j.enzmictec.2008.04.005

Liu, Y.-Q., Liu, Y., & Tay, J.-H. (2005). Relationship between size and mass transfer resistance in aerobic granules. *Letters in Applied Microbiology*, *40*(5), 312–315. https://doi.org/10.1111/j.1472-765X.2005.01695.x

Liu, Y., Gu, J., & Zhang, M. (2020). Approaches to energy and resource recovery from municipal wastewater. In *A-B Processes: Towards Energy Self-sufficient Municipal Wastewater Treatment* (pp. 29–67). IWA Publishing. https://doi.org/10.2166/9781789060089_0029

Liu, Y., & Tay, J.-H. (2004). State of the art of biogranulation technology for wastewater treatment. *Biotechnology Advances*, *22*(7), 533–563. https://doi.org/10.1016/j.biotechadv.2004.05.001

Lochmatter, S., Gonzalez-Gil, G., & Holliger, C. (2013). Optimized aeration strategies for nitrogen and phosphorus removal with aerobic granular sludge. *Water Research*, *47*(16), 6187–6197. https://doi.org/10.1016/j.watres.2013.07.030

Luo, J., Hao, T., Wei, L., Mackey, H. R., Lin, Z., & Chen, G.-H. (2014). Impact of influent COD/N ratio on disintegration of aerobic granular sludge. *Water Research*, *62*, 127–135. https://doi.org/10.1016/j.watres.2014.05.037

McCarty, P. L. (2018). What is the Best Biological Process for Nitrogen Removal: When and Why? *Environmental Science and Technology*, *52*(7), 3835–3841. https://doi.org/10.1021/acs.est.7b05832

Miller, M. W., Bunce, R., Regmi, P., Hingley, D. M., Kinnear, D., Murthy, S., Wett, B., & Bott, C. B. (2012). A/B Process Pilot Optimized for Nitrite Shunt: High Rate Carbon Removal Followed by BNR with Ammonia-Based Cyclic Aeration Control. *Proceedings of the Water Environment Federation*, *2012*(10), 5808–5825. https://doi.org/10.2175/193864712811709607

Mozumder, M. S. I., Picioreanu, C., van Loosdrecht, M. C. M., & Volcke, E. I. P. (2014). Effect of heterotrophic growth on autotrophic nitrogen removal in a granular sludge reactor. *Environmental Technology*, *35*(8), 1027–1037. https://doi.org/10.1080/09593330.2013.859711

Nancharaiah, Y. V., & Sarvajith, M. (2019). Aerobic granular sludge process: a fast growing biological treatment for sustainable wastewater treatment. In *Current Opinion in Environmental Science and Health* (Vol. 12, pp. 57–65). Elsevier B.V. https://doi.org/10.1016/j.coesh.2019.09.011

Ni, B.-J., Xie, W.-M., Liu, S.-G., Yu, H.-Q., Wang, Y.-Z., Wang, G., & Dai, X.-L. (2009). Granulation of activated sludge in a pilot-scale sequencing batch reactor for the treatment of low-strength municipal wastewater. *Water Research*, *43*(3), 751–761. https://doi.org/10.1016/j.watres.2008.11.009

Nsenga Kumwimba, M., Lotti, T., Şenel, E., Li, X., & Suanon, F. (2020). Anammox-based processes: How far have we come and what work remains? A review by bibliometric analysis. In *Chemosphere* (Vol. 238, p. 124627). Elsevier Ltd. https://doi.org/10.1016/j.chemosphere.2019.124627

Peyong, Y. N., Zhou, Y., Abdullah, A. Z., & Vadivelu, V. (2012). The effect of organic loading rates and nitrogenous compounds on the aerobic granules developed using low strength wastewater. *Biochemical Engineering Journal*, *67*, 52–59. https://doi.org/10.1016/J.BEJ.2012.05.009

Regmi, P., Bunce, R., Miller, M. W., Park, H., Chandran, K., Wett, B., Murthy, S., & Bott, C. B. (2015). Ammonia-based intermittent aeration control optimized for efficient nitrogen removal. *Biotechnology and Bioengineering*. https://doi.org/10.1002/bit.25611

Sarma, S. J., & Tay, J. H. (2018). Aerobic granulation for future wastewater treatment technology: challenges ahead. *Environ. Sci.: Water Res. Technol*, *4*(9). https://doi.org/10.1039/c7ew00148g

Saxena, N., Nawaz, A., & Lee, M. (2019). Comprehensive Review of Control and Operational Strategies for Partial Nitration/ANAMMOX System. In *Industrial and Engineering Chemistry Research*. American Chemical Society. https://doi.org/10.1021/acs.iecr.9b01670

Schraa, O., Rosenthal, A., Wade, M. J., Rieger, L., Miletic´, I. M., Alex, J., & Miletic´, I. M. (2020). *Assessment of aeration control strategies for biofilm-based partial nitritation/anammox systems*. https://doi.org/10.2166/wst.2020.174

Xu, M., Weissburg, M., Newell, J. P., & Crittenden, J. C. (2012). Developing a Science of Infrastructure Ecology for Sustainable Urban Systems. *Environ. Sci. Technol*, *46*, 7929. https://doi.org/10.1021/es3025534

Yuan, S., Gao, M., Zhu, F., Afzal, M. Z., Wang, Y. K., Xu, H., Wang, M., Wang, S. G., & Wang, X. H. (2017). Disintegration of aerobic granules during prolonged operation. *Environmental Science: Water Research and Technology*, *3*(4), 757–766. https://doi.org/10.1039/c7ew00072c

Zheng, Y. M., Yu, H. Q., Liu, S. J., & Liu, X. Z. (2006). Formation and instability of aerobic granules under high organic loading conditions. *Chemosphere*, *63*(10), 1791–1800. https://doi.org/10.1016/j.chemosphere.2005.08.055

Chapter 6

Conclusions and Engineering Significance

6.1. Overview

One of the main goals of water resource recovery facilites (WRRFs) is to achieve nitrogen removal to meet effluent standard goals while, at the same time, reduce energy and resource needs to achieve this. The biological nitrogen removal (BNiR) technology landscape has been continuously evolving over the last few decades in search of such an ideal system. Currently, aerobic granular sludge reactors (GSR) are emerging as prime technology to address this need. At the same time, novel reactor configurations as well as novel microbial processes such as partial nitritation and anammox (PN/A) have gained popularity due to their potential to reduce aeration and carbon demand, and minimize excess sludge production. Therefore, combining AGS with PN/A for mainstream wastewater treatment has bottlenecks that still need significant advancement for wide spread full-scale adaptation. In fact, in the last two decades only 20 full-scale AGS systems have been implemented (Orhon, 2015). Some of the bottlenecks occur because of the difficulty associated with achieving granulation with low strength mainstream wastewater (We et al., 2020). However, once granules are formed, it is possible to maintain stable granules over long period of time (Franca et al., 2018). Stable granules suppress or out-select undesired microbial groups such as NOBs that compete for critical resources (Nsenga Kumwimba et al., 2020), and allow for the integration of PN/A with heterotrophic denitrification to improve N removal. This dissertation set out to address some of these bottleneck in coupled GSR-PN/A systems to support its development and adoption toward full-scale implementation. The outcomes of this dissertation suggest that some of these challenges can be addressed by further

optimizing the process using a robust control strategy that takes into considerations the dynamics that exists in GSR-PNA systems under low loading rates.

Chapter 3 of this dissertation focuses on estabilishing the necessary ground work needed to successfully integrate GSR and PN/A, which was demonstrated in a lab-scale SBR by using anaerobically treated effluent as one of the use cases. We demonstrated that under low organic loading it is possible to develop aerobic granules. We also developed and demonstrated a novel sensor mediated control (SMC) scheme that successfully supressed NOB to achieve nitration, paving the way for anammox to become established and contribute to improved N removal. In Chapter 4, further optimization of the SMC and long-term stability of the GSR under different influent condition was investigated and established. Our results show that GSR coupled with SMC was able to achieve high (~90%) N removal with a low aeration expense in a dilute (mainstream) simulated wastewater. Chapter 5 introduced an extensive model-based investigation of the proposed system to assess its feasibility and robustness beyond the infuent characteristics conducted in the lab-scale system. The results indicate that the developed strategy of GSR coupled with SMC can be applied to a wider range of influent VFA and NH_4^+ concentrations, owing to the flexible nature of the developed SMC. Overall, this disseration gives new insights about how GSR with PN/A can be practically applied as a promising B-stage mainstream N removal system by overcoming the aforemention bottlenecks.

6.2. Main findings and significance

The first challenge addressed by the disseration work was formation of granules and thier subsequent long-term stability. Towrds that end, long term experimental work was performed and demonstrated that granulation can be achieved using a dilute mainstream wastewater with organic loading rates as low as 0.2 kg-COD/d/m^3. The lower limit was demonstrated through work reported on in Chapter 5, where OLR was gradually increased until sufficient granulation was achieved in the system. Furthermore, the work revealed that a minimum OLR is needed to

develop granules and sustain them over long operational periods and under low nitrogen and organic load conditions. This finding delineates the lower limit needed to develop GSR reactors for mainstream systems. Hence, we can hypothesize that for scaling up, such systems might might actually require a larger OLR than this to develop granules and sustain them for longer period of time.

Another bottleneck addressed during this disseration work was NOB suppression and nitritation in dilute mainstream wastewater. Regardless of the reactor configuration, one of the main bottlenecks reported detering the implementation of mainstream PN/A is NOB suppression while sustaining partial nitritation (Gu et al., 2020; Ma et al., 2020). The work reported here reveals that by combining a low DO setpoint and intermittent aeration, the SMC control strategies effectively supress NOB and attain partial nitritation. The success of this strategy can be attributed to (1) the differential oxygen affinity between AOB and NOB in our system, as it was revealed through 16sRNA squence analysis (Chapters 3 and 4), (2) the lag of NOB activity due to creation of a transient anoxia condition that was created through intermittent aeration, as suggested by Gilbert et al., (2014) and Kornaros et al., (2010). Hence, this disseration work further reinforces the findings by others that NOB suppression can easily be overcome by implementing a control scheme that creates these conditions.

At the core of this dissertation, we investigated operational strategies for the successful integration of anammox and OHOs for improved N-removal, which is consistent with the motto of a sustainable WRRF. Theoretically, it might be possible to achieve N-removal to ~ 90% by only using PN/A; however, the organic carbon present in the wastewater has to be removed to achieve PN/A. An obvious option is to aerobically oxidize it, then proceed to partial nitritation; however, this means imposing higher aeration expense as outlined by Daigger (2014). By properly designing the aeration strategy, at least some of the organic carbon can be used for heterotrophic N-removal, which could marginally increase the overall N-removal. Thus, in this disseration we used intermittent aeration cycled between anaerobic phases as the first step to allow

heterotrophic denitrification to occur by using NO_2^- and NO_3^- residual from the previous batch cycles. As a result, we were able to demonstrate in Chapters 3 and 4 that the OHOs contributed 40 to 60% of the overall N removal, which is a significant ammount. At the same time, we were able to demonstrate the integration of anammox for N-removal. As a result, our experiment and modeling results in Chapter 4 demonstrate the integration of PN/A and heterotrophic denitrification in GSR for low strength wastewater.

The success of all the above results strongly relied on the the SMC strategy developed during this work that combined a DO setpoint, intermittent aeration, and ammonium-based aeration control (ABAC). In addition to achieving a high level of N removal, which reached ~90%, our extensive simulation work demonstrated that it is also possible to achieve comparable performance in a GSR receiving different influent compositions. All in all, the work in this disseration offers a promising proposal that GSR coupled with an adaptive SMC can be used to further advance the adoption of GSR in large scale systems as a competitive B-stage technology.

6.3. Recommendations for future research

The insights and findings from this research gives us a glimpse of the potential that aerobic GSRs coupled with SMC can achieve using one type of wastewater composition; hence, its applicability to dilute but different wastewater compositions needs to further investigated. As described above, the research in this disseration mainly used a synthetic AnMBR reactor effluent to simulate an A-stage system; thus, other A-stage effluent compositions (such as, from high rate activated sludge and chemically enhanced primary treatment) need further evaluation. This is especially important because effluent from these sources contain particulate matter, which will add aditional complexity to the granulation process as reported by others.(de Kreuk et al., 2010; Derlon et al., 2016; Wagner et al., 2015). Hence, future research on these systems can evaluate the broader feasibility of the approach demonstrated in this work.

It was possible to successfully develop granules in the experiments conducted for this dissertation, which produced relatively large granules with an average diameter of 1 mm during the first experiment (Chapter 3) and smaller granules with an average dameter of 0.4 mm during the second run, although the organic loading rates were similar. What was different, however, was the operational strategy. Similar behavior is also report in the literature where the same influent load produced significantly different granule sizes (Derlon et al., 2016; Ni et al., 2009b; Peyong et al., 2012a; Pishgar et al., 2019; Wagner et al., 2015). Hence, other than the obvious differences observed in operational conditions, there is limited fundamental understanding of the underlying mechanism or identifying the correlation between granulation, performance and loading rate. This is important because it could mean reproducibility may not be garanteed, which will be a significant implication when scaling the system to full-scale application.

Related to granule size, more research should be done to explore the correct TSS concentration related to specific influent loading and operating conditions. During the work presented here, we tried to address this question indirectly through the use of a simulation experiment where we looked at different scenarios with different granule concentrations and diameters. We used the final active biomass fraction as a good proxy to assess the validity of the assumption and to indicate the integrity of the granules. Therefore, at least emperical work can be done to establish a relationship or guideline to determine the expected TSS concentration for healty granules.

Finally, in addition to testing the system with different influent composition, future modeling or experimental work can be done using a dynamic influent composition for each batch (i.e., the influent composition or loading rate changed from batch to batch in a cyclic manner). This kind of scenario could mimic a real wastewater, which is expected to change from time to time. Modeling can tell us the maximum potential of the system, while experimental work can capture the impact of the dynamic loading on granule integrity.

Appendices

Appendix A Supplementary Information for Chapter 3

Sensor-Mediated Granular Sludge Reactor for Nitrogen Removal and Reduced Aeration Demand using a Dilute Wastewater

1. SRT calculation

Solids are wasted from the reactor in each cycle only during the decanting period and sludge retention time (SRT) was calculated according to Eq. (A-1). Figure A-1 gives the box plot for the calculated SRT values for the four operation phases.

$$SRT = \frac{TSS_r \cdot V_r}{TSS_{eff} \cdot Q_{eff}} \qquad \text{(Eq. A-1)}$$

Where:

TSS_r: TSS concentration in the reactor (gTSS L^{-1});
V_r: reactor volume (L);
$TSS_{eff.}$: TSS concentration in the effluent (gTSS L^{-1});
$Q_{eff.}$: effluent flow rate (L d^{-1});

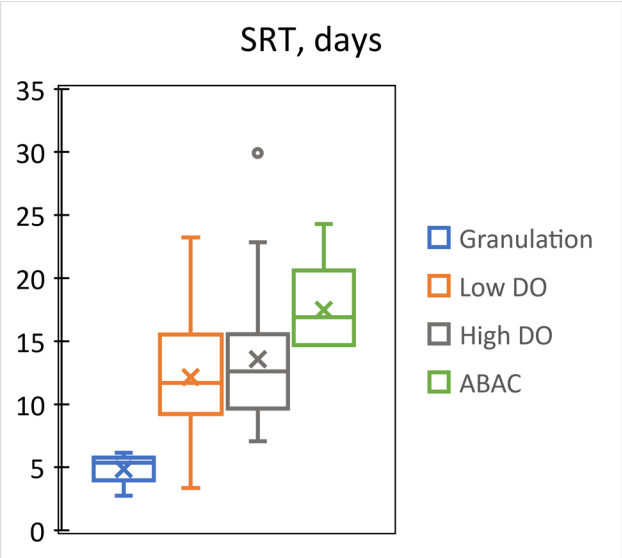

Figure A-1: Box plot for SRT values during the four operation phases.

2. Granule size distribution

Granules were taken from the reactor, transferred to clear plate, and image was taken which was analyzed in ImageJ software for size distribution. Figure A-2 gives granules size distributions for samples taken during Phase 1 and Phase 2.

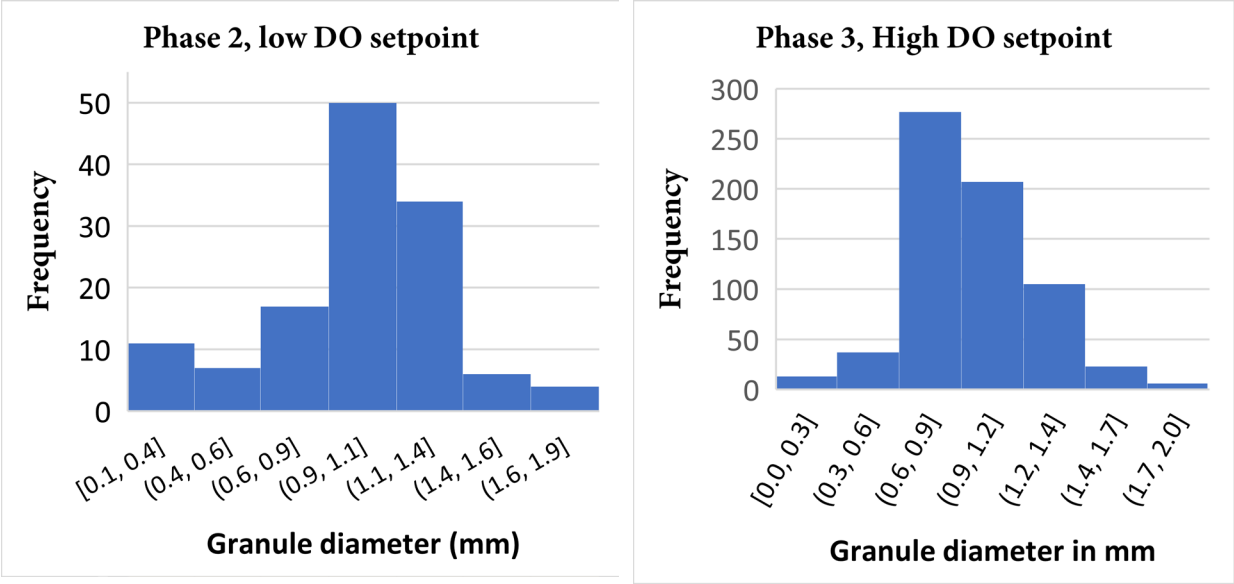

Figure A-2. Granule size distribution from ImageJ software analysis.

3. Solids concentration and SVI

To determine biomass production and sludge volume index (SVI), total suspended solids (TSS), volatile suspended solids (VSS) and sludge volume were measured regularly. The sludge volume was measure by directly reading the settled granule depth from the reactor at 5 min and 30 min. The SVIs at 5 and 30 min were calculated by dividing the granule volume (mL) with reactor volume (4.5L) and TSS (g TSS L^{-1}).

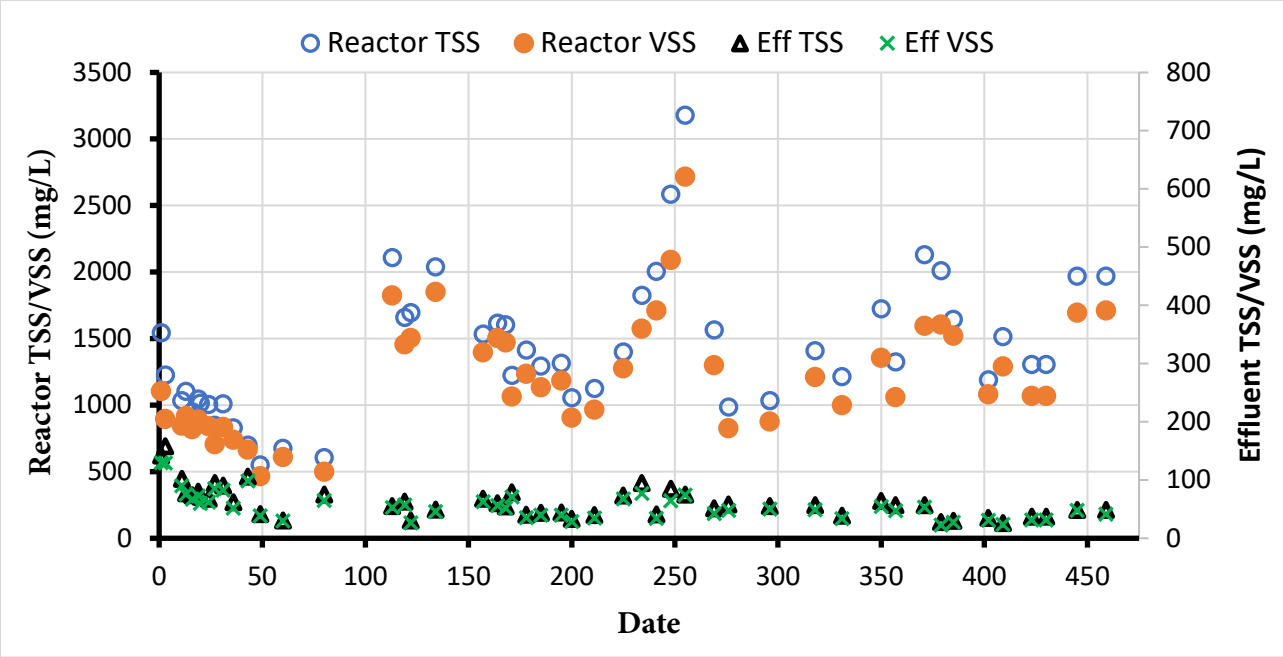

Figure A-3. Solids concentration in the reactor and effluent.

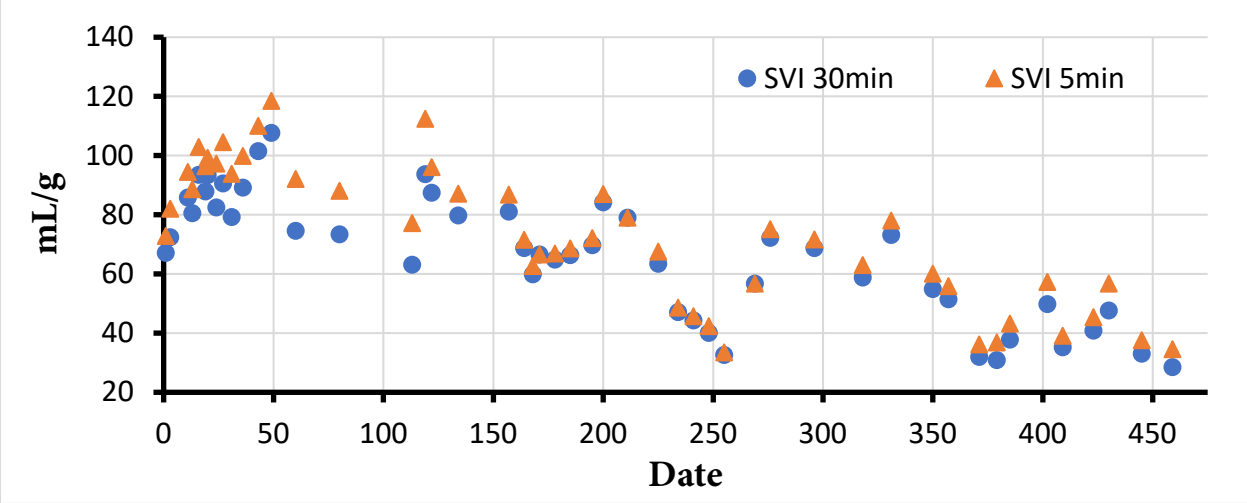

Figure A-4. Calculated SVI for 5 and 30 minutes.

4. Long-term reactor's performance data

Figure A-5 gives the reactor's N removal performance data from day 0 to day 474. In this figure ammonium concentration for the influent and effluent samples and all three N species (i.e., ammonium, nitrite, and nitrate) for effluent samples are shown. In addition, Table A-I1 gives reactor's data that are not included in the analysis due to known operational issues for completeness.

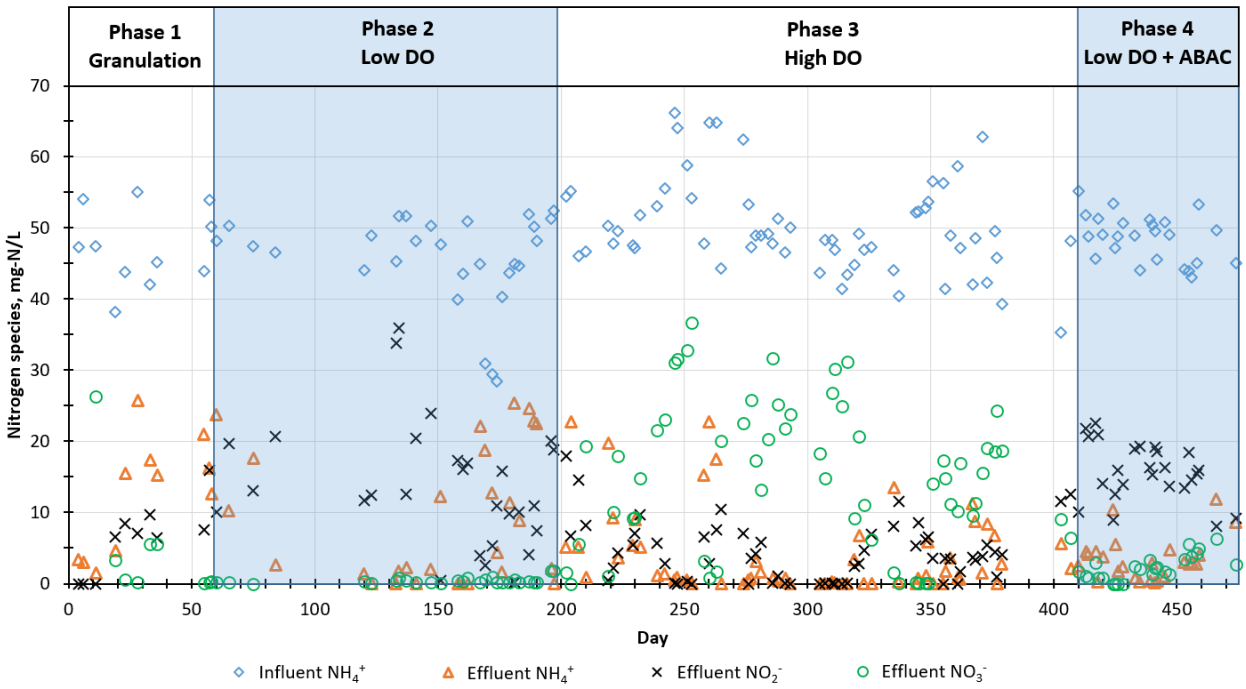

Figure A-5. The reactor performance over 474 days of operation over four phases: Phase 1 granulation**;** Phase 2 low DO (~0.5 mg/L) setpoint**;** Phase 3 high DO (0.75 – 1 mg/L) setpoint**;** and Phase 4 ABAC with a DO setpoint of 0.5 mg/L. Samples for days when operational failures occurred are not shown but are summarized in Table SI A-1. Water quality data shown based on analytical measurements and not sensor-based measurements.

Table A-1: Summary of days the reactor has system failure

Day	Influent NH_4^+	Effluent NH_4^+	Effluent NO_2^-	Effluent NO_3^-	Problem
17	18.73	0.54	0.00	0.16	Influent tubing leaking
144	66.29	25.96	3.50	0.02	Air tank ran out overnight
200	51.79	28.17	4.10	0.00	Diffusor stone clogged with biomass
212	50.16	0.14	0.15	35.97	Nitrogen gas run out
215	48.07	28.20	1.02	2.56	The DO was high probably air was leaking into the reactor
256	46.61	28.62	2.88	1.74	Very low DO in the reactor due air supply issue
299	48.14	22.87	0.00	15.41	Low Do in the reactor due to diffusor stone clogging
301	45.96	0.00	0.02	39.53	Too much air supply to the reactor
383	48.05	0.00	0.00	38.11	Problem with nitrogen gas supply
390	48.47	28.23	0.07	0.00	Air tank was empty
391	43.52	27.75	1.09	0.65	Reactor overflow due to decant pump failure
395	51.27	22.03	1.24	27.00	Nitrogen gas run out
467	51.85	18.55	8.31	4.37	Too low DO in the reactor
468	54.99	24.04	3.04	3.68	Error in ammonium sensor

5. Aeration control scheme

The aeration control strategy developed uses a known intermittent aeration cycles with a DO setpoint and residual ammonium control (See Figure A-6). Up to phase 3 only intermittent aeration with different DO setpoint (0.5 and 0.75 mg/L) was implement. This implies during these phases once the number of intermittent aeration and the durations of aerobic and anoxic cycles are fixed the total cycle duration is also fixed. For the last phase the residual ammonium control was used in addition to the intermittent aeration with a DO setpoint. This means, even if the number of intermittent cycles and the duration of aerobic and anoxic periods are fixed, the aerobic duration is variable as a result the total cycle duration becomes variable (i.e., it could be less than the predefined duration).

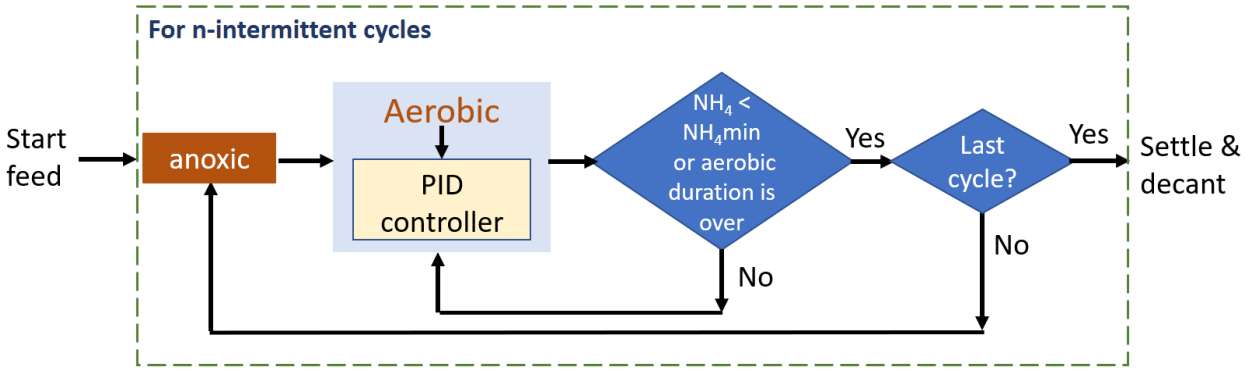

Figure A-6: Aeration control design.

6. VFA profile data

A batch cycle done volatile fatty acids (VFAs) profile measurements were done using ion chromatography as described in Smith et al. (Smith et al., 2013). Data for samples taken during Phase 1 and Phase 2 operation period are given in Figure A-7.

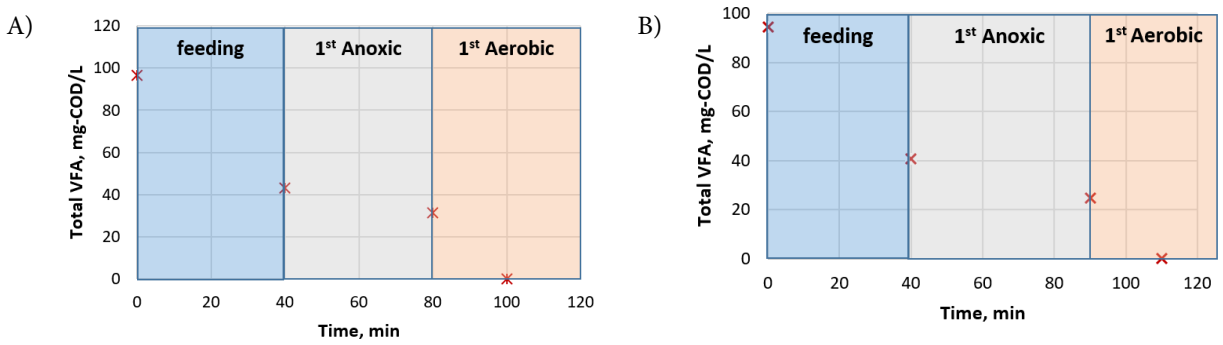

Figure A-7: Total VFA profile during (a) Low DO day 127 and (b) High DO day 321.

7. Reactor operation phases

The different operation phases implemented for the entire operation period of the reactor are summarized in Table A-2.

Table A-2. Different phases of operation and aeration controls used.

	Phase I Granulation	**Phase 2 Low DO control**	**Phase 3 High DO control**	**Phase 4 Low DO+Ammonium control**
Operation days	0-60	61-200	201-410	411-474
DO setpoint (mg/L)	1.5	0.5	0.75	0.5

8. In-situ anammox and nitrification activities test

The data for the in-situ anammox and nitrification test conducted for Phase 2 through Phase 4 are given from Table A-3 to A-7.

Table A-3: In-situ anammox activity test during Phase 2 (low DO setpoint control) on day 155.

Time (min)	Nitrite		Nitrate		Ammonia	
	mg-N/L	Error	mg-N/L	Error	mg-N/L	Error
0	39.2	2.1	24.2	0.1	27.5	2.9
30	36.3	3.5	24.5	0.1	24.8	2.3
60	35.7	1.9	25.0	0.2	18.4	2.3
90	35.5	1.6	23.6	0.2	18.7	0.6
120	34.6	2.2	24.3	0.1	18.1	2.9
150	30.5	0.8	22.7	0.1	13.7	1.9
180	31.0	2.2	26.8	3.5	16.3	0.9
210	29.5	2.7	29.2	0.1	12.4	2.8
240	28.4	1.2	28.5	0.2	14.3	1.1

Table A-4: In-situ anammox activity test during Phase 3, high DO setpoint control on day 362.

Time (min)	Nitrite		Nitrate		Ammonia	
	mg-N/L	Error	mg-N/L	Error	mg-N/L	Error
Start fed	0.0	0.0	0.0	0.0	27.4	1.0
0	20.2	0.3	8.1	0.0	25.4	0.8
30	20.5	0.1	8.2	0.0	22.6	0.5
45	19.5	0.2	8.5	0.5	22.0	0.3
60	19.0	0.1	8.8	0.5	21.5	1.1
75	19.5	0.1	8.8	0.0	20.6	1.1
90	19.0	0.1	9.0	0.0	20.8	0.7
105	17.4	0.1	9.1	0.0	20.4	0.5
120	17.2	0.2	9.6	0.0	19.3	0.8

Table A-5: In-situ anammox activity test during Phase 4, low do setpoint plus ABAC control on day 463.

Time (min)	Nitrite		Nitrate		Ammonia	
	mg-N/L	Error	mg-N/L	Error	mg-N/L	Error
Start fed	28.4	0.7	0.0	0.0	30.0	1.0
0	23.5	0.7	24.2	0.1	25.3	0.4
30	18.2	0.5	24.5	0.1	20.5	1.5
60	15.2	0.2	25.0	0.2	18.2	1.0
90	13.2	0.3	25.5	0.2	15.2	0.7
120	12.1	0.5	26.0	0.1	14.0	1.3
150	11.3	0.5	26.7	0.1	13.2	2.1
180	10.5	0.4	26.8	3.5	12.2	1.0

Table A-6: In-situ nitrification activity test during phase 2, low do setpoint control on day 179.

Time (min)	Nitrate		Nitrite		Ammonia	
	mg-N/L	Error	mg-N/L	Error	mg-N/L	Error
0	0.0	0.0	0.0	0.0	46.1	2.6
20	1.6	0.3	5.5	0.0	38.2	1.0
40	3.2	0.4	8.8	0.2	31.3	0.1
60	5.0	0.4	14.3	0.1	23.0	1.2
80	6.7	0.7	19.7	0.1	15.3	0.4
100	7.0	0.1	26.2	0.1	8.1	0.2
120	7.5	0.3	32.0	0.1	1.7	0.3

Table A-7: In-situ nitrification activity test during Phase 3, high do setpoint control on day 376.

Time (min)	Nitrate		Nitrite		Ammonia	
	mg-N/L	Error	mg-N/L	Error	mg-N/L	Error
0	0.0	0.0	0.0	0.0	46.1	2.6
20	5.5	0.0	2.4	0.1	38.2	1.0
40	9.8	0.2	5.1	0.7	31.3	0.1
60	13.9	0.0	7.4	0.5	23.0	1.2
80	18.9	0.0	10.4	0.8	15.3	0.4
100	24.9	0.2	9.1	0.5	8.1	0.2
120	30.1	0.3	10.1	0.4	1.7	0.3

Table A-8: In-situ nitrification activity test during Phase 4, low DO and ABAC on day 459

Time (min)	Nitrate		Nitrite		Ammonia	
	mg-N/L	Error	mg-N/L	Error	mg-N/L	Error
0	4.6	0.1	5.8	0.0	51.7	0.4
20	10.5	0.2	9.3	0.0	41.7	0.5
40	14.5	0.2	11.3	0.0	33.5	1.0
60	19.5	0.1	14.1	0.1	25.5	0.5
80	23.7	0.1	16.0	0.0	18.6	1.1
100	26.2	0.1	17.5	0.1	13.7	0.4
120	28.6	0.1	18.2	0.1	10.5	0.7
140	35.7	0.9	19.5	0.2	3.4	0.5

9. Methane data

Dissolved methane samples were directly taken from the reactor and analyzed in gas chromatography. Figure A-7 shows methane profile for sample taken on day 420 during phase 4 of the reactor operation.

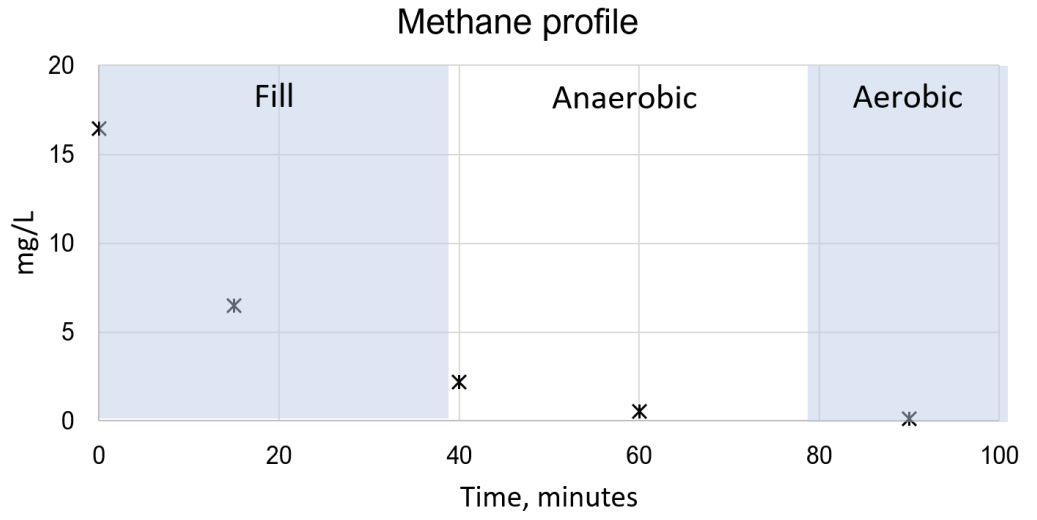

Figure A-8. Methane profile taken on day 420 during Phase 4.

10.Profile (Cross-cycle) data analysis

Routine time profile (cross-cycle) monitoring of N species was done by taking sample at the different stages within one batch cycle. Tables A-9 through A-26 give the data for samples taken during the different operation stages of the reactor. These data were used to estimate the relative contribution of anammox vs OHOs for N removal. From the VFA data we noticed that by the

end of the first aerobic period all VFA in the fed was consumed, hence we assumed N removal that has happened starting the second anoxic period is due to anammox plus N used for maintenance. With this assumption we used the following standard stoichiometric equations to determine the contribution of OHOs in N removal from fed to the end of the first anoxic period based on how much NO_X was lost for each cross-cycle data. We calculated OHOs contribution for a range of VFA fractions from 0 to 1 consumed for denitrification, while the remaining fraction is assumed to be oxidized in first aerobic period. Among the range of values, the maximum stoichiometrically possible VFA value was used to report the contribution of OHOs in N removal. This is done not to overestimate anammox contribution in N removal.

NO_3^- as electron acceptor

$$0.125CH_2COO^- + 0.106NO_3^- + 0.0235NH_4^+ + 0.106H^+ = 0.155H_2O + 0.031CO_2 + 0.053N_2 + 0.0235C_5H_7O_2N \quad \text{(Eq. A-2)}$$

NO_2^- as electron acceptor

$$0.125CH_2COO^- + 0.177NO_2^- + 0.0235NH_4^+ + 0.177H^+ = 0.1898H_2O + 0.031CO_2 + 0.088N_2 + 0.0235C_5H_7O_2N \quad \text{(Eq. A-3)}$$

Table A-9: Cross-cycle samples data for phase 2 taken on day 78

Time from start (min)	**Stage**	**NH_4^+ (mg·N/L)**	**NO_2^- (mg·N/L)**	**NO_3^- (mg·N/L)**
	Influent	48.27	0	0
0	Anoxic 11	25.66	9.85	0.64
50	Anoxic 12	22.89	6.31	0.67
140	Aerobic 12	17.77	9.28	4.20
190	Anoxic 22	16.83	9.94	3.91
280	Aerobic 22	4.91	18.10	2.16
285	Effluent	3.05	19.71	1.28

Table A-10: Cross-cycle samples data for phase 2 taken on day 89

Time from start (min)	Stage	NH_4^+ (mg·N/L)	NO_2^- (mg·N/L)	NO_3^- (mg·N/L)
	Influent	50.11	0.00	0.00
0	Anoxic 11	32.94	4.61	0.18
50	Anoxic 12	32.10	3.75	0.14
140	Aerobic 12	28.55	6.18	0.17
190	Anoxic 22	23.98	6.14	0.15
280	Aerobic 22	20.55	9.66	0.21
285	Effluent	15.76	11.21	0.35

Table A-11: Cross-cycle samples data for phase 2 taken on day 109

Time from start (min)	Stage	NH_4^+ (mg·N/L)	NO_2^- (mg·N/L)	NO_3^- (mg·N/L)
	Influent	51.04	0.00	0.00
0	Anoxic 11	29.31	3.12	1.22
50	Anoxic 12	24.44	1.63	1.19
140	Aerobic 12	17.21	2.67	1.29
190	Anoxic 22	13.56	3.12	1.34
280	Aerobic 22	8.50	5.64	1.65
285	Effluent	7.58	6.06	2.44

Table A-12: Cross-cycle samples data for phase 2 taken on day 120

Time from start (min)	Stage	NH_4^+ (mg·N/L)	NO_2^- (mg·N/L)	NO_3^- (mg·N/L)
	Influent	51.04	0.00	0.00
0	Anoxic 11	26.24	8.30	0.17
50	Anoxic 12	23.53	1.01	0.03
140	Aerobic 12	20.30	11.89	0.13
190	Anoxic 22	18.52	18.70	0.13
280	Aerobic 22	10.23	19.21	0.39
285	Effluent	8.51	20.52	0.33

Table A-13: Cross-cycle samples data for phase 2 taken on day 134

Time from start (min)	Stage	NH_4^+ (mg·N/L)	NO_2^- (mg·N/L)	NO_3^- (mg·N/L)
	Influent	51.04	0.00	0.00
0	Anoxic 11	33.02	17.95	0.17
50	Anoxic 12	18.12	18.80	0.41
140	Aerobic 12	8.13	30.76	0.27
190	Anoxic 22	3.36	36.14	0.24
280	Aerobic 22	0.10	38.66	0.26
285	Effluent	15.00	35.90	0.33

Table A-14: Cross-cycle samples data for phase 2 taken on day 148

Time from start (min)	Stage	NH_4^+ (mg·N/L)	NO_2^- (mg·N/L)	NO_3^- (mg·N/L)
	Influent	51.04	0.00	0.00
0	Anoxic 11	33.02	4.02	0.17
50	Anoxic 12	24.44	1.81	1.19
140	Aerobic 12	17.21	6.14	1.29
190	Anoxic 22	13.56	5.12	1.20
280	Aerobic 22	8.50	7.85	0.95
285	Effluent	7.58	8.52	0.33

Table A-15: Cross-cycle samples data for phase 2 taken on day 159

Time from start (min)	Stage	NH_4^+ (mg·N/L)	NO_2^- (mg·N/L)	NO_3^- (mg·N/L)
	Influent	50.14	0	0
0	Anoxic 11	31.41	5.01	1.22
50	Anoxic 12	27.90	8.61	1.19
140	Aerobic 12	20.08	15.21	1.29
190	Anoxic 22	19.27	14.98	1.2
280	Aerobic 22	12.67	16.68	0.95
285	Effluent	12.67	17.32	2.44

Table A-16: Cross-cycle samples data for phase 2 taken on day 171

Time from start (min)	Stage	NH_4^+ (mg·N/L)	NO_2^- (mg·N/L)	NO_3^- (mg·N/L)
	Influent	45.22	0	0
0	Anoxic 11	30.22	5.845	0.24
50	Anoxic 12	29.57	3.98	0.15
140	Aerobic 12	23.53	6.71	0.19
190	Anoxic 22	21.18	8.28	0.15
280	Aerobic 22	14.55	12.99	0.33
285	Effluent	15.22	13.69	0.48

Table A-17: Cross-cycle samples data for phase 3 taken on day 201

Time from start (min)	Stage	NH_4^+ (mg·N/L)	NO_2^- (mg·N/L)	NO_3^- (mg·N/L)
	Influent	52.83	0.00	0.00
0	Anoxic 00	28.13	8.81	0.07
25	Anoxic 11	15.68	8.63	0.16
50	Anoxic 12	29.58	3.99	0.13
75	Aerobic 11	27.83	2.12	0.12
100	Aerobic 12	26.21	2.13	0.19
150	Anoxic 22	24.40	1.91	0.16
175	Aerobic 21	22.78	4.81	0.13
200	Aerobic 22	20.94	5.29	0.05
250	Anoxic 32	17.35	7.75	0.16
275	Aerobic 31	14.09	9.42	0.13
300	Aerobic 32	12.10	10.72	0.35
205	Effluent	13.44	12.61	0.13

Table A-18: Cross-cycle samples data for phase 3 taken on day 219

Time from start (min)	Stage	NH_4^+ (mg·N/L)	NO_2^- (mg·N/L)	NO_3^- (mg·N/L)
	Influent	55.17	0.00	0.00
0	Anoxic 00	38.96	3.71	0.07
25	Anoxic 11	29.24	4.78	0.16
50	Anoxic 12	35.09	1.09	0.13
75	Aerobic 11	32.44	1.26	0.12
100	Aerobic 12	29.21	1.73	0.19
150	Anoxic 22	26.78	3.33	0.16
175	Aerobic 21	23.50	4.26	0.13
200	Aerobic 22	20.00	6.05	0.05
250	Anoxic 32	20.42	8.96	0.16
275	Aerobic 31	16.34	11.67	0.13
300	Aerobic 32	13.64	10.68	0.35
205	Effluent	22.75	7.41	0.13

Table A-19: Cross-cycle samples data for phase 3 taken on day 239

Time from start (min)	Stage	NH_4^+ (mg·N/L)	NO_2^- (mg·N/L)	NO_3^- (mg·N/L)
	Influent	53.06	0.00	0.00
0	Anoxic 00	27.09	2.85	10.80
25	Anoxic 11	23.21	2.56	12.51
50	Anoxic 12	21.60	1.29	12.74
75	Aerobic 11	17.97	2.97	13.28
100	Aerobic 12	14.83	4.30	15.12
150	Anoxic 22	12.96	4.29	15.66
175	Aerobic 21	9.68	4.75	16.41
200	Aerobic 22	7.41	5.93	17.89
250	Anoxic 32	6.19	5.66	18.47
275	Aerobic 31	5.15	5.73	18.77
300	Aerobic 32	4.00	5.57	19.97
205	Effluent	1.12	5.70	21.61

Table A-20: Cross-cycle samples data for phase 3 taken on day 246

Time from start (min)	Stage	NH_4^+ (mg·N/L)	NO_2^- (mg·N/L)	NO_3^- (mg·N/L)
	Influent	53.06	0.00	0.00
0	Anoxic 00	26.77	0.02	15.53
25	Anoxic 11	9.70	0.00	23.59
50	Anoxic 12	25.29	0.00	11.57
75	Aerobic 11	21.84	1.94	12.55
100	Aerobic 12	19.10	2.23	13.79
150	Anoxic 22	15.37	2.19	15.78
175	Aerobic 21			
200	Aerobic 22			
250	Anoxic 32	5.27	3.26	23.70
275	Aerobic 31	3.82	2.44	24.84
300	Aerobic 32	0.69	0.57	29.62
205	Effluent	0.48	0.47	31.05

Table A-21: Cross-cycle samples data for phase 3 taken on day 253

Time from start (min)	Stage	NH_4^+ (mg·N/L)	NO_2^- (mg·N/L)	NO_3^- (mg·N/L)
	Influent	54.16	0.00	0.00
0	Anoxic 00	27.08	0.00	16.82
25	Anoxic 11	17.19	0.00	19.81
50	Anoxic 12	17.07	0.00	18.33
75	Aerobic 11	14.58	1.41	19.26
100	Aerobic 12	9.20	2.49	22.89
150	Anoxic 22	6.72	2.73	25.26
175	Aerobic 21	2.84	3.03	29.58
200	Aerobic 22	0.94	0.75	34.35
250	Anoxic 32	0.28	0.00	35.86
275	Aerobic 31	0.21	0.00	36.11
300	Aerobic 32	0.02	0.00	36.87
205	Effluent	0.01	0.00	36.64

Table A-22: Cross-cycle samples data for phase 3 taken on day 274

Time from start (min)	Stage	NH_4^+ (mg·N/L)	NO_2^- (mg·N/L)	NO_3^- (mg·N/L)
	Influent	62.45	0.00	0.00
0	Anoxic 00	31.24	3.55	13.28
25	Anoxic 11	25.29	5.60	9.45
50	Anoxic 12	25.24	5.78	4.88
75	Aerobic 11	21.38	7.26	6.25
100	Aerobic 12	14.65	9.73	9.93
150	Anoxic 22	13.46	9.79	10.74
175	Aerobic 21	7.08	6.66	13.97
200	Aerobic 22	3.74	10.26	17.01
250	Anoxic 32	2.58	9.05	17.09
275	Aerobic 31	0.51	8.89	19.32
300	Aerobic 32	1.07	7.55	21.59
205	Effluent	0.04	7.11	22.56

Table A-23: Cross-cycle samples data for phase 3 taken on day 284

Time from start (min)	Stage	NH_4^+ (mg·N/L)	NO_2^- (mg·N/L)	NO_3^- (mg·N/L)
	Influent	49.25	0.00	0.00
0	Anoxic 00	25.43	5.00	9.50
25	Anoxic 11	42.84	0.00	1.03
50	Anoxic 12	35.42	1.06	0.63
75	Aerobic 11			
100	Aerobic 12	33.83	3.10	2.97
150	Anoxic 22	22.67	7.98	7.33
175	Aerobic 21			
200	Aerobic 22	13.83	11.36	12.91
250	Anoxic 32	9.72	12.49	15.10
275	Aerobic 31			
300	Aerobic 32	3.32	10.39	19.75
205	Effluent	3.12	9.98	20.36

Table A-24: Cross-cycle samples data for phase 3 taken on day 326

Time from start (min)	Stage	NH_4^+ (mg·N/L)	NO_2^- (mg·N/L)	NO_3^- (mg·N/L)
	Influent	47.29	0.00	0.00
0	Anoxic 00	23.68	2.93	0.76
25	Anoxic 11	22.61	0.14	0.00
50	Anoxic 12	22.39	0.00	0.00
75	Aerobic 11			
100	Aerobic 12	17.71	3.30	0.70
150	Anoxic 22	17.08	3.17	0.86
175	Aerobic 21			
200	Aerobic 22	7.21	7.26	2.69
250	Anoxic 32	3.06	8.36	3.45
275	Aerobic 31			
300	Aerobic 32	0.09	8.90	6.18
205	Effluent	0.06	6.92	6.23

Table A-25: Cross-cycle samples data for phase 4 taken on day 434

Time from start (min)	Stage	NH_4^+ (mg·N/L)	NO_2^- (mg·N/L)	NO_3^- (mg·N/L)
	Influent	44.02	0.00	0.00
0	Anoxic 00	15.97	5.90	0.41
30	Anoxic 11	15.15	3.73	0.12
60	Anoxic 12	12.58	0.95	0.47
90	Aerobic 1	10.88	3.94	0.68
120	Anoxic 21	8.19	3.57	0.71
150	Anoxic 22	7.97	2.37	1.12
180	Aerobic 2	6.38	4.36	1.28
210	Anoxic 31	3.10	4.07	1.51
240	Anoxic 32	2.49	2.68	3.99

Table A-26: Cross-cycle samples data for phase 4 taken on day 447

Time from start (min)	Stage	NH_4^+ (mg·N/L)	NO_2^- (mg·N/L)	NO_3^- (mg·N/L)
	Influent	44.02	0.00	0.00
0	Anoxic 0	22.67	9.47	0.00
40	Anoxic 1	21.33	9.33	0.29
70	Aerobic 11	17.06	13.05	0.44
100	Aerobic 12	13.05	13.56	0.58
140	Anoxic 2	12.79	14.53	0.89
170	Aerobic 21	8.98	15.30	0.72
200	Aerobic 22	6.67	18.04	0.84
240	Anoxic 3	6.52	19.54	1.07
270	Aerobic 31	3.79	21.59	1.24
300	Aerobic 32	3.33	21.26	1.15

11.Physical characterization of granules

To determine biomass production and sludge volume index (SVI), total suspended solids (TSS), volatile suspended solids (VSS) and sludge volume were measured weekly or biweekly. The sludge volume was measure by directly reading the settled granule depth from the reactor at 5 min and 30 min. The SVIs at 5 and 30 min were calculated by dividing the granule volume (mL) with reactor volume (4.5L) and TSS (g TSS L-1). The morphology of the granules was monitored periodically using a digital camera (Canon G7X) and ImageJ software (Rasband & S., 2012) for image analysis of the granules' size distribution. Solids were wasted at the end of each cycle during the decanting period only and was considered when calculating the solids retention time (SRT) as described in the Section 1.

12.Synthetic media

The influent fed to the reactor was a synthetic anaerobic effluent freshly prepared every 2-days. Twenty liters of influent was prepared every 2-3 days by combining an acidic trace metals, basic trace metals and NaEDTA (10.08g/L) each 20 mL. The acidic trace metals stock solution was prepared by mixing (per liter): $CoCl_2 \cdot 6H_2O$, 0.28 g; $ZnSO_4 \cdot 7H_2O$, 0.34 g; H_3BO_3, 37 mg; $MnCl_2 \cdot 4H_2O$, 0.11 g; $AlCl_3 \cdot 6H_2O$, 28 mg; $NiCl_2 \cdot 6H_2O$, 0.14 g; $CuCl_2 \cdot 2H_2O$, 0.10 g. The basic trace metals stock solution was prepared by mixing (per liter): $(NH_4)_2MoO_4 \cdot 4H_2O$, 0.16 g;

Na_2SeO_4, 22 mg; $Na_2WO_4 \cdot 2H_2O$, 39.5 mg. Next, 100 mL of a 56g/L ammonium bicarbonate stock was added. After thoroughly mixing these in a flask, 20 mL of a chloride salts solution made up of (per liter): $CaCl_2 \cdot 2H_2O$, 5g; $MgCl_2 \cdot 6H_2O$, 33 g; KCl, 16 g; KH_2PO_4, 11 g, was added to the mixture. This mixture was combined with 65 mL of 1 N HCL and diluted with DI water to make 20 liters of influent solution. Following this, the solution was sparged with methane gas for 25 minutes, after which 95 mL of a 30 g/L sodium bicarbonate stock and 20 mL of a 6.6 g/L $FeSO_4 \cdot 7H_2O$ stock (stored in an anaerobic glove chamber) were added. Finally, the influent solution was sparged for 5 more minutes with methane gas. For the addition of VFAs, a separate bottle containing equivalent COD proportions of sodium acetate and sodium propionate was fed via a peristaltic pump to get 100 mg COD/L. All glassware used for preparing the feed stock was autoclaved every time before making influent.

13.In-situ activity batch tests

In-situ batch activity tests were conducted to determine the extent of nitrification and anaerobic ammonium oxidation (anammox). For these in-situ tests the reactor was operated for at least one hour under aerobic conditions at the end of the prior cycle to remove any remaining organic carbon present in the system. Next, the supernatant was decanted completely, granules were taken out of the reactor, and rinsed with VFA- and methane-free influent media. The washed granules were returned to the reactor, which was filled with VFA- and methane-free influent media containing inorganic nitrogen chemicals tailored for each test. Specifically, ammonium was the only inorganic nitrogen chemical added for the in-situ nitrification test, while ammonium, nitrite and nitrate (to create an appropriate redox condition and avoid sulfate reduction (Loosdrecht et al., 2016)) were added for the in-situ anammox activity test. For the in-situ nitrification test, the reactor was operated under aerobic conditions by mixing with dry air gas and taking samples after a stable bulk DO > 1 mg/L was achieved. For the in-situ anammox test, the reactor was operated anaerobically by mixing with nitrogen gas (99.998% purity), and taking samples after achieving stable anaerobic conditions, defined by waiting 10 minutes after no DO was detected (detection limit = 0.00 mg/L O_2). Seven to nine samples were taken over 2 to 4 hours for each test and analyzed for ammonium, nitrite and nitrate according to the methods described in Section 2.5. One of each kind of test occurred during each of Phase 2, 3 and 4. The maximum specific anammox rate (mg-N/mg-VSS/day) was determined by first doing linear

regression using the data to determine the nitrogen removal rate (i.e., ammonium removal rate plus nitrite removal rate minus nitrate production rate) then dividing it by the volatile suspended solids.

14.References

Loosdrecht, M. C. M. van, Nielsen, P. H., Lopez-Vazquez, C. M., & Brdjanovic, D. (2016). Experimental procedures in wastewater treatment. In *Experimental procedures in wastewater treatment*. IWA Publishing. http://www.iwapublishing.com/books/9781780404745/experimental-methods-wastewater-treatment

Rasband, W. S., & S., W. (2012). ImageJ: Image processing and analysis in Java. *Astrophysics Source Code Library, Record Ascl:1206.013*. http://adsabs.harvard.edu/abs/2012ascl.soft06013R

Appendix B Supplementary information for Chapter 4

Long-term stability and performance of aerobic granular sludge reactor for nitrogen removal with an adaptive sensor-mediated control

1. Solids concentration and SVI

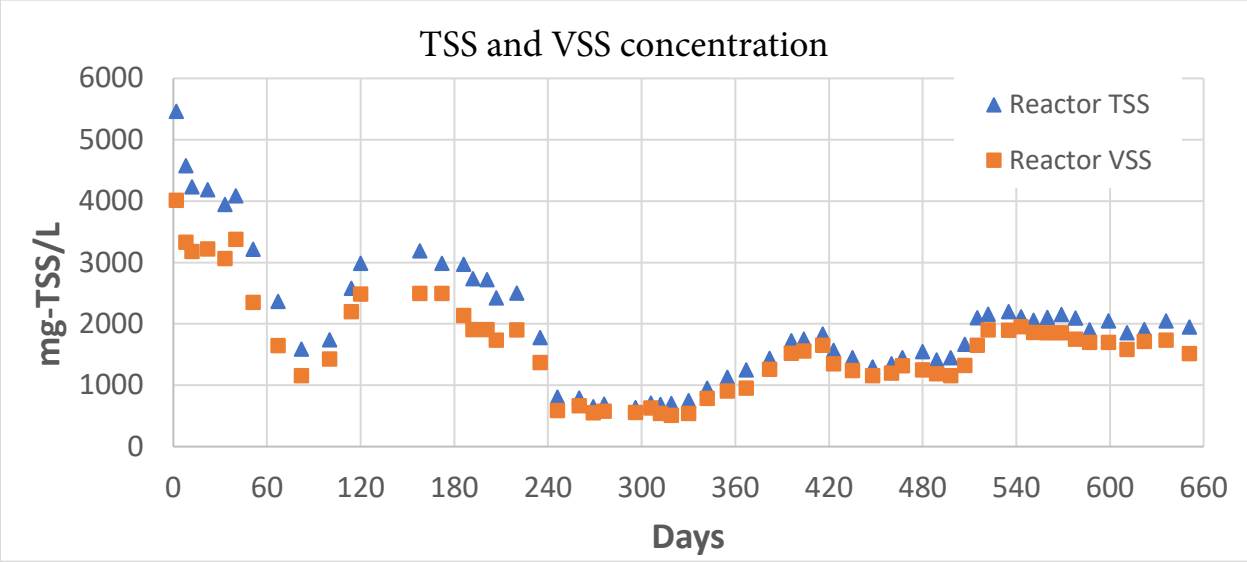

Figure B-1: Solids concentration in the reactor in mg-TSS/L

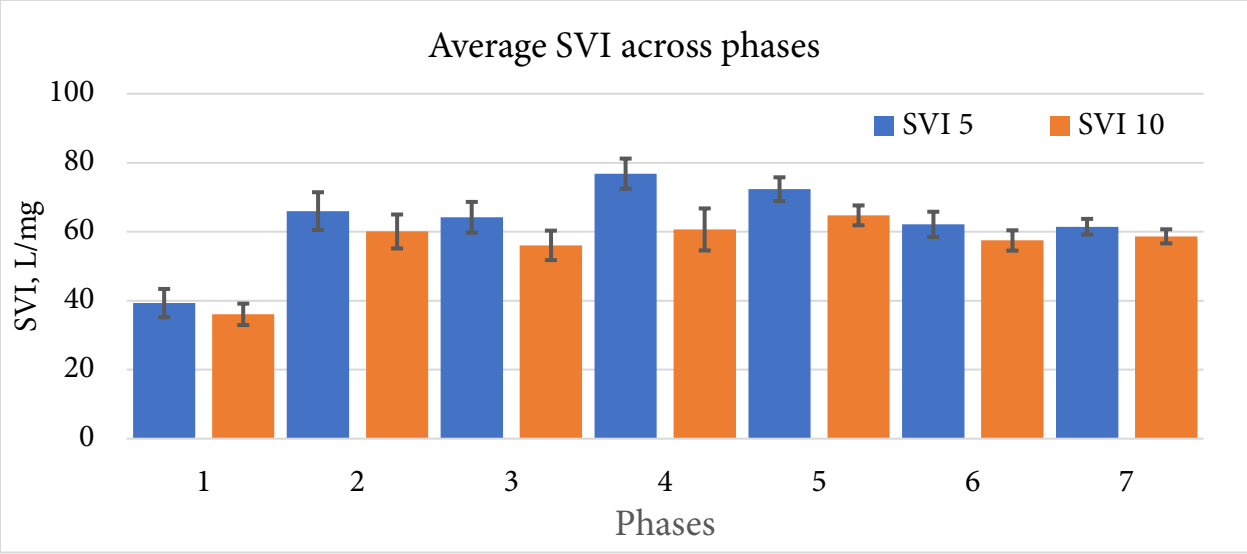

Figure B-2: Sludge volume index after 5 and 30 minutes of settling.

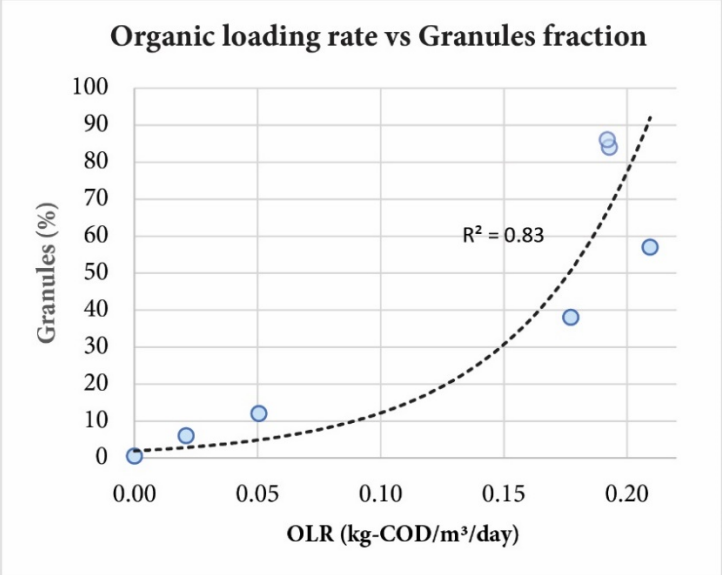

Figure B-3: Organic loading rate vs granules fraction by mass.

2. SRT calculation

Solids are wasted from the reactor in each cycle only during the decanting period and sludge retention time (SRT) was calculated according to Eq. (B-1). Figure B-3 gives the box plot for the calculated SRT values for the four operation phases.

$$SRT = \frac{TSS_r \cdot V_r}{TSS_{eff} \cdot Q_{eff}} \qquad \text{(Eq. B-1)}$$

Where:

TSS_r: TSS concentration in the reactor (g TSS L^{-1})
V_r: reactor volume (L)
$TSS_{eff.}$: TSS concentration in the effluent (g TSS L^{-1})
$Q_{eff.}$: effluent flow rate (L d^{-1})

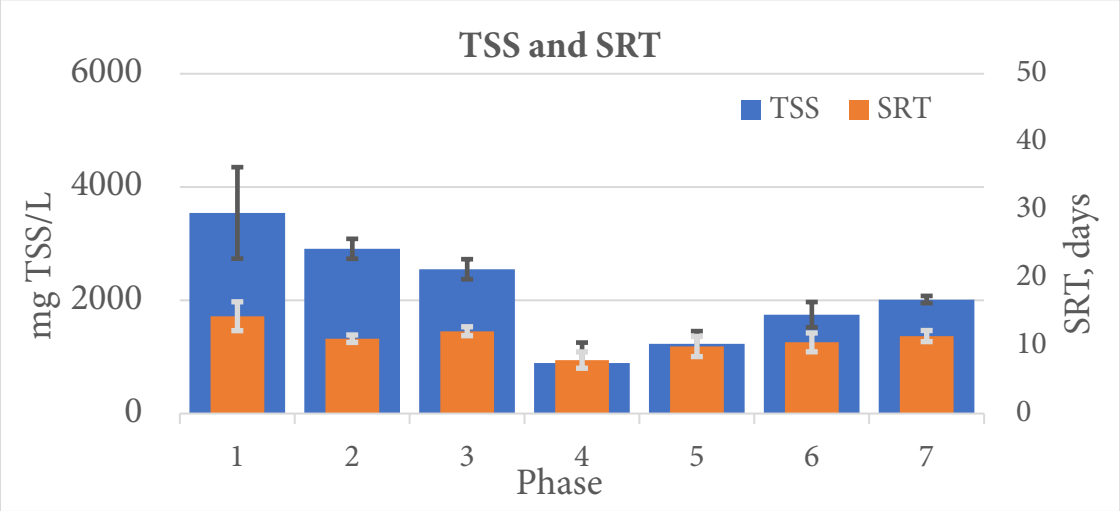

Figure B-4 Average TSS concentration and SRT across different phases

3. Influent and effluent N species profile

Figure B-1 presents the concentrations of N species for influent and effluent taken throughout the operation of the reactor. Influent samples were taken from the influent line during fed time and effluent samples from effluent line after settling during discharge.

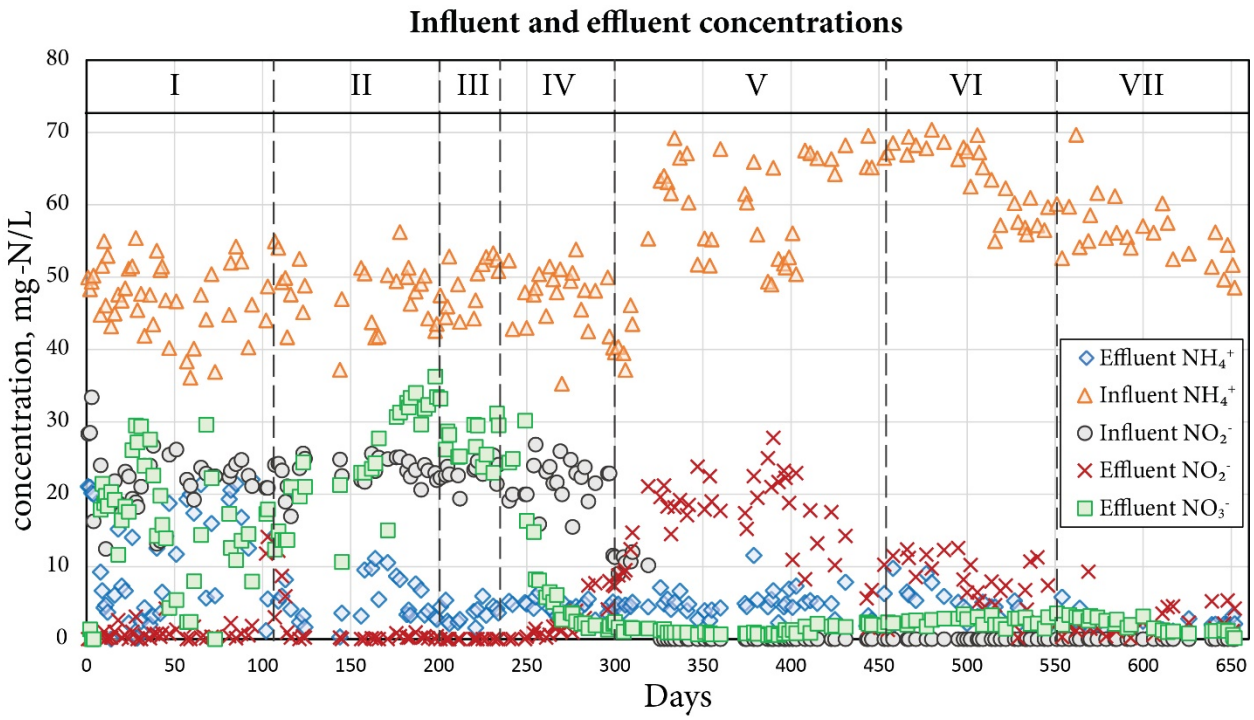

Figure B-5: Nitrogen species profile for the entire span of the reactors operation taken for samples taken from influent and effluent.

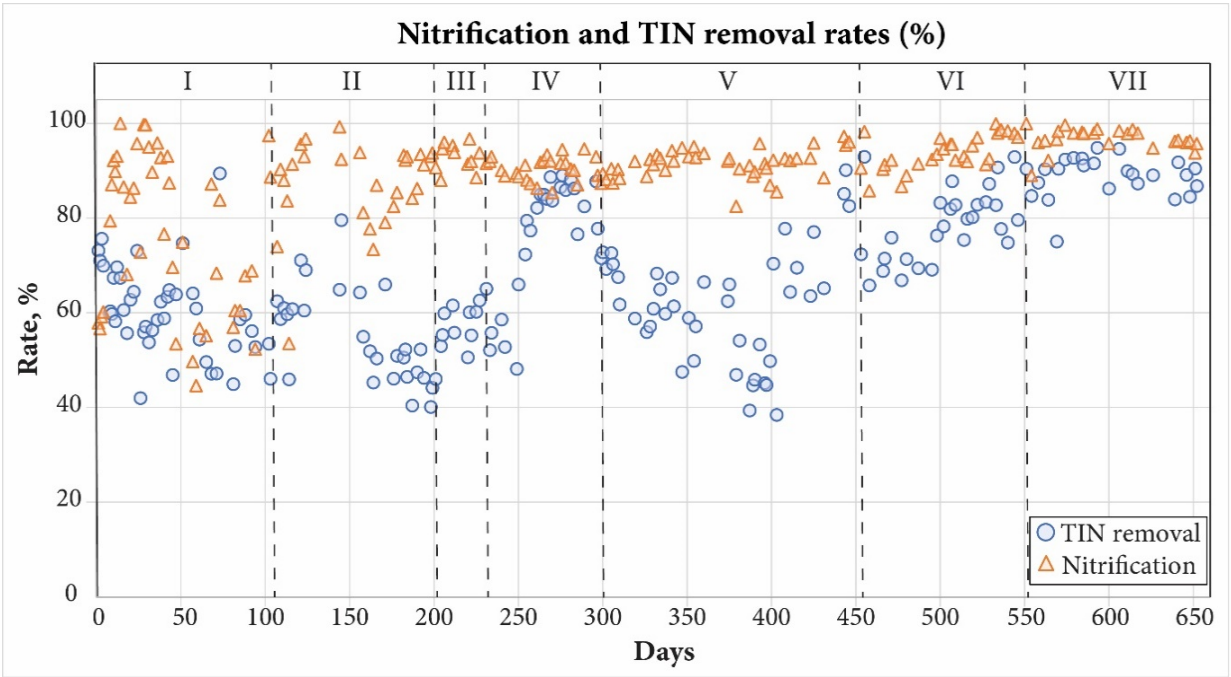

Figure B- 6: Nitrification and TIN removal efficiency across 7 operation phases.

4. Microbial community data

Biomass samples were taken from the reactor during Phase 5, 6, and 7, then the biomass was separated into flocs and granules by using a 200 μm sieve. Then, DNA samples were extracted from the flocs, granules, and the mix (the original sample taken directly from the reactor) and 16S rRNA sequencing was done to study the microbial composition between granules and flocs.

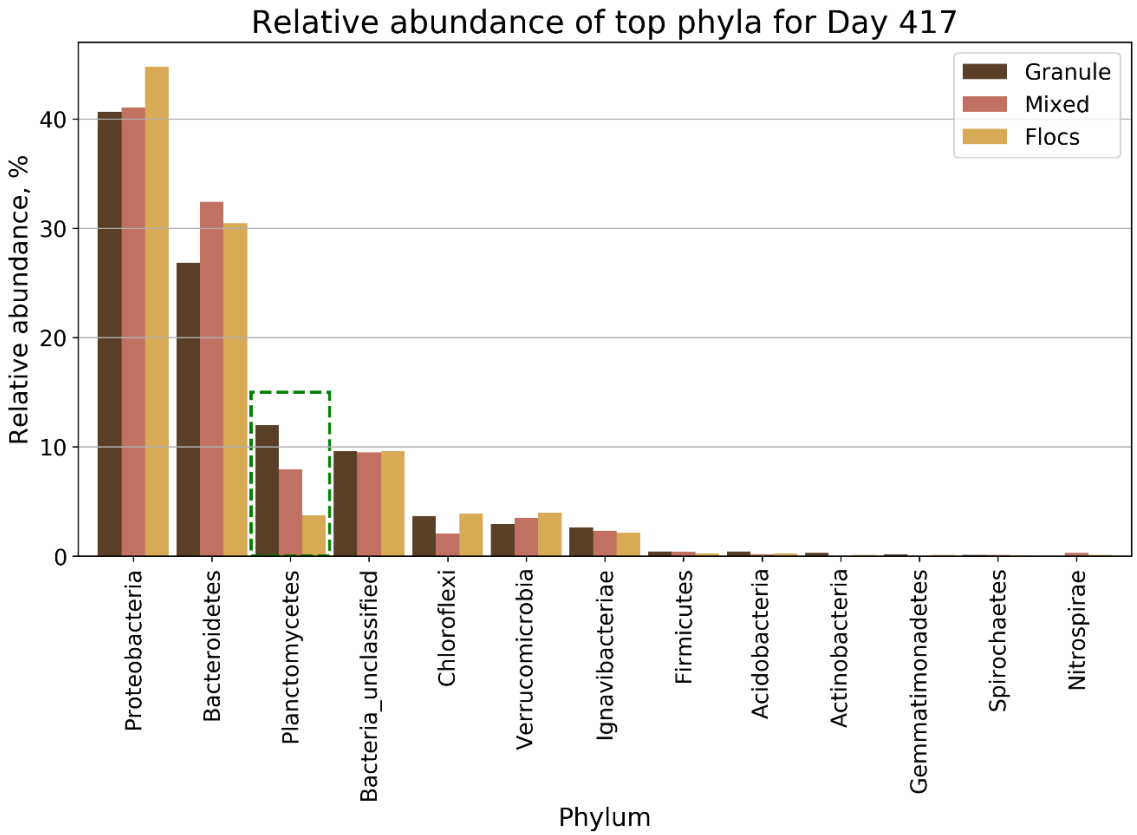

Figure B-7: Relative abundance (%) of top phyla comparison among granules, flocs and a mix of granules and flocs take from the reactor at the same time. The sample was taken on operation day 417 (Phase 5).

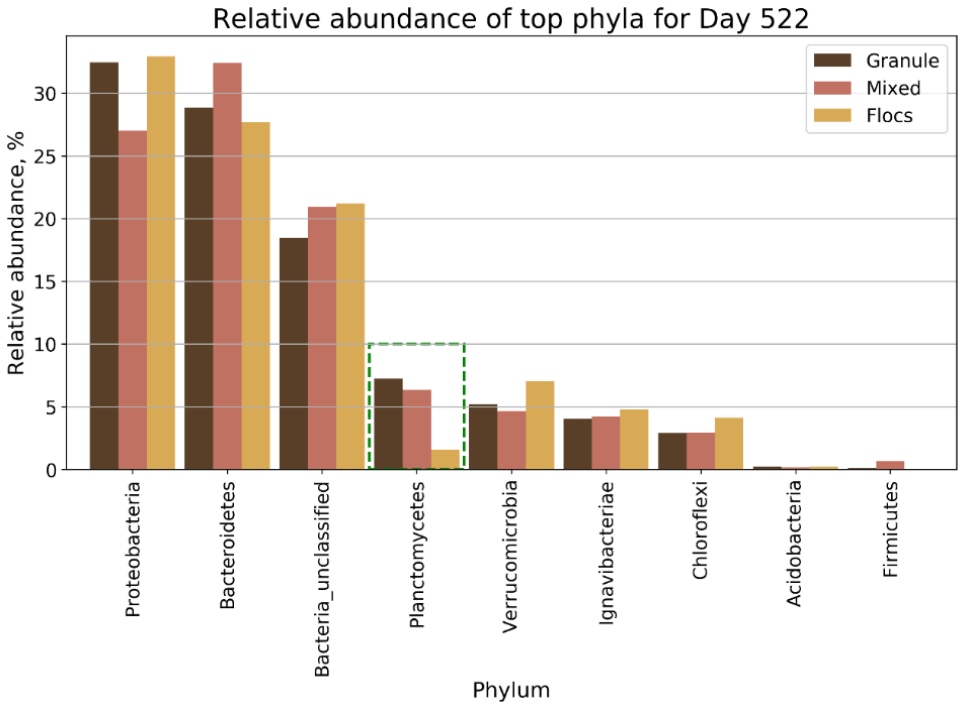

Figure B- 8 Relative abundance (%) of top phyla comparison among granules, flocs and a mix of granules and flocs take from the reactor at the same time. The sample was taken on operation day 522 (Phase 6).

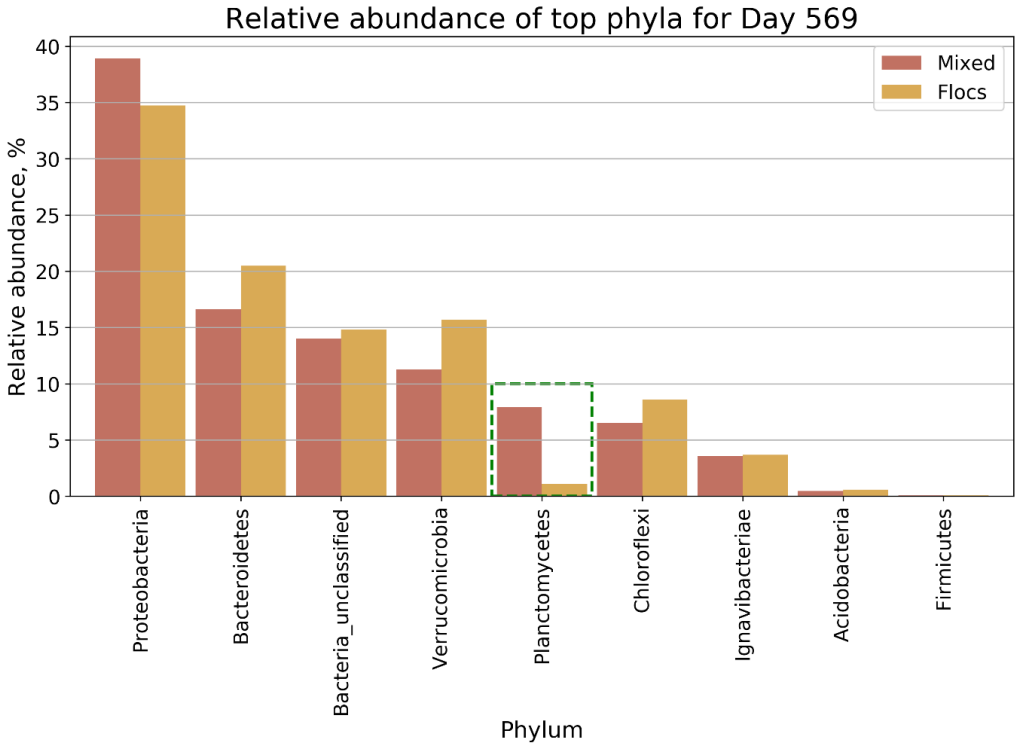

Figure B- 8 Relative abundance (%) of top phyla comparison among granules, flocs and a mix of granules and flocs take from the reactor at the same time. The sample was taken on operation day 569 (phase 7).

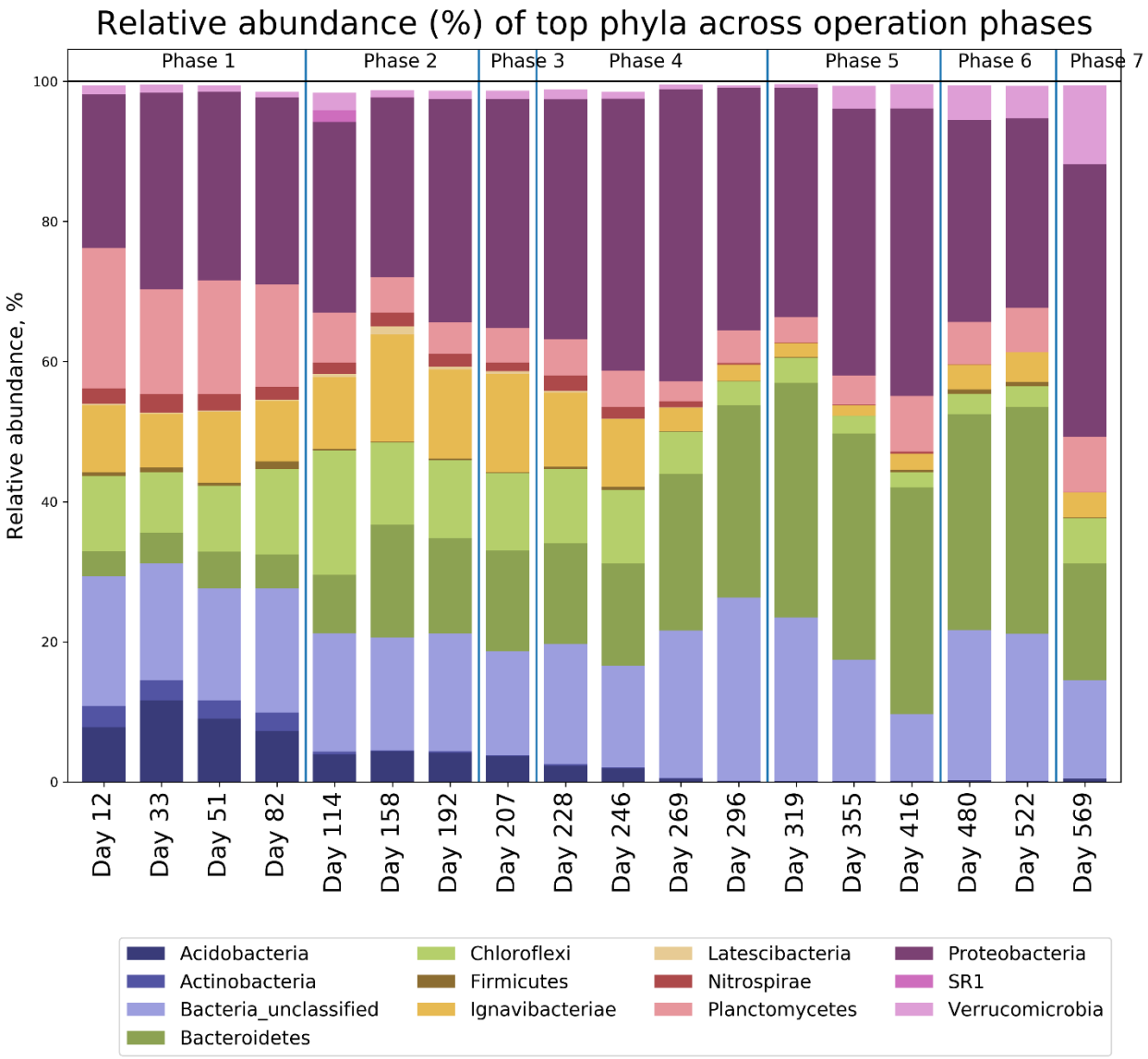

Figure B-9: Microbial community data taken from the reactor (granules + flocs) over the course of the 7 operation phases of the reactor. The data presented here is at phylum with relative abundance > 0.2%.

5. Anammox specific activity test results

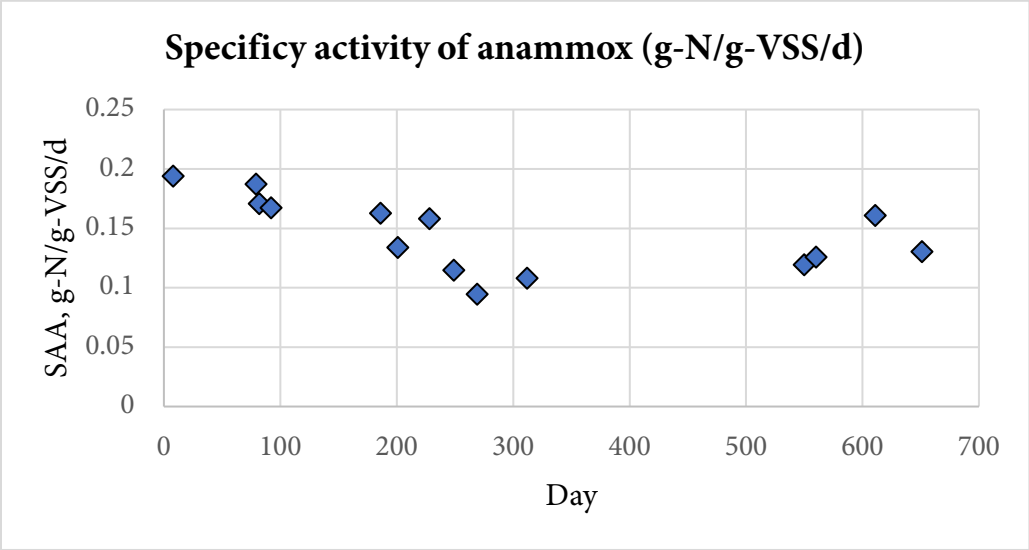

Figure B-10: Specific activity of anammox (SAA) for samples taken on different days throughout the operation phases.

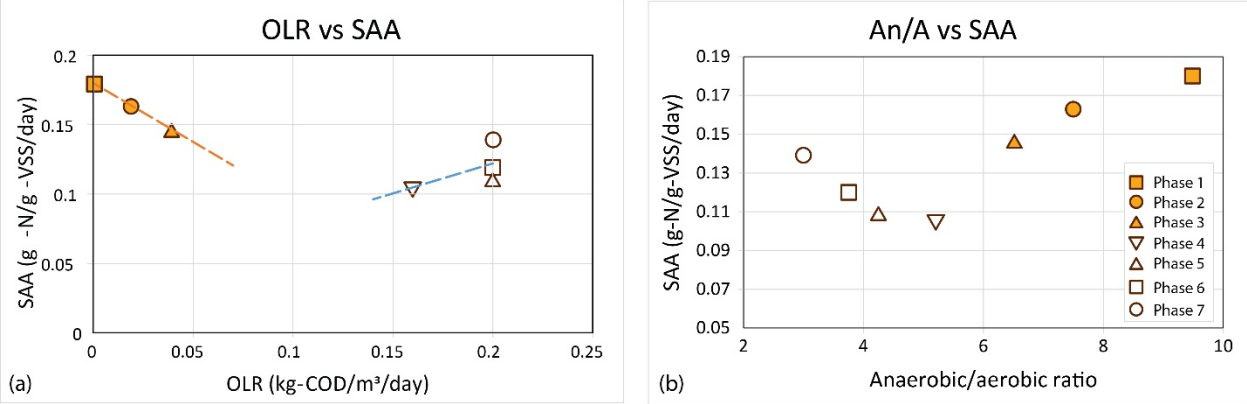

Figure B-12: (a) Organic loading rate vs specific anammox activity rate for the different phases. (b)Anaerobic to aerobic duration ratio vs specific anammox activity rate for the 7 operation Phases.

6. Profile (cross-cycle) data

Table B-1: Cross-cycle samples data for phase 1 taken on day 20

Total Time (min)	Stage	NH_4^+ (mg·N/L)	NO_2^- (mg·N/L)	NO_3^- (mg·N/L)
0	Influent	49.04	22.03	0.00
37	Anoxic 11	23.51	15.27	2.77
67	Anoxic 12	22.70	14.12	3.10
97	Anoxic 13	22.27	13.37	3.43
127	Anoxic 14	21.21	12.74	4.50
157	Aerobic 1	20.17	11.90	6.23
177	Anoxic 21	14.59	9.07	7.46
207	Anoxic 22	12.76	7.49	8.02
237	Anoxic 23	10.93	6.56	9.58
267	Anoxic 24	10.11	5.63	9.82
297	Aerobic 2	8.92	3.48	9.53
317	Effluent	7.62	1.29	10.02

Table B-2: Cross-cycle samples data for phase 1 taken on day 68

Total Time (min)	Stage	NH_4^+ (mg·N/L)	NO_2^- (mg·N/L)	NO_3^- (mg·N/L)
0	Influent	48.22	26.03	0.00
7	Anoxic 11	28.96	21.01	2.65
37	Anoxic 12	27.51	16.27	5.77
67	Anoxic 13	23.70	12.12	6.10
97	Anoxic 14	22.27	10.37	6.43
122	Aerobic 1	20.82	7.74	8.00
152	Anoxic 21	20.17	7.90	9.74
182	Anoxic 22	17.59	6.07	10.96
212	Anoxic 23	15.76	3.49	11.52
237	Aerobic 2	13.93	2.56	13.08
267	Anoxic 31	15.11	1.63	13.32
297	Anoxic 32	11.92	0.48	13.03
327	Anoxic 33	**11.62**	0.29	13.52
352	Aerobic 3	11.87	0.06	12.84

Table B-3: Cross-cycle samples data for phase 2 taken on day 120

Total Time (min)	Stage	NH_4^+ (mg·N/L)	NO_2^- (mg·N/L)	NO_3^- (mg·N/L)
0	Influent	54.02	21.85	0.00
40	Anoxic 11	23.33	18.45	2.02
80	Anoxic 12	15.09	10.21	4.75
95	Aerobic 1	9.42	7.34	7.28
135	Anoxic 21	6.84	6.90	9.33
175	Anoxic 22	4.05	4.02	13.34
190	Aerobic 2	2.52	1.03	14.31
230	Anoxic 31	1.26	1.13	14.87
270	Anoxic 32	1.06	0.00	15.07
285	Aerobic 3	0.86	0.00	14.78
300	Effluent	0.45	0.00	14.63

Table B-4: Cross-cycle samples data for phase 2 taken on day 158

Total Time (min)	Stage	NH_4^+ (mg·N/L)	NO_2^- (mg·N/L)	NO_3^- (mg·N/L)
0	Influent	48.50	21.72	0.00
0	Anoxic 11	27.73	13.51	8.73
30	Anoxic 12	25.74	9.05	9.32
60	Anoxic 13	21.45	4.84	10.52
90	Aerobic 1	22.22	0.19	11.39
105	Anoxic 21	15.63	0.00	14.46
135	Anoxic 22	11.93	0.00	15.60
165	Anoxic 23	12.92	0.00	14.12
195	Aerobic 2	11.89	0.00	14.38
210	Anoxic 3	10.30	0.00	15.65
225	Aerobic 3	9.54	0.00	16.25

Table B-5: Cross-cycle samples data for phase 3 taken on day 201

Total Time (min)	Stage	NH_4^+ (mg·N/L)	NO_2^- (mg·N/L)	NO_3^- (mg·N/L)
0	Influent	51.65	26.56	0.00
37	Anoxic 11	34.85	20.81	4.62
67	Anoxic 12	33.04	19.74	5.25
97	Anoxic 13	34.52	18.35	5.32
127	Anoxic 14	30.89	14.91	5.46
142	Aerobic 1	25.69	13.96	9.10
172	Anoxic 21	24.26	11.66	11.69
202	Anoxic 22	22.59	9.87	11.62
232	Anoxic 23	21.54	6.83	11.69
247	Aerobic 2	16.00	6.78	15.26
277	Anoxic 31	13.81	4.84	17.57
307	Anoxic 32	13.57	3.19	17.64
337	Anoxic 33	12.38	2.59	17.50
352	Aerobic	7.80	0.47	20.65

7. Model sensitivity analysis and calibration result

Global sensitivity analysis was done using Morris's elementary effect method (Saltelli et al., 2008). The elementary effect method calculates the average derivatives of a factor over n-level of discretized space of the input using Equation B-2. The elementary effect (EE) is calculated at each grid point and the average of the absolute values are calculated. The average EE (μ) are calculated for all factors considered, then it will be used to rank on the factors. Figure B-13 presents the results of the global sensitivity analysis.

$$\mu_i^* = \frac{1}{r}\sum_{j=1}^{r}\left|EE_i^j\right| \qquad \text{Equation B-2}$$

Figure B-13 presents the results of the global sensitivity analysis.

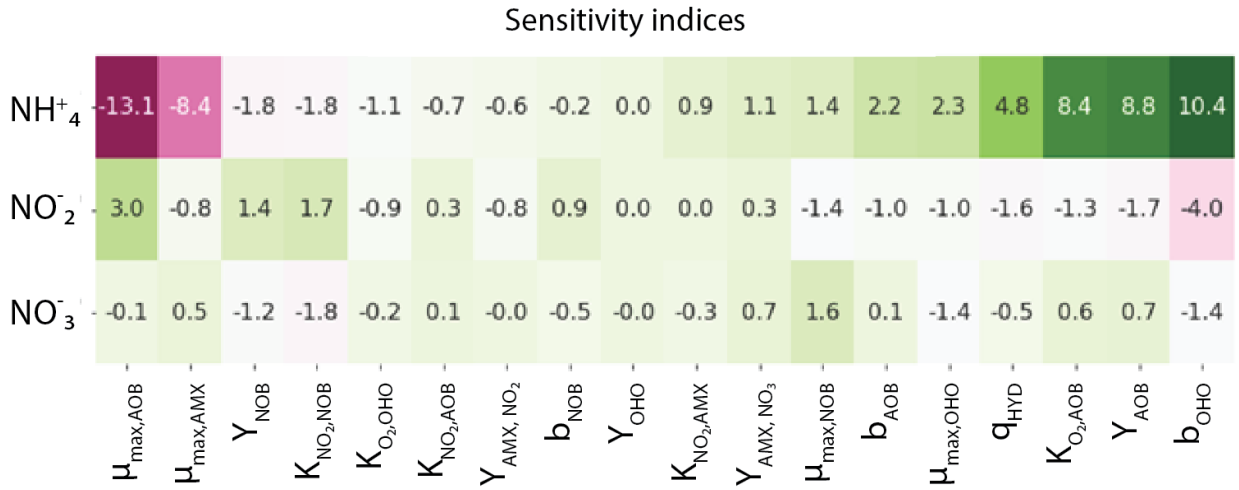

Figure B-13. Sensitivity indices measured as the mean overall effect of model parameters on the concentration of NH_4^+, NO_2^-, and NO_3^-. A positive value means the concentration increases with a unit increase in the of the parameter, and a negative value means the concentration decreases with a unit increase in the value of the parameter.

The range of parameters used in the calibration for the top sensitivity parameters ($\mu_{max,AOB}$, b_{OHO}, $k_{O2,AOB}$, $\mu_{max,AMX}$, $\mu_{max,OHO}$, and q_{HYD}) are presented in Table B-6. The best parameter which resulted in the lowest standard of error of estimate (Eq. B-3) was chosen.

Table B-6: Calibration parameters range for grid search algorithm

Parameters	$\mu_{max,AOB}$	$k_{O2,AOB}$	$\mu_{max,OHO}$	$\mu_{max,AMX}$	b_{OHO}	q_{HYD}
Unit	per day	mg-O_2/L	per day	per day	per day	per day
Range	0.7-1.5	0.1-0.5	2.5-5.5	0.07-0.12	0.4- 0.7	0.09-0.3

$$X^2 = \sum_{i=1}^{n} \frac{\left(S_{measured,\,i} - S_{calculated,\,i}\right)^2}{\sigma_{measured}} \qquad \text{Eq. B-3}$$

Figure B-14 presents the calibration results profile comparing the measured and simulated result. Figure B-15 presents the validation results comparing the measured and the simulated profile.

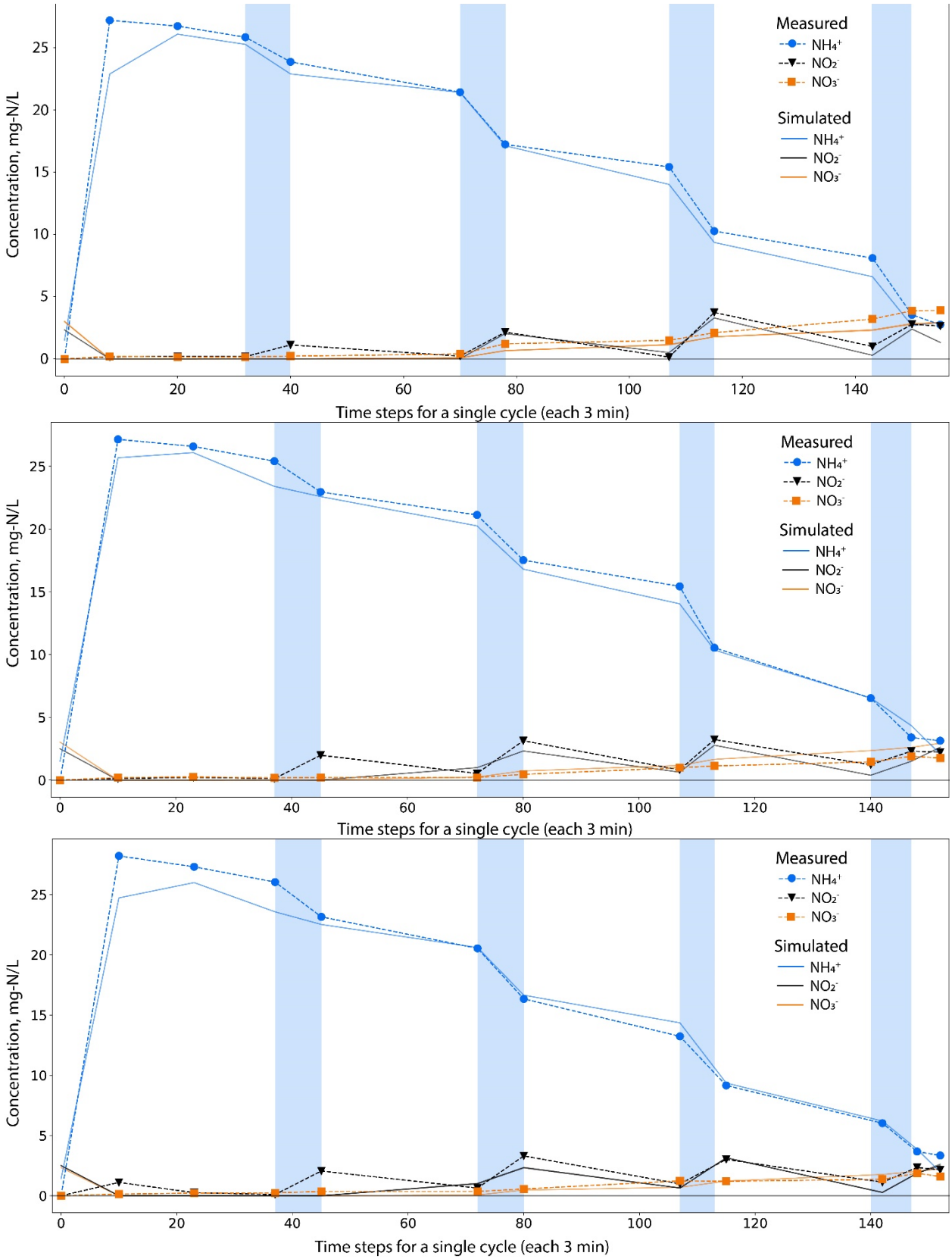

Figure B-14: Calibration results comparing the measured values with the calibration values for three different cross cycle profiles. The blue strips are aerobic phases, while the blank is anaerobic phases

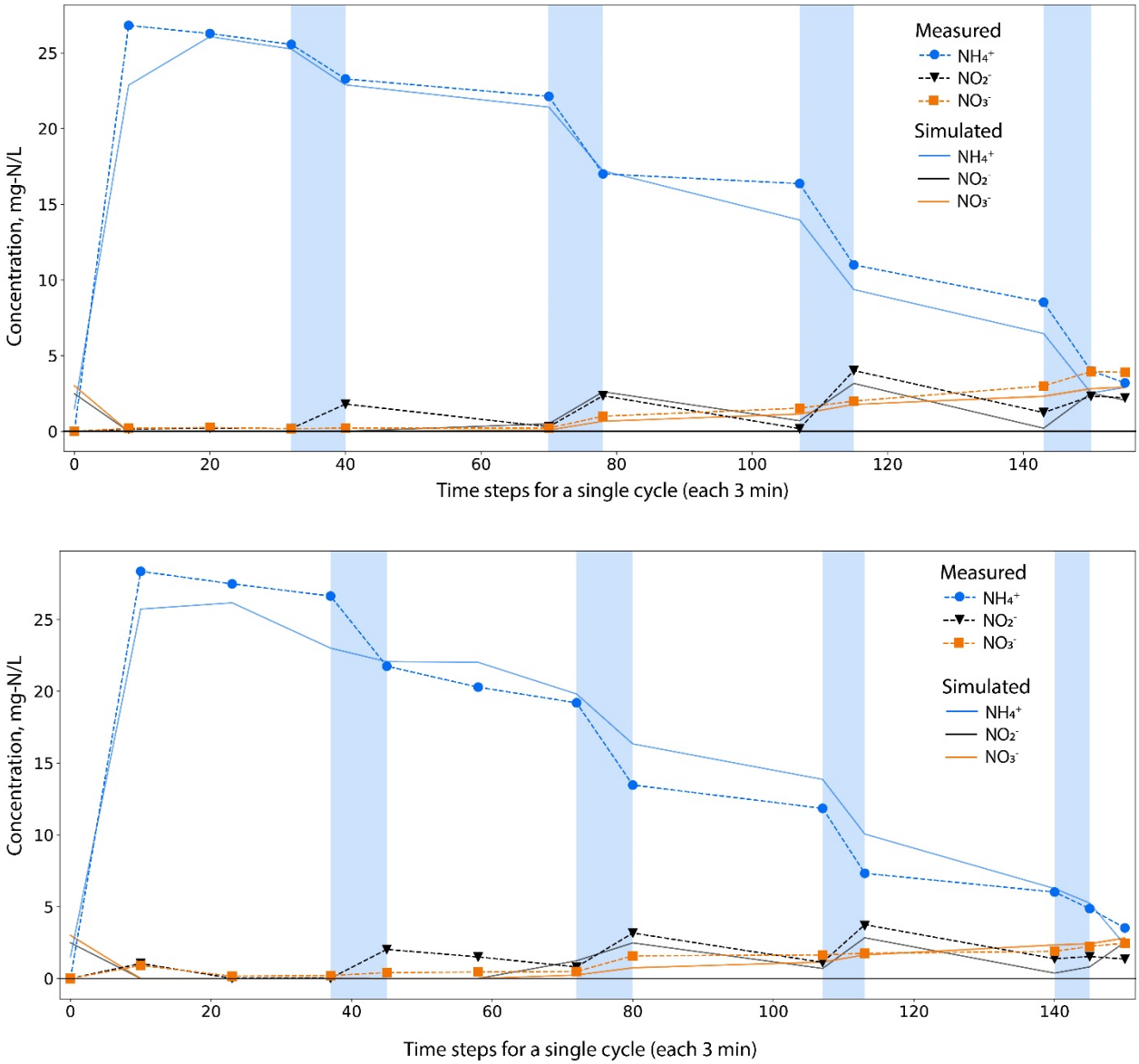

Figure B-15: Validation results for two different cross cycle profile data comparing simulation and measured data. The blue strips are aerobic phases, while the blank is anaerobic phases

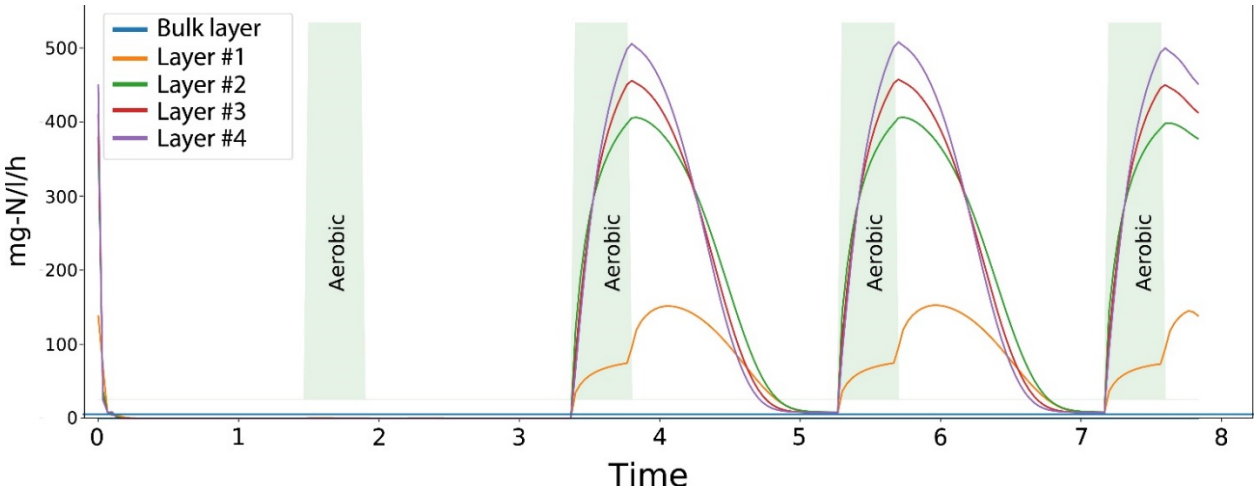

Figure B-16: Anammox nitrogen production rate over one cycle (simulation result)

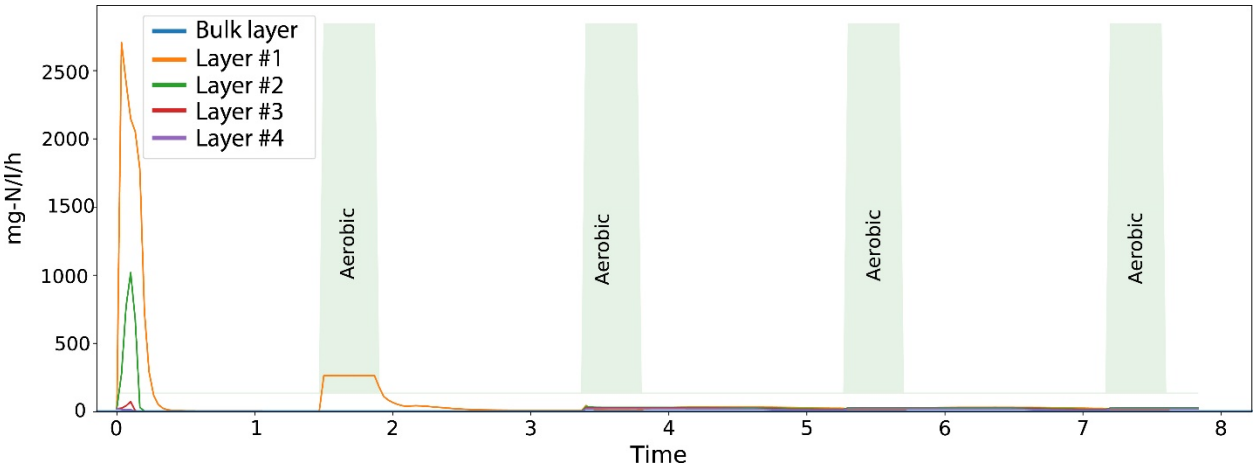

Figure B-17: OHO nitrogen production rate over one cycle (simulation result)

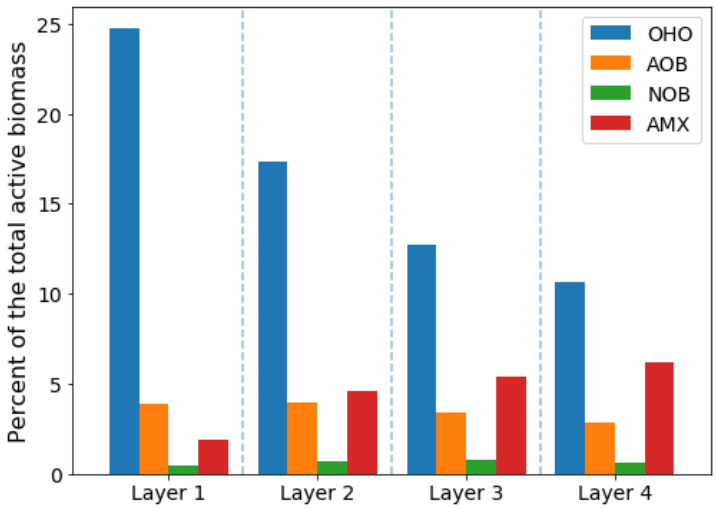

Figure B-16: Percent active biomass distribution in the granule layers (simulation result)

Table B-7: Relevant model parameters used in the final model that are different from the default values in Sumo 19

Symbol	Name	Value	Unit
μAOB	Maximum specific growth rate of AOBs	0.7	day^{-1}
$KO_{2,AOB,AS}$	Half-saturation of O2 for AOBs (AS)	0.25	mg O_2/L
$KO_{2,NOB,AS}$	Half-saturation of O2 for NOBs (AS)	0.7	mg O_2/L
μNOB	Maximum specific growth rate of NOBs	0.7	day^{-1}
qHYD	Rate of hydrolysis	0.09	day^{-1}
bOHO	Decay rate of OHOs	0.45	day^{-1}
μAMX	Maximum specific growth rate of AMX	0.12	day^{-1}
bAMX	Decay rate of AMXs	0.03	day^{-1}

Appendix C Supplementary information for Chapter 5

Simulation based evaluation of various feed conditions on the nitrogen removal performance of an aerobic granular sludge reactor with sensor-mediated control

Table C-1. The best calibration parameters values with lowest standard of errors

Parameters	$\mu_{max,AOB}$	$k_{O2,AOB}$	$\mu_{max,OHO}$	$\mu_{max,AMX}$	b_{OHO}	q_{HYD}
Values	0.7	0.15	6.0	0.08	0.6	0.1

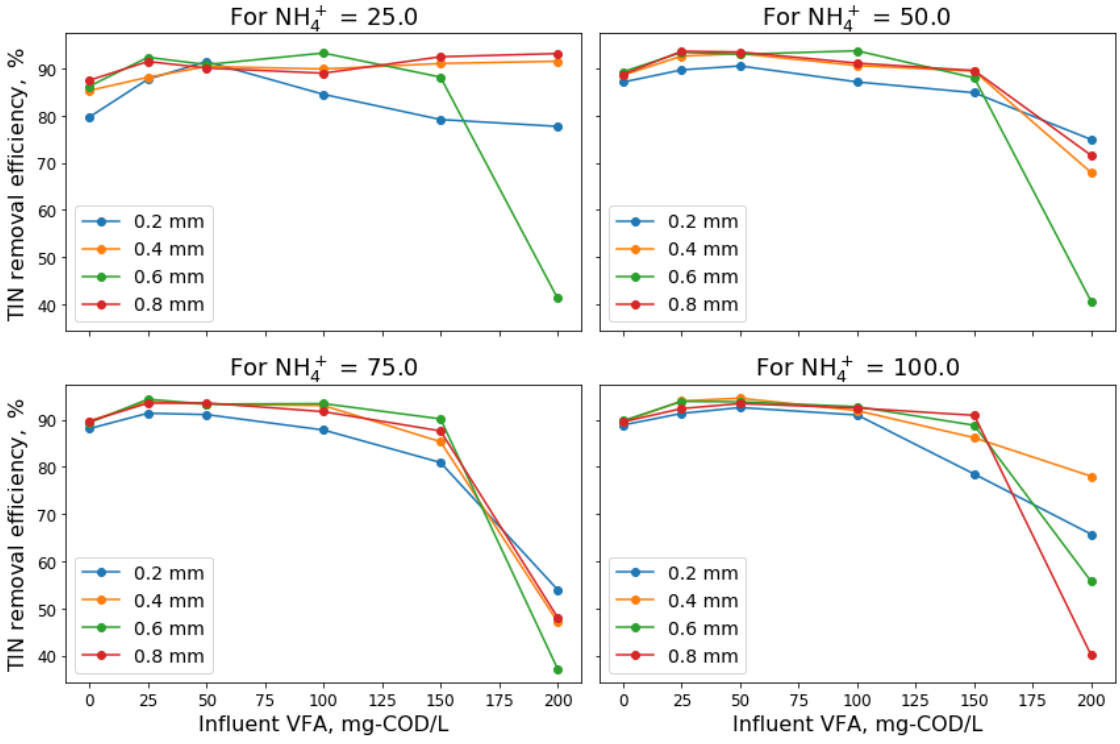

Figure C-1: TIN removal efficiency for different influent VFA and NH_4^+ (mg-N/L) across different granule diameter

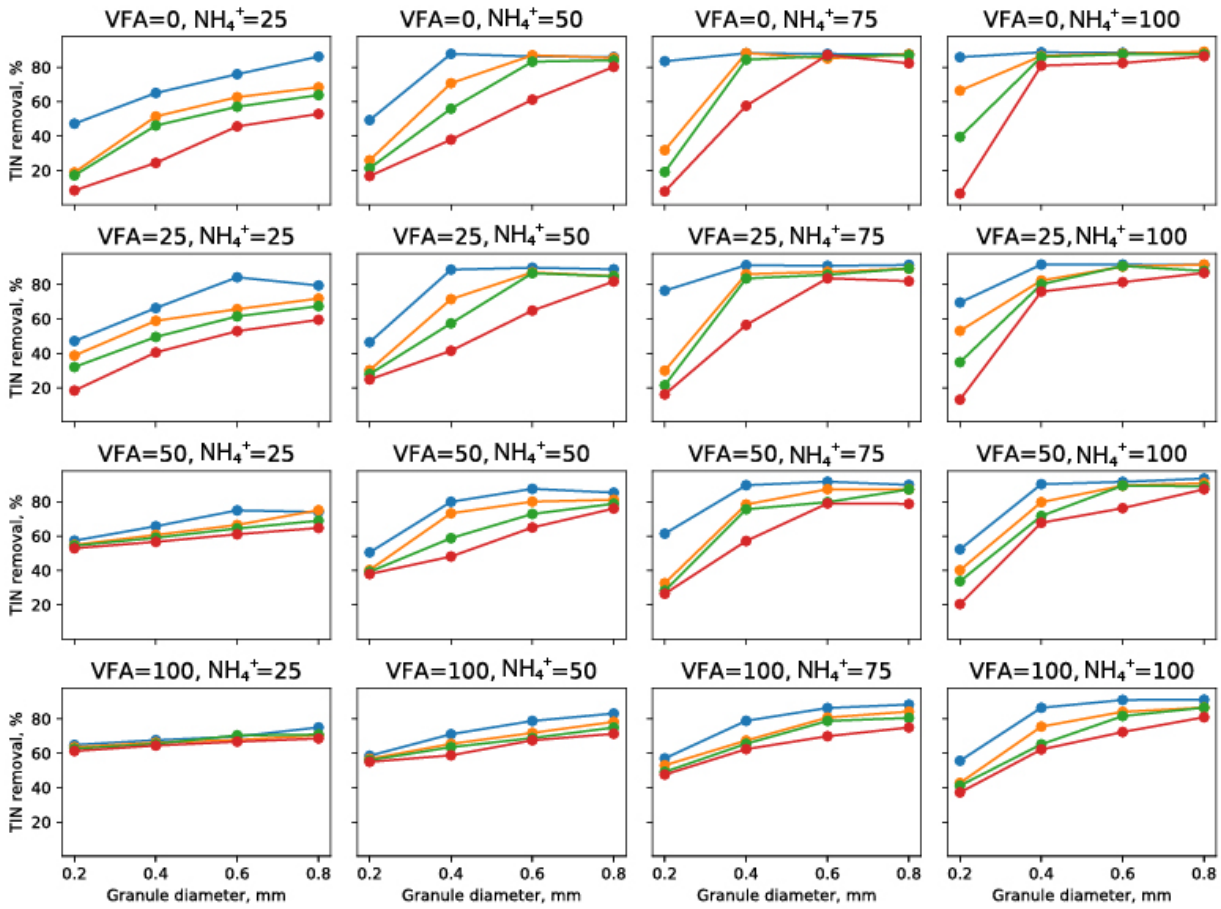

Figure C-2: TIN removal efficiency vs granule diameter for different influent VFA and ammonium combinations, and for max. aerobic time = 45 and max. anaerobic time=30 mins. The four different line represent the different DO setpoints (blue: 0.2 mg/L, orange: 0.4 mg/L, green: 0.5 mg/L, and red:0.75 mg/L)

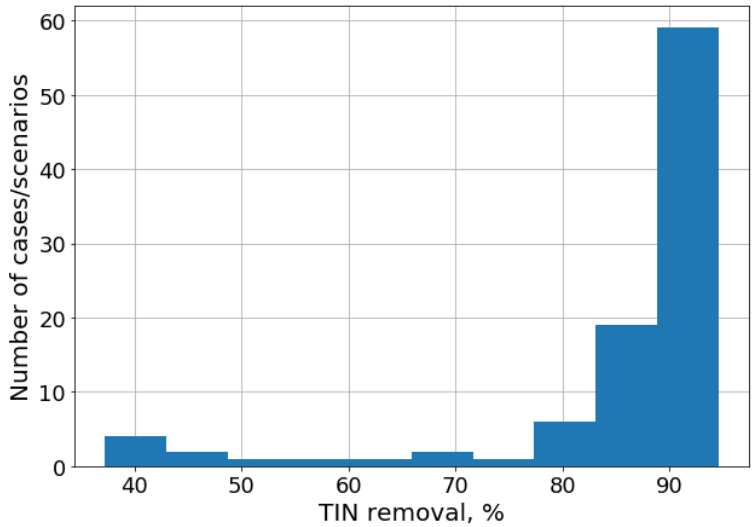

Figure C-3: Histogram showing the distribution of the best TIN removal achieved for the 96 simulation scenarios.

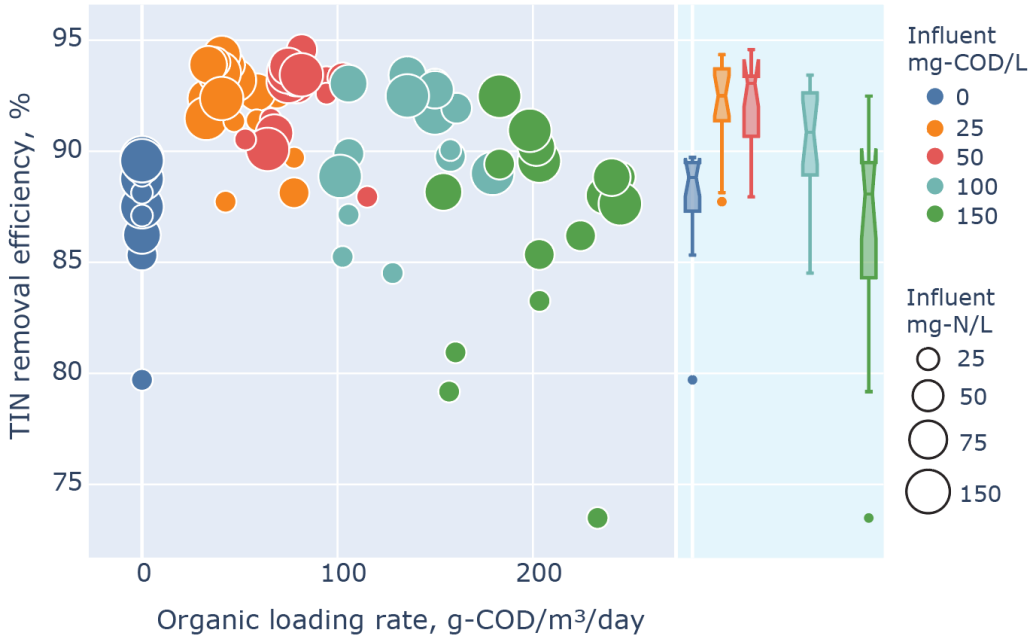

Figure C-4: Showing organic loading rate vs TIN removal efficiency for those input conditions resulting in total cycle less 12 hrs and influent VFA less than 200 mg-COD/L.

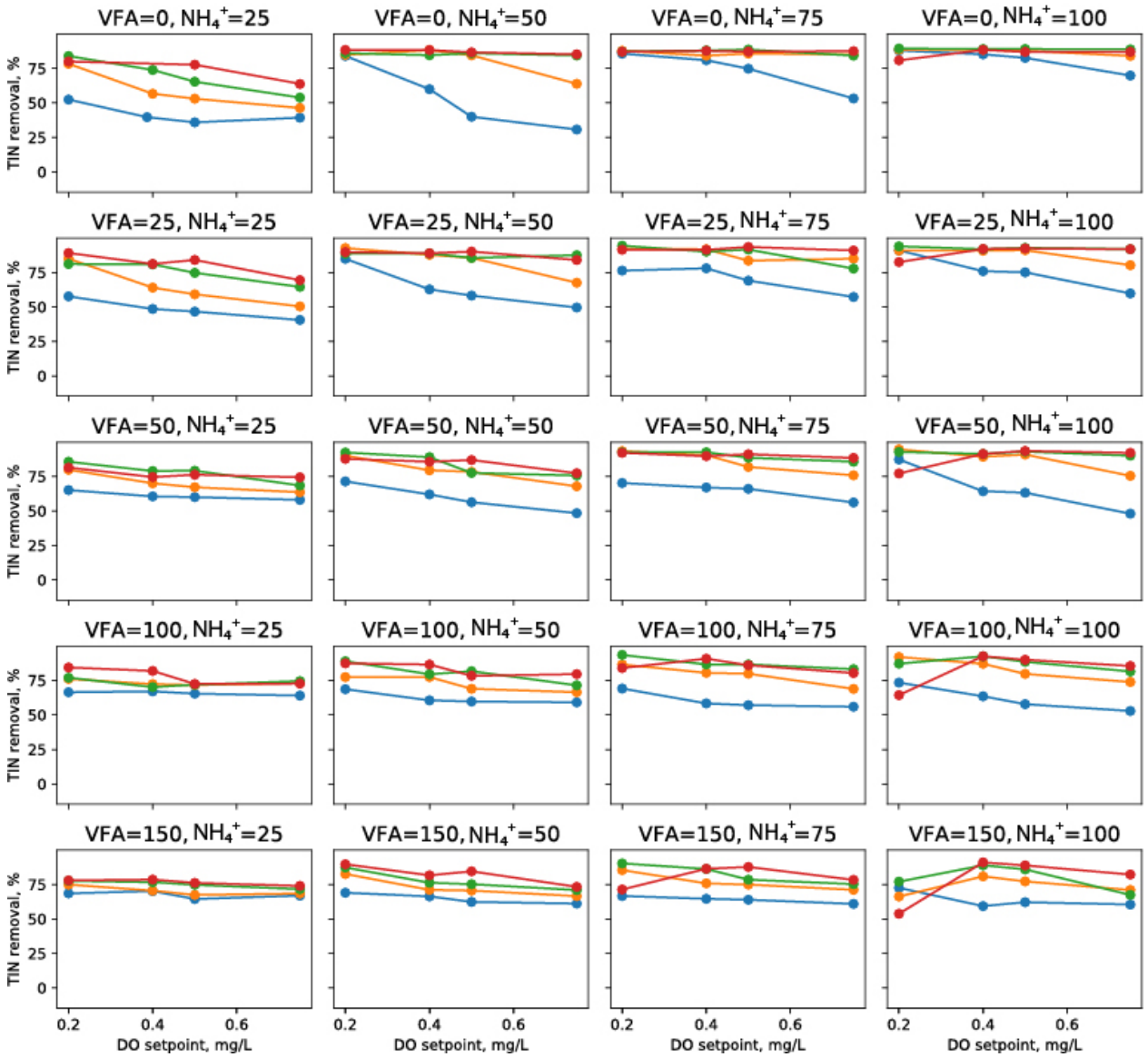

Figure C-5: TIN removal efficiency vs DO setpoint for different influent VFA and ammonium combinations, and for max. aerobic time = 30 and max. anaerobic time=60 mins. The four different line represent the different granule sizes (blue: 0.2 mm, orange: 0.4 mm, green: 0.6 mm, and red: 0.8 mm)

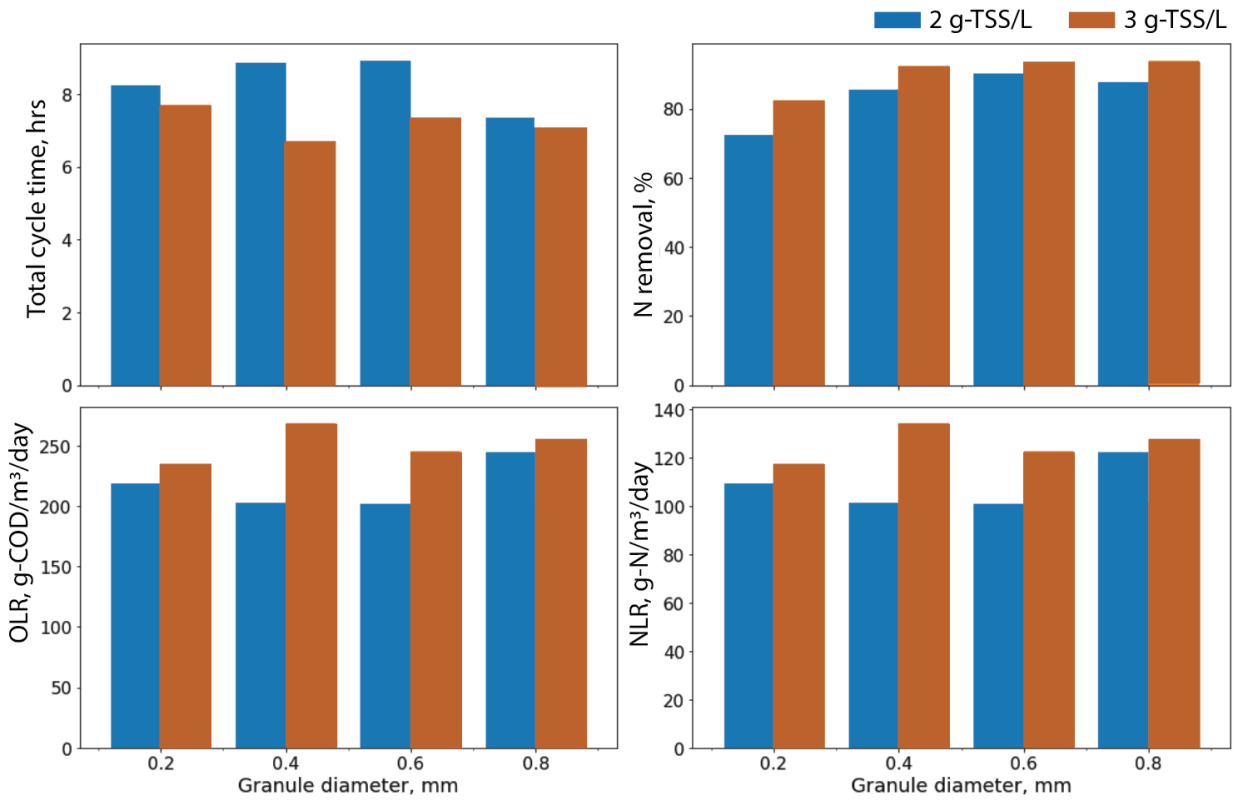

Figure C-6: Performance comparison between target TSS concentration of 2 g-TSS/L and 3 g-TSS/L